RESUM

L' objectiu d'aquest projecte consisteix en el desenvolupament aerodinàmic de l'aleró posterior del prototip de Fórmula 1 que l'equip Epsilon Euskadi prepara per la temporada 2011. La quantitat de recursos informàtics pel seu desenvolupament en CFD (Dinàmica Computacional de Fluids) limita constantment les fases d'evolució del monoplaça, i per tant es requereix una optimització del procediment.

Per tal d'accelerar el desenvolupament i de millorar la presa de decisions a l'hora de provar nous alerons, s'utilitza el programa ModeFrontier per tal d'automatitzar tot el procés de disseny en 3D, simulació de dinàmica de fluids i posterior tractament dels resultats. A més, mitjançant l'ús d'algoritmes interns d'aquest programa, es busquen automàticament nous candidats per millorar l'aleró sense la intervenció de l'enginyer.

Amb la finalitat d'obtenir un disseny que pugui ser millorat automàticament, es fa un estudi de la simulació de fluids del Fórmula 1 en StarCCM+, i es fa un disseny totalment parametritzat de l'aleró posterior amb CATIA V5. A més, es redueix la complexitat de la malla i del model a simular per tal de reduir fins a 30 vegades la quantitat de càlculs que s'han de processar, tot i que implica unes certes limitacions a l'hora del desenvolupament de la part inferior de l'aleró (aleró de suport/estructural d'unió amb la carrosseria).

Finalment, un cop implementat el model reduït i amb resultats de correlació positius amb el model inicial, es posa en funcionament en un ordinador d'altes prestacions, buscant el millor aleró possible, revisant periòdicament els resultats i decidint les noves línies de desenvolupament en les reunions amb el Departament d'Aerodinàmica. Mitjançant diverses fases de millora, s'assoleix un nou aleró posterior que fa el monoplaça més d'una dècima de segon més ràpid per volta.

Tot el projecte ha estat desenvolupat al Departament d'Aerodinàmica de l'equip Epsilon Euskadi treballant conjuntament amb el grup de desenvolupament del prototip de Fórmula 1, el que suposa que el projecte s'ha guiat constantment per les necessitats del monoplaça i pels criteris de desenvolupament que implica aquest esport, buscant sempre el màxim rendiment possible amb els recursos disponibles amb dates límit molt estrictes. Això incrementa notablement el valor del projecte ja que reflecteix perfectament el desenvolupament real en un equip de Fórmula 1 d'un aleró posterior.

ABSTRACT

The main goal of this project consists in the aerodynamic development of the rear wing of the Epsilon Euskadi Formula One prototype, which is being prepared for 2011 season. The quantity of computing resources for its development in CFD (Computational Fluid Dynamics) limits the evolution of the car. Therefore an optimization of the procedure is needed.

In order to accelerate the development and improve the decision-making when testing new wings, it is used ModeFrontier to automate all the 3D design, CFD simulation and further data treatment. Moreover, through internal algorithms of this software, new candidates are found to improve the wing without the intervention of any engineer.

To obtain a design which can be automatically improved, CFD Formula One model is analyzed with StarCCM+, and it is created a parametric design of the rear wing in CATIA V5. Moreover, mesh complexity and model size is reduced up to 30 times the original CFD model of the full car, although entails some limitations when developing the lower beam wing of the rear wing.

Finally, once implemented the reduced model and with positive correlation results with the full model, it is started in a powerful workstation, looking for the best rear wing design, periodically reviewing the results and deciding new development paths in meeting with the Aero Team. Through several improvement stages, a new rear wing is obtained, which improves race car lap time by more than one tenth of a second.

The full project has been developed in the Aerodynamics Department of Epsilon Euskadi team, working together with the Formula 1 development team, which means that the project has been driven by the full car requirements, and by the development style of this sport, looking for the maximum performance with the resources available, working under very tight deadlines. This increases notably the value of this project, as it reflects perfectly the real development inside a Formula One team of a rear wing.

Table of Contents

epsilon EUSKADI

Figure index

epsilon EUSKADI

epsilon EUSKADI

Table index

Equation index

Glossary

Beam wing	Lower element of the rear wing, with both structural and aerodynamic functions.
CFD	Computational Fluid Dynamics
Diffuser	Aerodynamic device under the rear wing to extract air from the underfloor, generating a huge amount of downforce
Downforce	Negative lift, produced by wings in race cars to improve grip
Drag	Force of the fluid against the relative motion of an object through it.
Endplate	Aerodynamic fences to reduce wing tip vortex
F-Duct	Duct used over the engine cover in Formula One to stall the rear wing in order to increase straight line speed
Flap	Small wing behind the main plane, with high angle of attack.
Gurney	Small flat tab, over the trailing edge of the flap, usually 90º to the pressure side surface of the airfoil
Lift to drag ratio	Efficiency of the wing, or downforce value divided by drag
Main wing/plane	Main part of the rear wing, on top of the rear wing, with low angle of attack
NACA (airfoil)	Standard airfoil shaped developed by the National Advisory Committee for Aeronautics.

epsilon EUSKADI

PART 1 - Introduction

1.1- Project Motivation

Formula One is one of the most challenging competitions where an engineer can develop its work. Specially in the aerodynamic department, where very strict rules limit the bodywork of each race car. After joining the master in Epsilon Euskadi and discovered the aerodynamic development of a Formula One for 2011 season, there was no doubt that it was the right place to develop a top engineering project.

After some years without major technical modifications, the period between 2009-2011 seems to be one of the most active in aerodynamic development (Double diffuser, F-ducts, new adjustable rear wing for 2011 season), specially in the rear end of the car. That is why this project will be dealing with the rear wing optimization, as it will be a critical zone after the ban of the F-Duct for 2011 season. Epsilon Euskadi team has awesome wind tunnel facilities and a CFD (Computational Fluid Dynamics) department with some clusters available, so the CFD development of a whole rear wing and the correlation with wind tunnel data allows to improve the lap times of a Formula One by some tenths of a second, which is an invaluable achievement for any engineer.

1.2- Objective

The objective of this project is to develop the rear wing of the current Epsilon Euskadi Formula One for 2011 season. Development will be done in three main areas:

- Wing and flap profile
- Rear wing 3D geometry (Angle of attack, gap, overlap…)
- Beam wing

The procedure will start with CFD development (with Star-CCM+) with the objective of maximize downforce and lift to drag ratio. These optimizations will be guided automatically by an optimizer software (ModeFrontier) using genetic algorithms.

Aerodynamics is not an exact science, as turbulence behavior is not fully understood. And the current technology limits the aerodynamic development of the race car. For an aerodynamic simulation of a whole Formula One, teams need one to three days depending on computing resources. So the size of the model (that is, the accuracy) should be compromised to get faster calculations. That is the first decision of the CFD engineer, the settings of the mesh for the calculation. The second step is to decide in which ways the model can be reduced in order to make more calculations in less time (use only half symmetrical car,

study only the rear part of the car without the front…). The third step is to decide which modifications will affect more the performance of the car, and as a result, are more profitable (economically – do not forget that Formula One is a business). Finally, the decision of which new parameters and values must be tested is crucial. In order to get the most representative calculations, genetic algorithms are used with the ModeFrontier software, which is programmed to redesign the 3D geometry of the car (with CATIA V5), launch the simulations in Star-CCM+, and calculate the resulting forces due to the geometrical changes, and decide how can the rear wing perform better. It is a really hard work, which implies parametrical design in CATIA V5, an absolute control of the mesh in StarCCM+, and some computing skills to make a 100% automated process. The final result: **to have a self-sufficient computing center, capable to develop and decide by itself, without any engineer in front of the computer.** This means that the computer will work during weekends, holidays, etc. so the resources will be 100% of the time working – which is the dream of any company – and it is faster than an engineer, and even better, it doesn't make mistakes.

Once the results are studied in the computer, wind tunnel test must be carried out. CFD simulations can show the fluid behavior, and aerodynamic improvements. However, they don't give us exact values of force, but approximations. The wind tunnel gives real results of the wind forces against a 50% scale model, which will show the correlation with CFD calculations and more accurate force values, to implement or not the new rear wing modifications. Anyway, this project is focused in the CFD-Optimization process, and the validation of these results corresponds to the wind tunnel department, but this project will also deal with it as a demonstration of the whole design process of a Formula One rear wing.

PART 2 – Formula One Rear Wing Optimization

2.1- Formula One Project Development Guidelines

When working for a Wind Tunnel department, the project guidelines must be followed strictly. It is very expensive to test parts in a wind tunnel (due to the fact that a giant fan of around 1000 HP has to be used and a moving belt at more than 200 Km/h. Apart from that, new parts should be machined (in this project a rear wing), so moulds have to be produced, and then a composite specialist should work for some hours laminating the wings in carbon fiber. So to sum up, a single rear wing tested during some hours costs thousands of Euros, wind tunnel time and manpower, so it must be developed and tested in CFD extensively.

The assembly of the rear wing is divided into three different projects, in order of importance: upper wing (Main Wing and Flap), lower beam wing and Endplates. The most difficult part is the Main Wing + Flap, as they must be developed together, so the optimum profile of the flap depends on the main wing and vice versa. After developing the wing profile, the 3D shape is the next process to focus on (this means, to extrude straight the profile, with w shape, etc.), and after that, chord/angle change along the extrusion. It is possible to go further, as changing the wing profile along the section of the rear wing, but it would require a huge amount of computing resources.

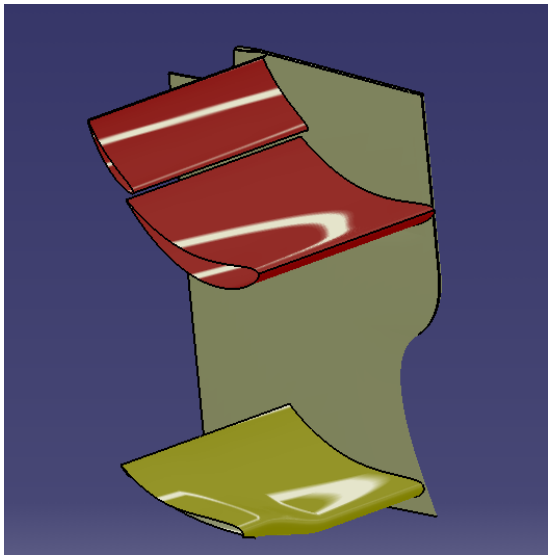

Fig. 2.1- Main wing and flap in red, lower beam wing in yellow, endplate in brown.

Talking about the lower beam wing, it is only one profile which should be optimized. However, the importance of this part is essentially due to its interaction with the diffuser, which could help extracting the

air from the underfloor. In this case, the 3D shape and torsion of the wing is more important due to the influence of the engine cover in front of it and the diffuser flow. Finally, the endplates are the last thing to improve, because its function is to maximize the performance of both upper wing and flap and lower beam wing. However, it is always as big as the regulation allows, and there is a small margin to improve.

Development Cycle (scheduled before starting the project)

1.-Upper rear wing – upper main wing and flap

1.1.- Main wing profile (NACA 4 digit with trailing edge refinement)

1.2.- Flap profile (NACA 4 digit with trailing edge refinement + gurney flap)

1.3.- **Baseline** positioning – always filling all the space allowed by the regulation box.

FIRST OPTIMIZATION GROUP WITH 8-10 VARIABLES

1.4.- Main wing profile (Parametric profile designed with CATIA).

1.5.- Flap profile (Parametric designed with CATIA).

1.6.- Param_Baseline positioning, superimposing previous NACA optimum design.

SECOND OPTIMIZATION GROUP WITH AROUND 40 VARIABLES AVAILABLE

1.7.- 3D shape (extrusion line) of the best design.

1.8.- Chord, angle of attack adjustments of the profile along the extruded wing.

THIRD OPTIMIZATION GROUP WITH AROUND 15 VARIABLES

2.- Lower beam wing

2.1.- Lower beam wing profile (NACA 4 digit with trailing edge refinement).

2.2.- Lower beam wing profile (RAM profile designed with CATIA).

2.3.- 3D Shape, combined with chord and angle of attack control.

FOURTH OPTIMIZATION GROUP WITH AROUND 25 VARIABLES

3.- *Endplates* (optional)

3.1.- Endplate shape (side view)

3.2.- Endplate profile

3.3.- Endplate louvers

FIFTH OPTIMIZATION GROUP – VARIABLES DECIDED BY CHIEF AERODYNAMICIST

WIND TUNNEL TESTING - End of cycle; Return to first point to continue improving.

epsilon EUSKADI

Baseline clarifications

The chief aerodynamicist set the criteria to draw the first Main Wing + Flap profile. The objective is to assure that we get the maximum downforce with the minimum drag possible. The regulation box says that it is mandatory to have 2 closed sections in a given volume. That means that the rear wing will consist in a main wing and a flap, and it is not allowed to add or remove any profile. The shape is totally free – provided that we are inside the volume allowed – and there is only a restriction, which says that the 2 sections must be separated by 15 mm at least.

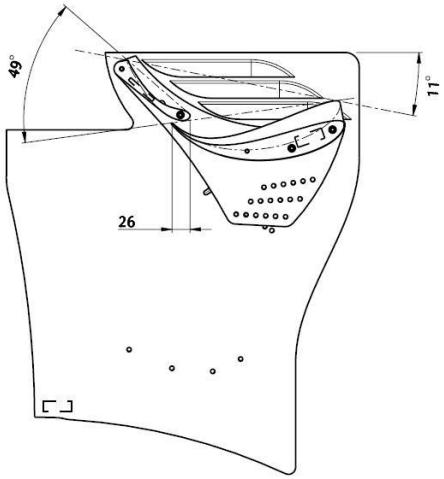

Fig 2.2 - Rear wing from a World Series by Renault car. Notice 18 whole for set-up adjustments.

Therefore, the next question is: how do we fill this volume? In Formula One, it was normal to have a rear wing with its angle of attack adjustable (you could tilt it forward or backward), like in any Formula Series like the World Series by Renault or similar. The problem with that is that you have to leave a margin with the profile to adjust the angle of the wings, and keep the profiles inside the regulation box, so the car will have a smaller wing, giving less downforce.

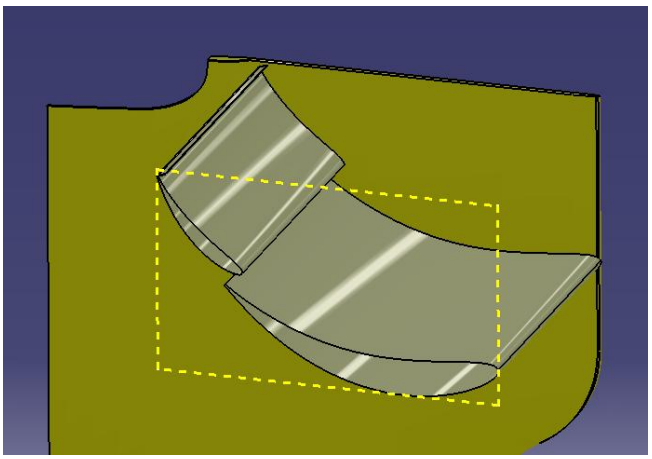

Fig 2.3 - Regulation box for the Main Wing and Flap, in yellow.

So, to get the maximum from the regulation box (because the Rear Wing is much smaller nowadays than some years ago), a range of different, fully optimized wings must be designed. Moreover, in Formula One the tracks are perfectly known by the engineers, so the Rear Wing is directly designed for a given track:

		TARGET 1		TARGET 2
Low DWF	Med-Low DWF	Medium DWF	Med-High DWF	High DWF
Monza	Turkey Belgium	**All others**	Silverstone	Monaco Budapest Singapur

Table 2.1- Track/Downforce groups

It is clear that the rear wing should be optimized for medium downforce tracks, as they represent more than 50% of the World Championship races. In this situation, the criteria for the optimization is to keep the same downforce as the former Epsilon Euskadi design (around 3000 N), but improving the drag. Once it is fully designed, the second wing designed is for high downforce tracks – where the rear wing is very important to have grip and traction. In this case, the priority is maximum downforce, no matter drag. Low downforce configuration tracks are not so critical, as the objective is to minimize drag with a small amount of downforce, therefore the regulation box will not be totally occupied.

So finally, a few decisions will govern our parametric design. First of all, the main wing leading edge will be tangent to the regulation box, and the lower surface will also be tangent to the regulation box. The trailing edge of the flap will also be tangent to the regulation box, and it will be some mm under the upper part of the regulation box, to allow enough space for the “gurney”, and assuring that is inside the box while rotating the flap during the optimization.

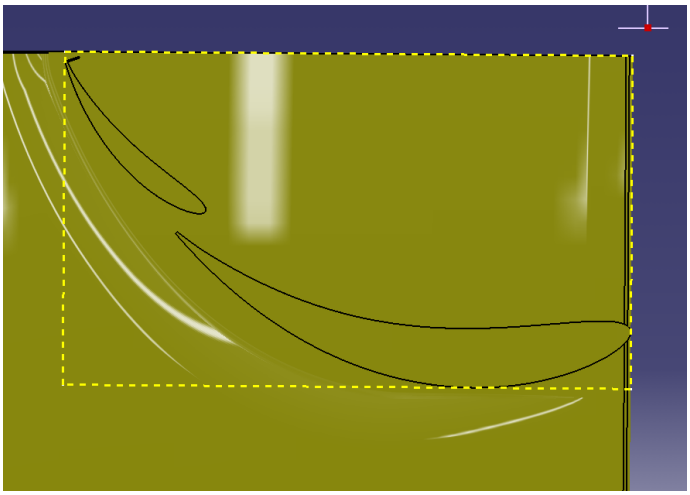

Fig 2.4 - Main wing and flap profiles, both closed sections tangent to the regulation box.

2.2- CFD Software Testing

2.2.1-Introduction

The software used in the Aero department of Epsilon Euskadi is StarCCM+ 5.04, a well-known CFD software with capable of make both pre-processing and post-processing apart from the CFD calculation. This means that we only need one software instead of three (which happens with other software like OpenFoam, where you need additional meshing software and a viewer), making the whole processing much easier.

CFD development is very complicated, and it has a lot of parameters to control, so the CFD department of Epsilon Euskadi has its own standards. However, as this project will deal with a new approach, a small study will be developed in order to fully understand the software, computing resources, and predict future problems, so the design can avoid them. Therefore, the list of the objectives is the following:

1- Practice with the software to **fully understand CFD simulations**.
2- Define **computer resources required** for each run (memory, file size, CPUs needed).
3- Define a **standard rear wing geometry** (according to the FIA Formula one Rules 2010) based on F-1 pictures, with NACA standard profiles.
4- Define **mesh size**, boundary layer thickness and number of prism layers required, influence of these parameters into file size and calculation's speed.
5- Study the **airflow** around the rear wing in order to achieve the maximum performance without stalling the flap.
6- Study the **rear wing sensitivity around the full range of velocities** for a F-1 race car.

To sum up, a complete study will be done to verify that it is possible to run the simulations on the Epsilon Euskadi computing centre, find the correct mesh size, file size, CPUs demand and adjust the planning depending on simulation length. However, the most important thing is the experience obtained from this test for to avoid further problems with the real Formula One model.

2.2.2- Test procedures

First of all, a number of parameters should be defined in order to make a "datum" simulation. A simplified rear wing will be designed according to the FIA Formula One 2010 rules, and its shape will be modified (if necessary) to achieve standard lift & drag values.

Once the shape of the rear wing is correct, mesh parameters will be regarded. In order to avoid "particular" simulations for a given speed, different test speeds will be simulated:

Airflow speed (m/s)	Airflow Speed (km/h)
30	108
40	144
50	180
70	252
100	360

Table 2.2- Airflow test speed in m/s and km/h

This particular selection has been done after some initial simulations to understand the software, which demonstrates that there is slightly more difference between tests in lower speeds than higher speeds. The maximum speed allowed has been selected with a small margin from 2009-2010 top speed recorded in Monza - Formula One Italian GP, which had the lowest downforce configuration.

Once the right wing profile has been chosen, the next step is to adjust the mesh to get every detail from the airflow (boundary layers, leading and trailing edge...). It will be tested with the standard K-Epsilon model, and the different parameters tested will be:

Surface mesh size: 12 mm
Boundary layer: Number of prism layers used (4) & Wall thickness (1mm)
Volumetric Controls: Leading/Trailing edge & wake

The selection of the correct mesh will be done by looking at the airflow and values obtained from the simulation. Moreover, while every simulation is being done, residual's convergence will be checked, and number of iterations needed to converge the simulation and iterations per minute done by the computer. In order to understand the correlation between iterations per minute and number of processors working, some simulations will be randomly run with 1, 4 or 8 processors.

Finally, different tests will be done while working with the K-Epsilon turbulence model to help the simulation to converge (that is, initialize flow before running, change under-relaxation factors...). K-Epsilon

epsilon EUSKADI

model has been chosen due to its capacity to handle more general flows (not only external aerodynamics), because the development of the rear aero package of a Formula 1 can involve some internal, complicated flows like F-Duct devices or the air intake manifold to the engine.

Fig. 2.5- F-Duct from Red Bull Racing and Mercedes GP Intake Manifold **[1]**

K-Epsilon turbulence model is the most used model in aerodynamics, although there is controversy between K-Omega and Spalart-Allmaras models. The current test will be done with K-Epsilon model because it is able to handle with many kind of flows, and converge successfully although non-accurate mesh/boundary conditions. However, some tests with K-Omega and Spalart-Allmaras will be done in order to check that there are no big differences between models.

2.2.3- Simulation Set Up

The basic geometry consists in a main wing and a flap, obtained with the Java Applet JavaFoil. The main wing is a simple NACA airfoil, thicker and with more camber, and the flap is a more slender wing with less camber, more or less half the chord of the main wing. The endplates are two simple rectangles not optimized, but accepted by the rules, and finally it has a central support, streamlined to minimize drag and to be connected with the rest of the wind tunnel. The wind tunnel size can be seen in the picture generated by CATIA:

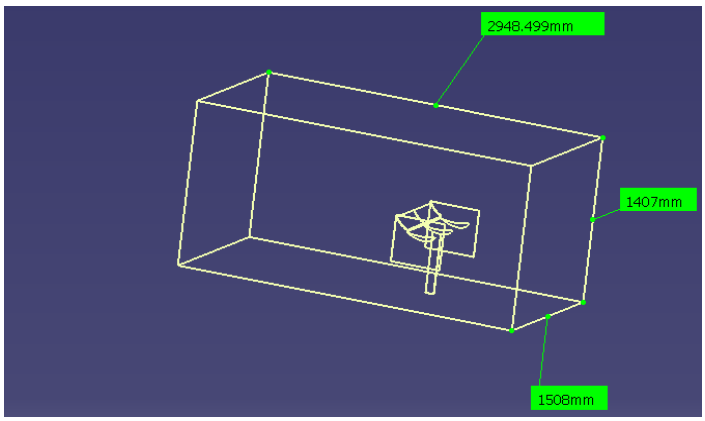

Fig. 2.6- Wind tunnel and rear wing inside it.

Different sizes have been chosen to develop the wake correctly, and to avoid blockage:

Cross Sectional Area:

-Wind tunnel: 2.122 m^2

-Rear Wing Assembly: 0.106 m^2

Blockage: 4.995%

This is a good value for standard race car wind tunnel facilities. However, blockage in wind tunnels is a serious problem which should be corrected, so a proper explanation can be read on reference book “Race Car Aerodynamics, by Joseph Katz” **[2]**.

So after checking the correct shape of the rear wing assembly and the wind tunnel, the final geometry is the one in the following picture.

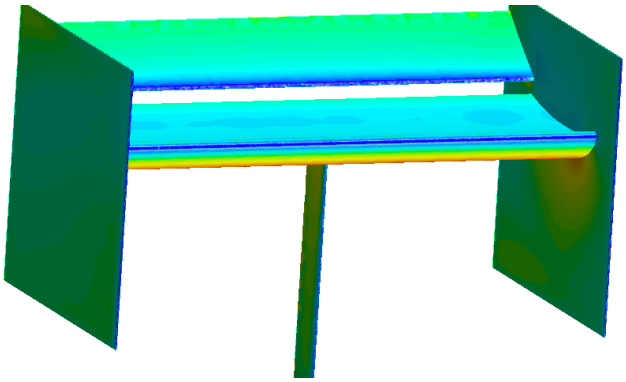

Fig. 2.7- First Assembly of the rear wing introduced into CFD software.

So, in order to test the performance of this rear wing, the first Star-CCM+ simulation must be defined. For this simulation, as it is the first one, different speeds will be tested to have a better understanding of the rear wing sensitivity. Particularly, in this first test, the following airflow speeds will be tested:

Airflow speed (m/s)	Airflow Speed (km/h)
30	108
40	144
50	180
60	216
70	252
100	360
130	468

Table 2.2b- Airflow test speed in m/s and km/h

Moreover, the most important thing in a first approach simulation is mesh properties. In this first test, based on the department experience from Epsilon Euskadi, the mesh will be generated according to the table below. Polyhedral mesh is also used due to its ability to deal with complex, non-accurate geometries, so it will not be discussed in this test. However, for the Formula One simulations, trimmed mesh (rectangular cells instead of polyhedral) is used, as it converges quicker than the polyhedral mesh.

StarCCM+ property	Values
Polyhedral Mesh - Base Size	15 mm
Boundary Layer - Number of prism layers / Wall thickness	4 layers/ 1 mm
Volumetric controls for mesh refinement	None

Table 2.3- StarCCM+ mesh properties

The final result with these properties can be seen in Fig.2.8 & 2.9, which is a mesh with enough cells to evaluate the rear wing. To have an idea of the size of the file in STAR-CCM+ of these characteristics, it is around **2 GB.**

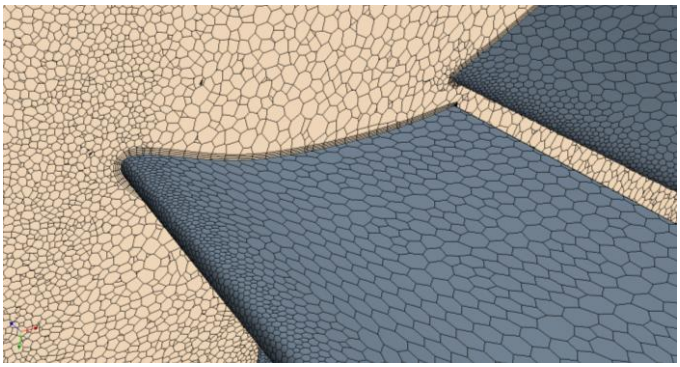

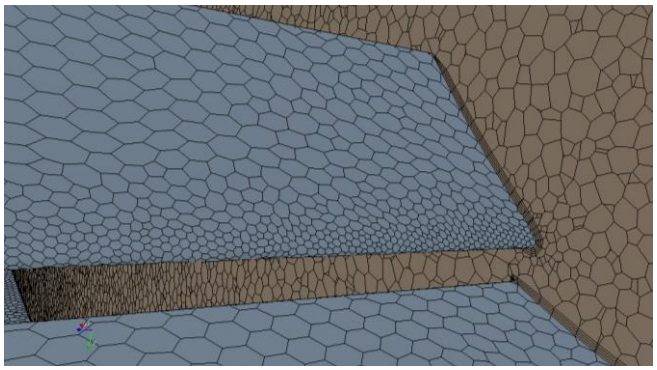

Fig. 2.8 & 2.9- Polyhedral mesh - Notice the boundary layer refinement with prism layers.

Next step is to define the parameters of the physic model. They are standard, so they will not be changed until the turbulence model testing.

Physic model selection in Star-CCM+	
Space	Three dimensional
Time	Steady
Material	Gas
Flow	Segregated flow
Equation of state	Constant density
Viscous Regime	Turbulent
Reynolds-Averaged Turbulence	K-Epsilon Turbulence

Table 2.4-StarCCM+ Physic model properties

2.2.4- Simulation Analysis

There are many measures to show the aerodynamic performance of a wing; Cx, Cz, Lift, downforce, Lift to drag Ratio... With the software Star-CCM+ it is possible to obtain them all, but in t his particular test, the parameter used will be the L/D Ratio, which is a non-dimensional value to compare different speeds, and it depends on both drag and lift generated by the airfoil.

Another issue to discuss is the time needed to develop the flow in a simulation. In this first test, the simulation will be considered as finished when the Drag and Lift (monitored in Star-CCM+) is stabilized. To be sure about that, the residuals will be regarded, waiting for their stabilization, which also indicates that the simulation is finished.

The final results expected for this kind of rear wing are:

L/D Ratio: around 6 (+/- 0.5) - notice that mesh is not optimised.

L/D Ratio Vs Speed: slightly increasing with speed.

epsilon EUSKADI

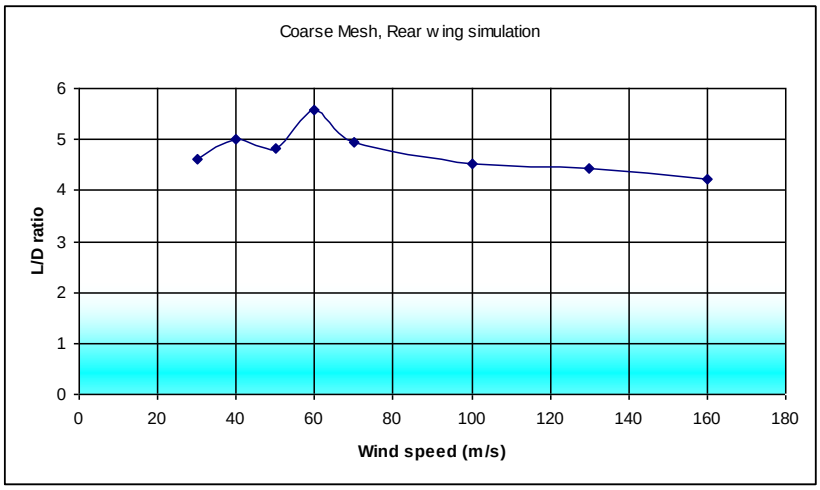

Fig. 2.10- Graph of L/D Ratio Vs Wind Speed - Note extra 160 m/s test.

As it can be seen in Fig.2.10, the results are far from expected. The L/D Ratio is below 6 (what was supposed to be) and the difference is huge depending on each simulation (or wind speed). The theory of wings does not match with this at all. Therefore, the simulation is not properly done, or there is a problem with the turbulence model - not very probable as it is the most standard one used in CFD.

2.2.5- The importance of a converged simulation

Analysing the process, there is only one step which is not very well defined - simulation length. So, here it is a table of each L/D value and number of iterations done. Cells in red are simulations with a reduced number of iterations, in yellow are intermediate calculations, and in green the ones "considered" already finished.

wind speed (m/s)	L/D ratio	Nº Iterations
30	4.616322	33
40	4.997164	106
50	4.826417	43
60	5.583973	142
70	4.935726	45
100	4.535094	40
130	4.445758	30
160	4.221972	21

Table 2.5- L/D Ratio table and stopping iteration

The following Fig. is massively representing the importance of number of iterations and convergence of flow to have a rigorous, correct study in race car aerodynamics:

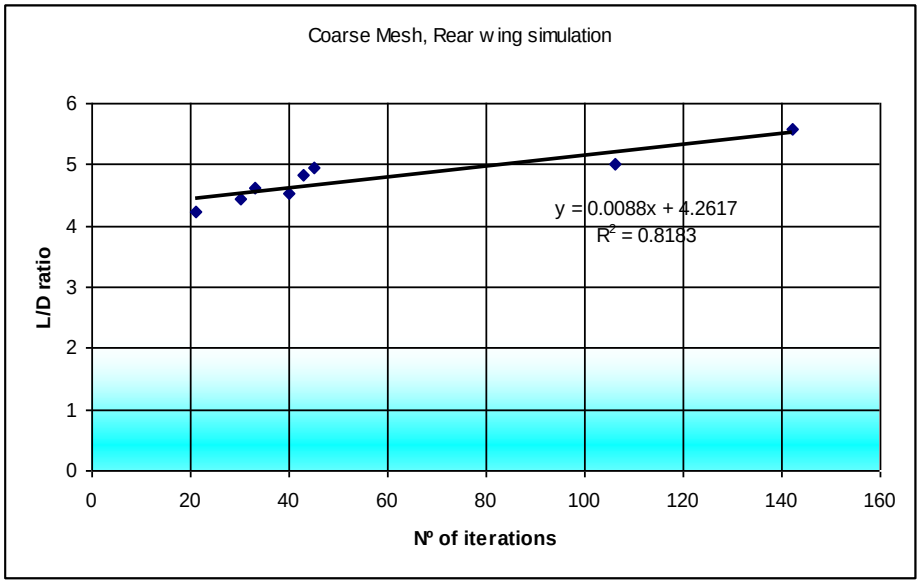

Fig. 2.11- Graph of L/D Ratio Vs number of iterations

The analysis of the rear wing cannot be done with this data, due to a huge dependency on the number of iterations of each simulation (!). There is a trend line on the graph which shows this phenomenon, with a R^2 factor of 0.8183, which can give a strong confidence that this relation really exists.

Analysing the equation of the trend line:

$$y=0.0088x+4.2617$$

So,

Δ10 iterations = 0.088 increase on L/D ratio (!).

Δ100 iterations = 0.88 increase on L/D ratio (!!!).

Notice that this study has been done with a reduced number of iterations compared to automotive industry standards (some thousands depending on each case). However, it shows an important rule of thumb - let the simulation **COMPLETELY** converges before considering it finished. Accuracy in Formula One is a must, and any aerodynamic development must be completely accurate.

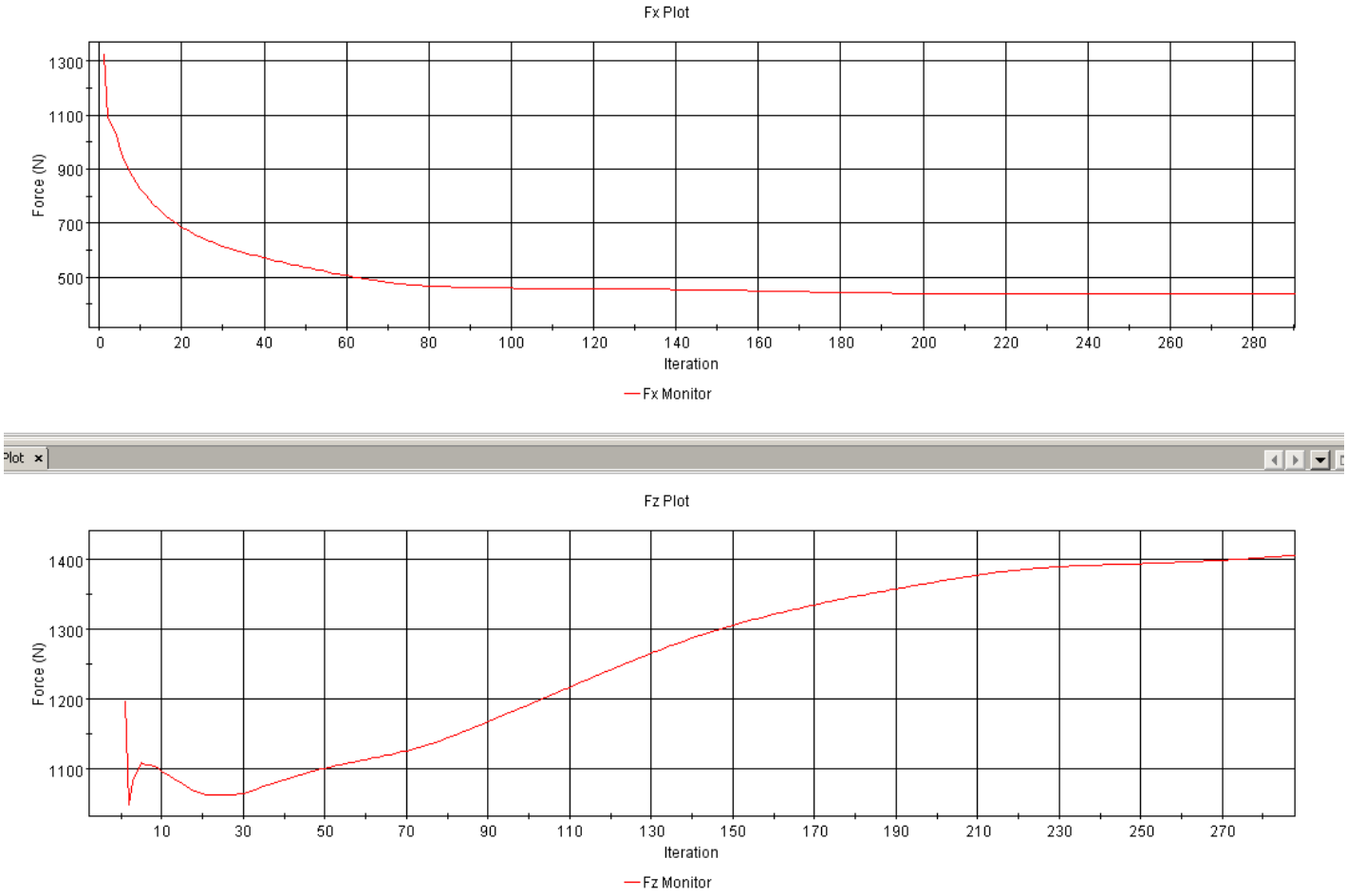

Fig. 2.12 - Evolution of drag (Fx) and downforce (Fz) values – Notice different time to convergence.

The author wanted to share this experience, because being a wrong simulation, it can teach young students an invaluable lesson in CFD. Further analysis in Residual's monitoring plot showed many non-converged simulations. There are two different ways in which a simulation can be considered finished:

1- Completely stable residuals, X,Y,Z Momentum, Continuity, Turbulence Kinetic Energy and Turbulence dissipation rate.

2- Stable simulation with a periodical perturbation, but with exactly the same shape.

If a simulation has not fully converged, it will NOT give the correct values, so the test (usually many hours, or even days in automotive industry) would be wrong. In figures 9 & 10, there is a good example of a converged simulation of type 1 and 2 explained:

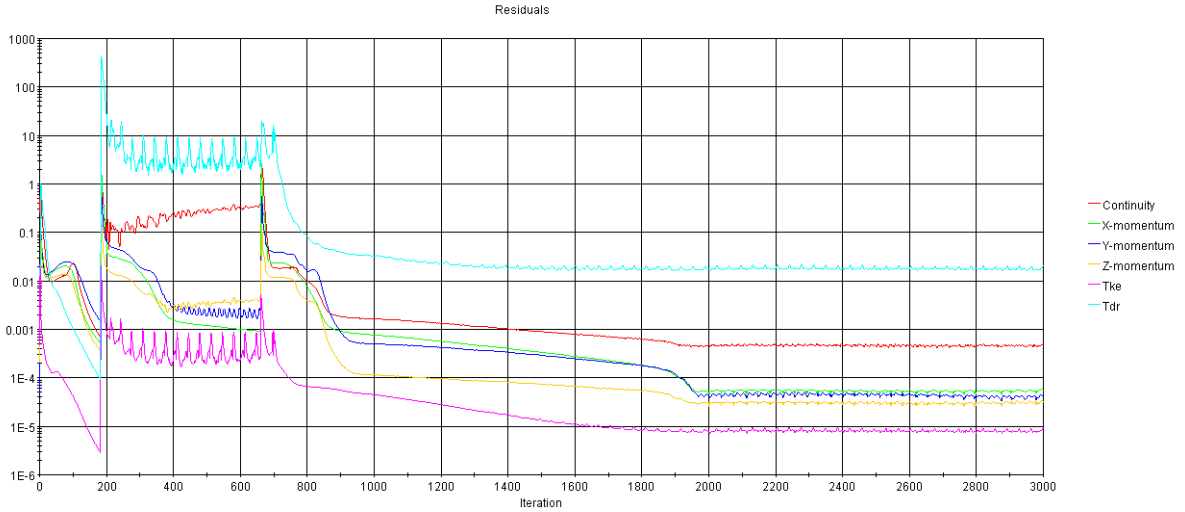

Fig. 2.13- Converged calculation with stable residuals

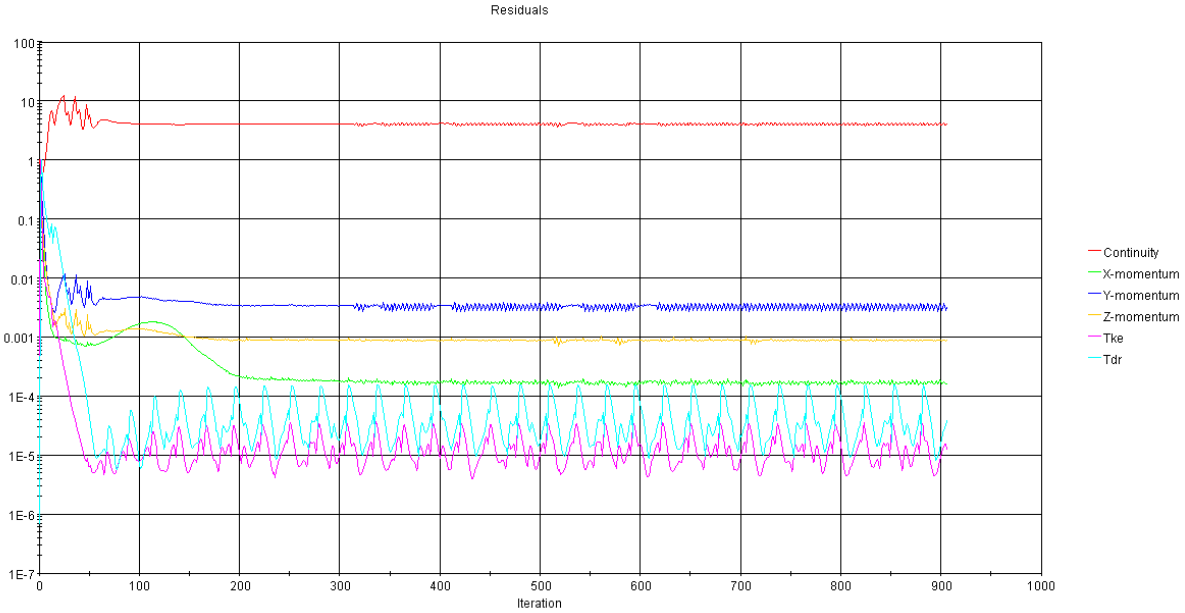

Fig. 2.14- Converged simulation with Tke and Tdr with a periodical perturbation

Looking in detail to the airflow, it is possible to see how the flow is attached on the first iterations of the simulation, but at the end of it, the flow is completely deattached of the flap. In the next figures, the visualization from Star-CCM+ of the complete wind tunnel and a detail of the flap can be seen from the velocity flow field - notice that the picture of the rear wing is upside-down (because the wing profile generated by Javafoil is like the one of an airplane), but it doesn't affect the simulation:

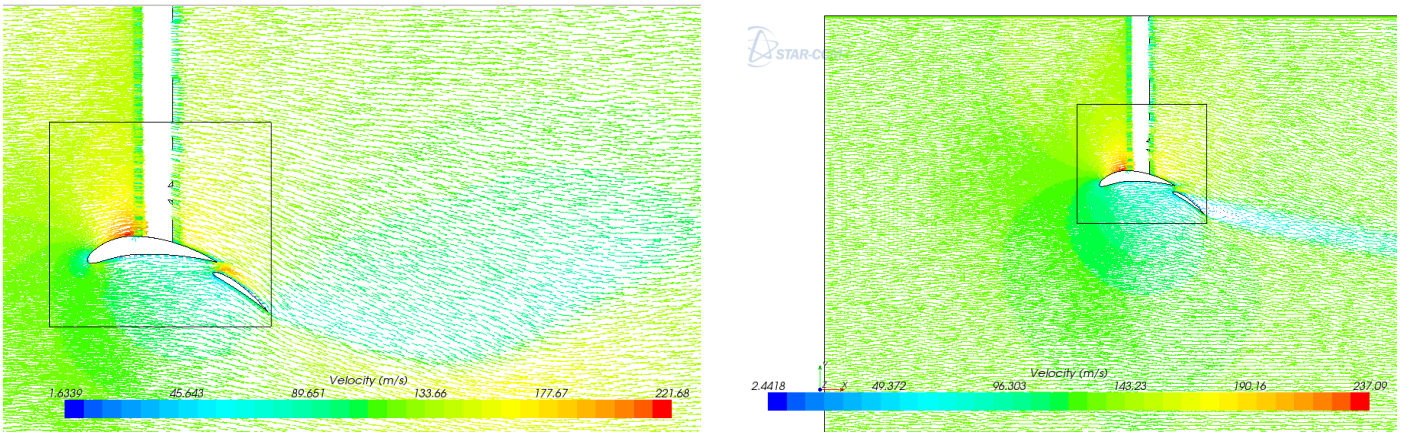

Fig. 2.15- Flow @ 130 m/s. Left side non-converged flow, right side fully converged with 200 it.

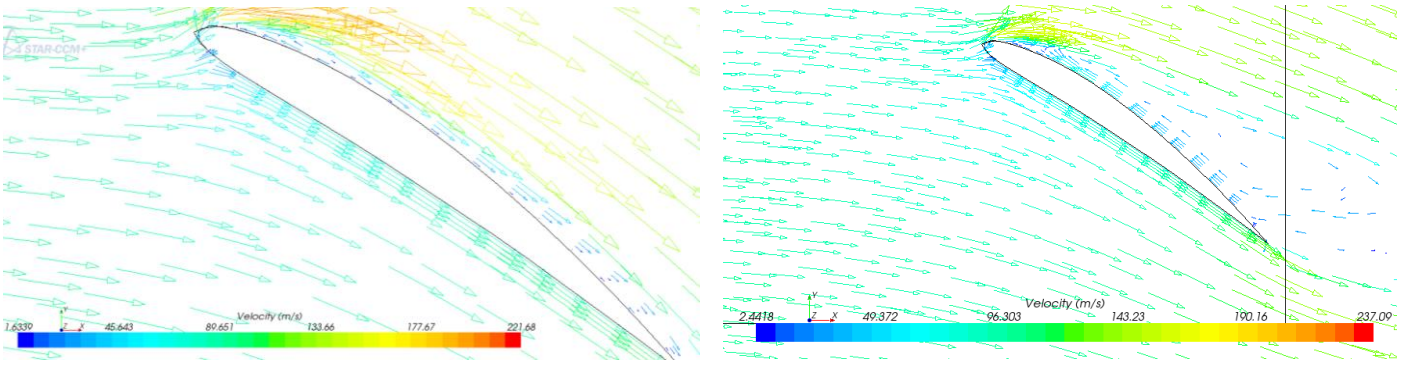

Fig. 2.16 & 2.17- Flow field detail. Notice attached flow with 30 it, but stalled flap with 200 iterations (!).

Taking a look at the pictures, the flap is not working properly - the flow is not attached to the flap, so in aeronautical terms, it is stalled. This means that the wing profile, size, overlapping, gap or angle of attack are not correct, so the full process should be started again from CAD design with CATIA V5. However, as said before, simulations have to be calculated again due to the small number of iterations, to have a perfectly accurate simulation. Star-CCM+ can resume already stopped simulations, which is very useful, as in this first simulations, the speed of processing is 33 iterations/hour with 1 processor (which is not linear with increasing number of processors), so each simulation should run around 200 iterations (or more), which means 6 hours per calculation (!) with this simplified model of around 6 million cells.

Once the correct way to simulate the rear wing has been set up, the only thing left to do is to run again the simulations and to analyse the tables with results. Apart from L/D Ratio, there are also the values of drag (Fx) and lift (Fz).

wind speed (km/h)	(m/s)	L/D ratio	Nº Iterations	Fx (N)	Fz (N)
108	30	5.541055	504	45.67	253.06
144	40	5.571729	652	80.79	450.14
180	50	5.596155	610	125.89	704.5
216	60	5.615274	212	182.32	1018.07
252	70	5.625689	173	246.72	1387.97
360	100	5.666401	200	501.2	2840
468	130	5.680554	233	847.56	4814.61

Table 2.6- L/D Ratio, drag and lift with longer convergence time

The table shows clearly a nearly constant (slightly increasing with speed) L/D Ratio, although slightly low. So the efficiency of the rear wing is not the expected one, probably due to a stalled flap. It should be checked with pictures from the airflow around the rear wing, and especially around the suction side of the flap.

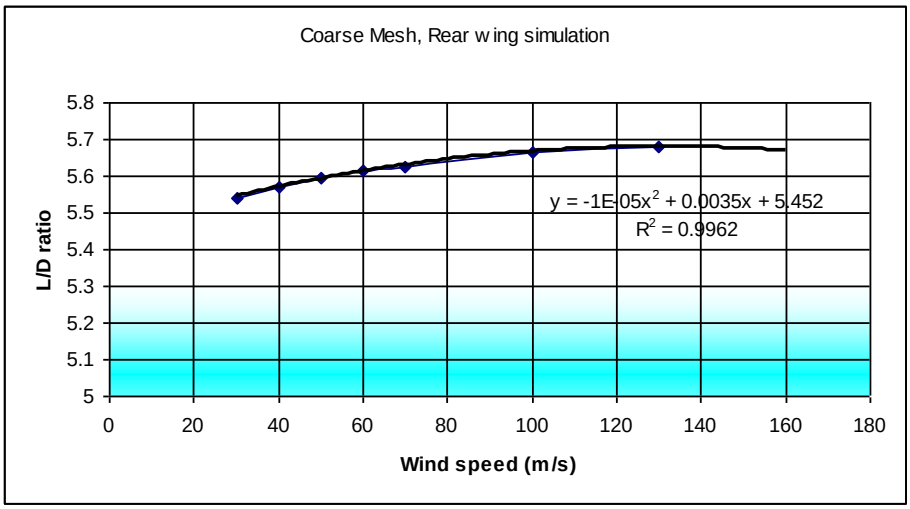

Fig. 2.18- Graph of L/D Ratio Vs wind speed - notice the slight increase with speed, and the R^2 nearly equal to 1 of the 2nd degree polynomial trend line.

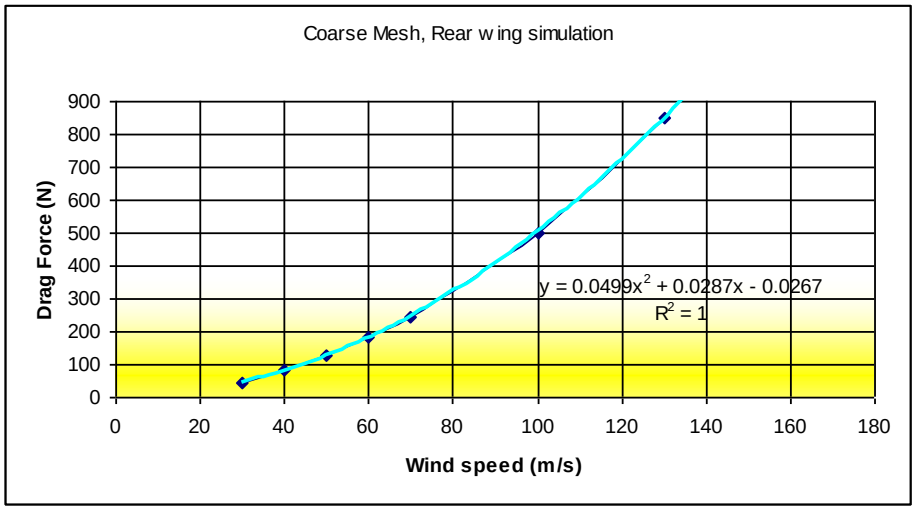

Fig. 2.19- Graph of Drag Force Vs Wind speed - notice R^2 equal to 1 of the 2nd degree polynomial trend line.

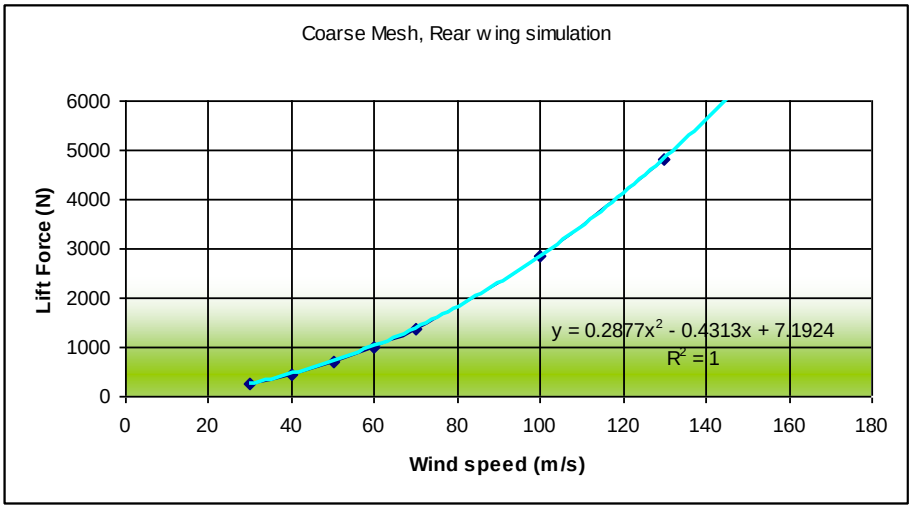

Fig. 2.20- Graph of Lift Force Vs Wind speed - notice R^2 equal to 1 of the 2nd degree polynomial trend line.

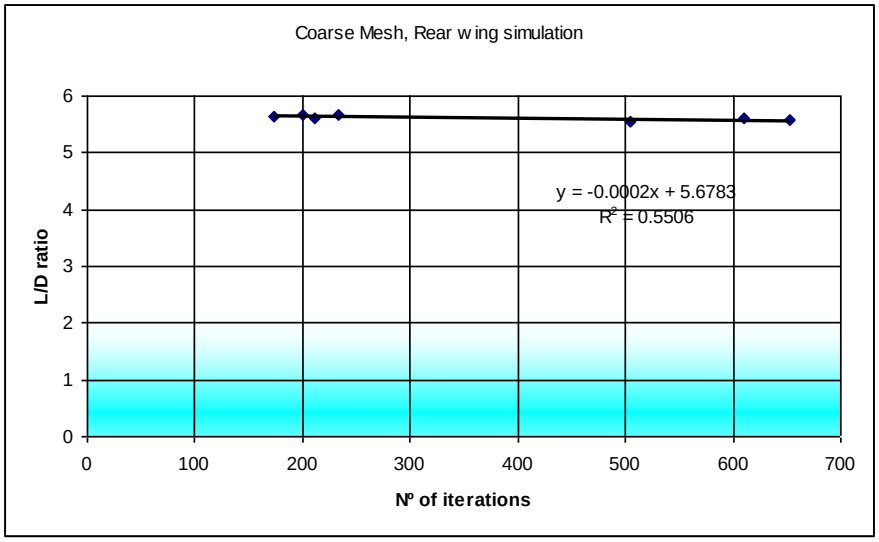

Fig. 2.21- L/D Ratio vs Nº of iterations - Notice that the correlation between iterations and L/D ratio (tendency to increase L/D with iterations) has completely disappeared.

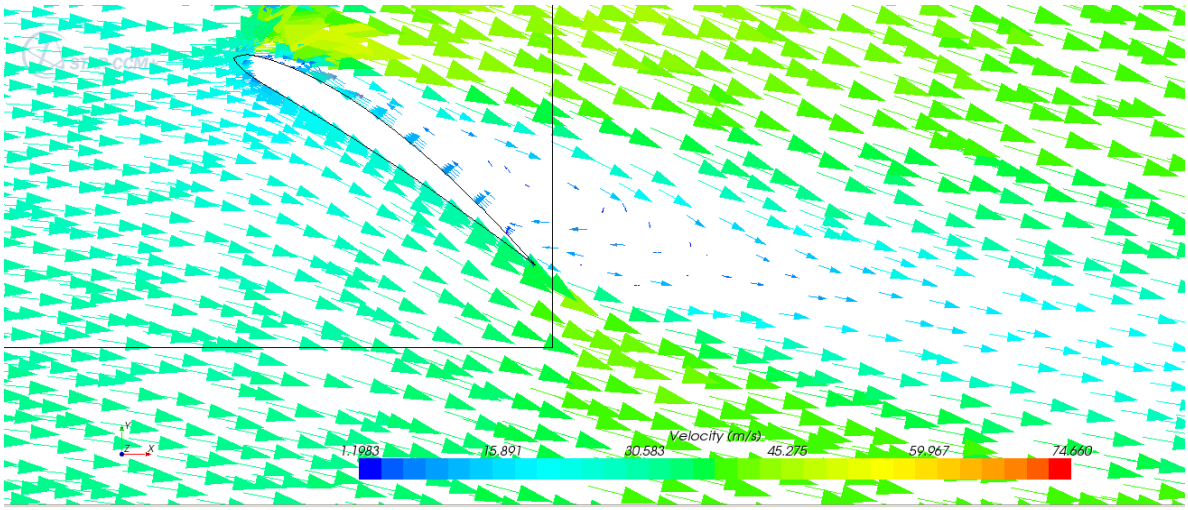

Fig 2.22- Velocity field around the flap stalled. Notice the velocity arrows in the suction surface.

2.2.6- Mesh sensitivity test set up

One of the most important areas in CFD is mesh building. There is always a compromise between the number of cells/size and quality of mesh. More cells will provide a better quality mesh, but the simulation will be slower. Fewer cells will result in a less accurate representation of the real model, and they can even suppose more problems in convergence, but will be faster, something essential when we are talking in days about the simulation time of a full Formula One car.

For the following test, three different wing models will be tested (the geometry has also been changed with a lower angle of attack of the flap to avoid stall). The previous mesh tested was done with

very small cells, but it was not well designed, so the calculation time was very high and the results were not really accurate. So in order to demonstrate the importance of the mesh, we will develop new meshes with smaller base size (which is proportional to file size and speed of calculations), with a new improvement each time. The new tests are:

Nº	Test	Mesh
1	Previous test, stalled flap	Polyhedral, base size 12 mm, 4 prism layers, 1 mm wall thickness
2	Flap corrected, coarse mesh	Polyhedral, base size 15mm, no prism layer used
3	Coarse mesh with boundary layer	Polyhedral, base size 15 mm 7 prism layers, 0.75 mm all thickness
4	Refined mesh, F-1 style	Polyhedral, base size 15 mm, 7 prism layers, 0.75 mm all thickness, leading edge and trailing edge of wing & flap refined with volumetric controls.

Table 2.7- Mesh testing properties

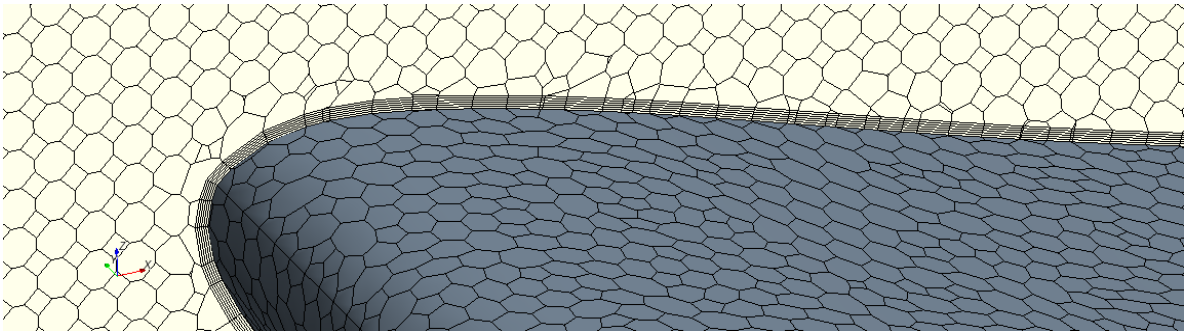

Fig 2.23- Coarse mesh with boundary layer, notice the smaller thickness of the prism layers.

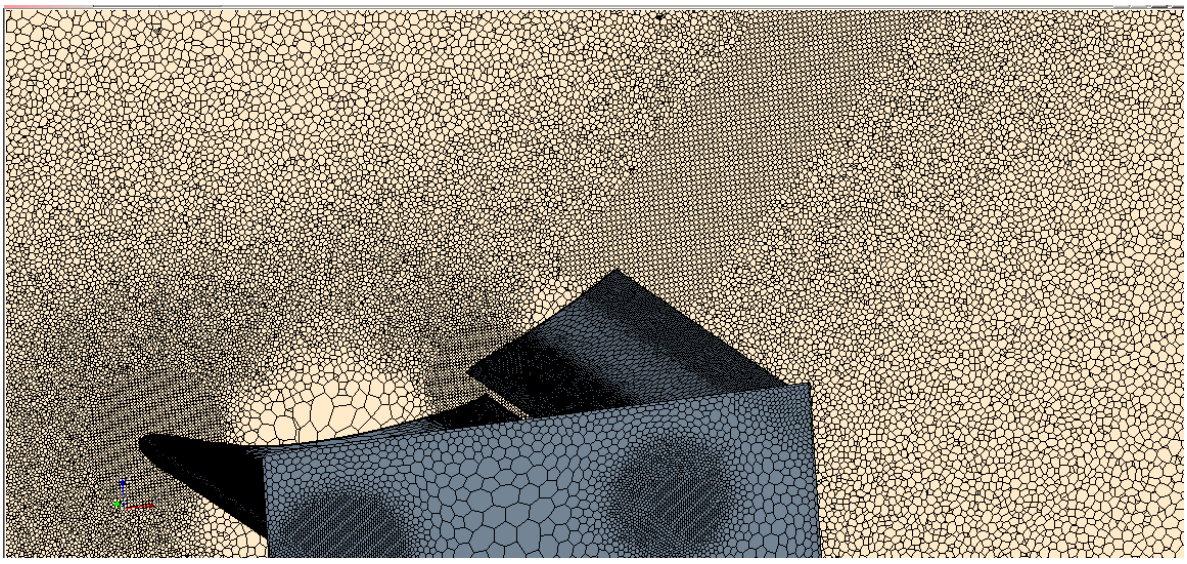

Fig 2.24- Refined mesh, with leading edge (circular) and trailing edge (tilted rectangle) refinement.

With the experience of previous tests, the new experiment will consist in the simulation of the three new models at 5 different speeds, according to a typical range in a Formula One track. The lower speed (108 km/h) is considered the smallest with aerodynamic relevance, and the top speed is the maximum speed achievable in a low downforce track like Monza:

Airflow speed (m/s)	Airflow Speed (km/h)
30	108
40	144
50	180
70	252
100	360

Table 2.8- Airflow test speed in m/s and km/h

In order to avoid convergence problems, all tests will not be stopped until fully converged, so the number of iterations will be around 1000. Partial results will be taken during the tests to check stability of the solution, and could be stopped if the simulation has already converged– never before 500 iterations.

2.2.7- Mesh sensitivity Analysis & Results

As expected, Test2 has a much better L/D ratio than the former simulation, as the flap is no longer in stall, and the rear wing is much more efficient. The tendency of a slight increase in L/D ratio as the speed increases is maintained, having something like a parallel of the former test with the stalled flap. However, a coarse mesh like that, without boundary layer and/or lack of refinement in leading/trailing edge, obtains a value slightly high – probably too much for this wing. This can be due to lack of shear stress caused by the friction due to the boundary layer – in this case, the model doesn't have prism layer to adapt correctly the boundary layer, so real drag would be higher than CFD results. Apart from that, as the mesh has fewer cells, the calculations are quite faster, around 30%.

Test3 with boundary layer improvement shows again a clear parallel downwards of the L/D ratio from the Test2, with an offset about 0.4. This is much closer to the 6.0 approximately expected by this kind of wing. So, the prism layers and the thin wall thickness catch perfectly this boundary layer, and consequently the drag force.

Finally, Test3 is a Formula 1 style mesh, with extra leading and trailing edge refinement. Results from this new mesh are very close to previous test with a refined boundary layer mesh, although some results are slightly different, but we are talking about a maximum difference of 3-4%. This difference could

be also due to small oscillations in the results, as the simulations were stopped as early as possible to cut simulation time.

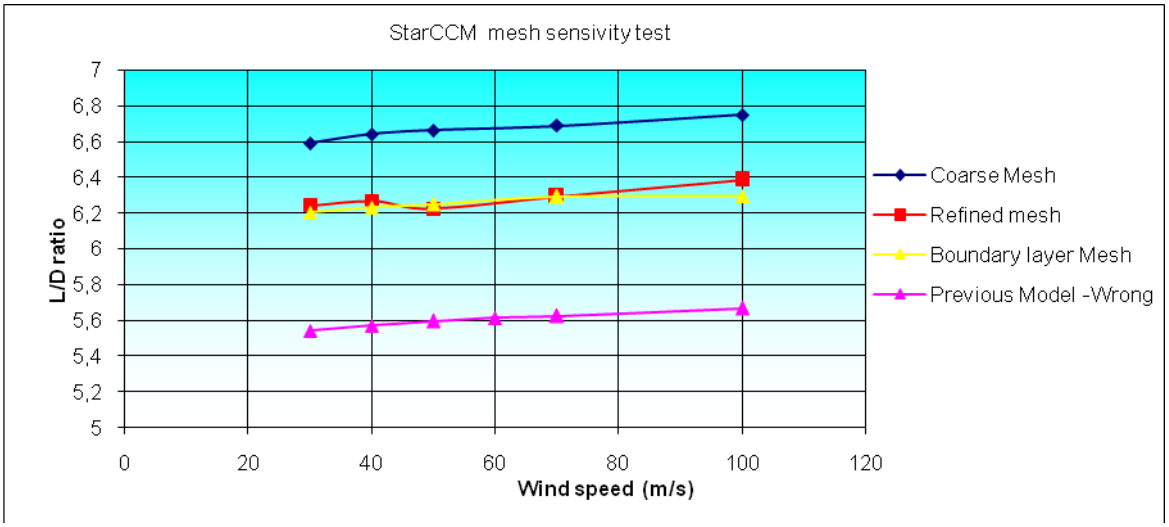

Fig 2.25- Mesh sensitivity study, representative of the influence of the mesh in the final result

PREVIOUS REAR WING MODEL -WRONG -STALLED FLAP				
km/h	wind speed (m/s)	L/D ratio	Fx (N)	Fz (N)
108	30	5,541055	45,67	253,06
144	40	5,571729	80,79	450,14
180	50	5,596155	125,89	704,5
216	60	5,615274	182,32	1018,07
252	70	5,625689	246,72	1387,97
360	100	5,666401	501,2	2840

Table 2.9 - First test, with the flap stalled, quite small mesh base size, but not correctly refined.

COARSE MESH				
km/h	wind speed (m/s)	L/D ratio	Fx (N)	Fz (N)
108	30	6,589532	37,64	248,03
144	40	6,640534	66,71	442,99
180	50	6,663365	104	692,99
252	70	6,688146	203,14	1358,63
360	100	6,748066	413,6	2791

Table 2.10 - Second test, with coarse mesh. Simulation is increased significantly.

INTERMEDIATE MESH, WITH BOUNDARY LAYER REFINEMENT				
km/h	wind speed (m/s)	L/D ratio	Fx (N)	Fz (N)
108	30	6,202742	37,93	235,27
144	40	6,229844	67,35	419,58
180	50	6,250357	105,13	657,1
252	70	6,291222	205,41	1292,28
360	100	6,296259	419,97	2644,24

Table 2.11 - Third test, with a refinement of the previous mesh in the boundary layer.

REFINED F1 STYLE MESH, LEADING AND TRAILING EDGE				
km/h	wind speed (m/s)	L/D ratio	Fx (N)	Fz (N)
108	30	6,243586	38,59	240,94
144	40	6,266589	68,57	429,7
180	50	6,270944	107,55	674,44
252	70	6,291222	205,41	1292,28
360	100	6,383821	424,99	2713,06

Table 2.12 - Fourth test, with leading and trailing edge refinement from previous mesh.

In conclusion, at the light of these results, it is possible to say that the accuracy of the mesh is as important as the geometry chosen, so it is very important to spend enough time to develop a mesh which is able to catch the flow behavior, but with the minimum number of cells to improve simulation time. Like everything in engineering, it is a compromise

2.2.8-Turbulence Models & Settings

In race car aerodynamics, there are three popular turbulence models: K-Epsilon, K-Omega and Spalart-Allmaras. The main characteristics of the models are:

K-Omega: -Two equation model
-Excellent treatment of boundary layers, especially for high adverse pressure-gradients.
-Excellent for external aerodynamics.

epsilon EUSKADI

-More stable variant of k-epsilon.

-Good treatment of separation/wake.

Spalart-Allmaras: -One-equation model

-Faster than k-omega.

-More robust than k-omega.

-Deals well with external aerodynamic flows, especially adverse pressure gradients.

-Smooth transition between laminar and turbulent flow.

-Poor treatment of separation/wake formation when compared with k-omega.

K-Epsilon: -Two equation model

-Standard turbulence model for most industrial flows.

-Poor treatment of strong adverse pressure gradients, particularly with regard to the under-prediction of separation.

-Poor development of boundary layer around leading edges and bluff bodies.

-Capable to deal with less accurate mesh/boundary condition simulations.

There is no perfect turbulence model, they have advantages and disadvantages, and the engineer must choose which one is the best. Some times (as happened in this project), the best turbulence model is not enough, so sometimes the flow must be initialized in K-Epsilon (which is the best one dealing with problematic cases) and then changed to another turbulence model (in this case, K-Omega). Therefore, the best way to decide which model is better for each case, a mixture between CFD stability and wind tunnel correlation must be done. In the Formula One projects for Epsilon Euskadi, the Chief Aerodynamicist decided to use K-Omega for the CFD simulations, so in order to have good correlation with this data, the rear wing development must also be done in K-Omega. Nevertheless, a couple of simulations with Spalart-Allmaras and K-Omega will be compared with the previous test with K-Epsilon to check that differences are very small (in this particular case, so this example cannot be extrapolated to other geometries).

For the three tests, the same conditions are applied. Wind speed is 40 m/s (144 km/h), and the mesh used is the F-1 style mesh, with boundary layer and leading/trailing edge refinement. This kind of simulation needs a lot of resources, apart from a calculation time around 6 hours (with 8 CPUs@ 2 GHz). The number of iterations will vary between cases, but they will not be stopped until fully converged.

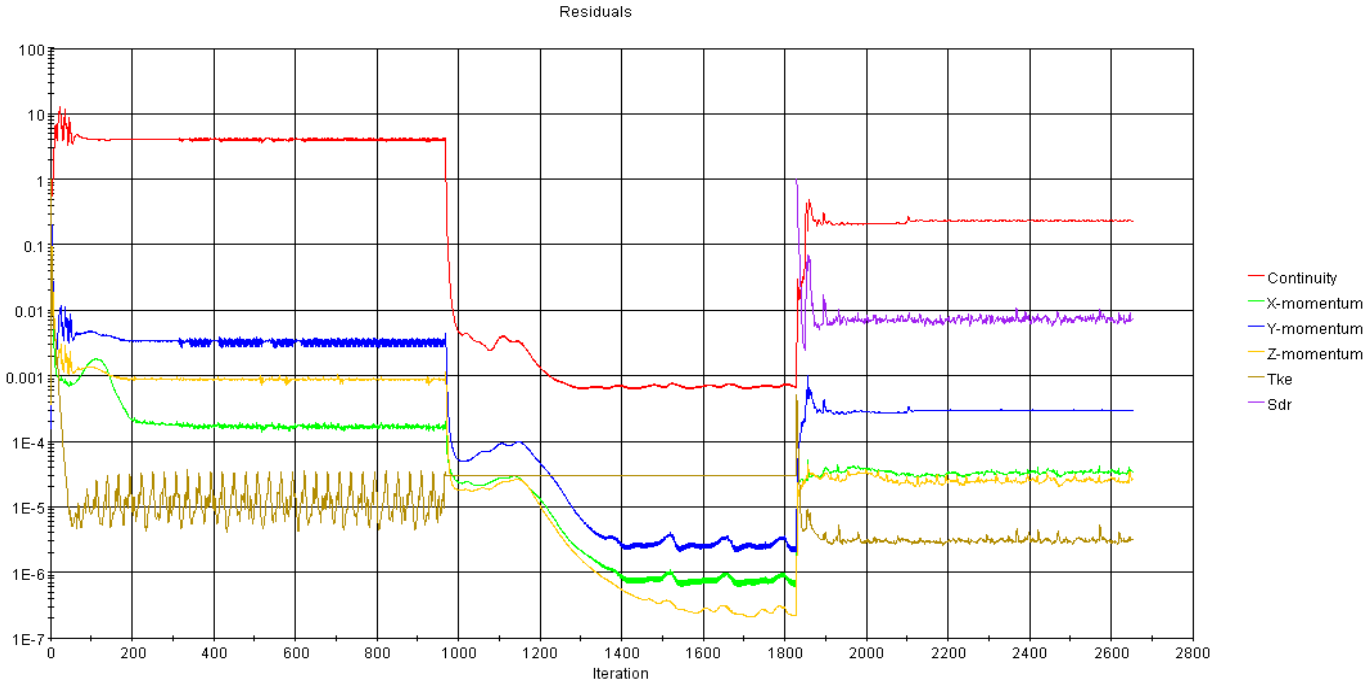

Fig 2.26 - Residuals from the three models. Notice the different behaviors, K-Epsilon (first 950 iterations), Spalart-Allmaras (from 950 to 1830 iterations) and K-Omega (from 1830 to 2650 iterations).

In Fig 2.26, there is a representation of the evolution of the residuals testing the same case. It is not only interesting to know time per iteration, but also the number of iterations needed to converge. K-Epsilon and K-Omega need around 300 iterations, whereas Spalart-Allmaras needs more than 600, although K-Omega number of iterations per hour is slightly smaller.

Turbulence Model	K-Epsilon	Spalart-Allmaras	K-omega
iterations to converge	310	700	320
iterations/hour	40	42	36.4

Table 2.13- Turbulence models convergence time comparison

In Fig 2.27, it is impossible to observe qualitative differences between models, although the measures of drag or lift can be slightly different (following page).

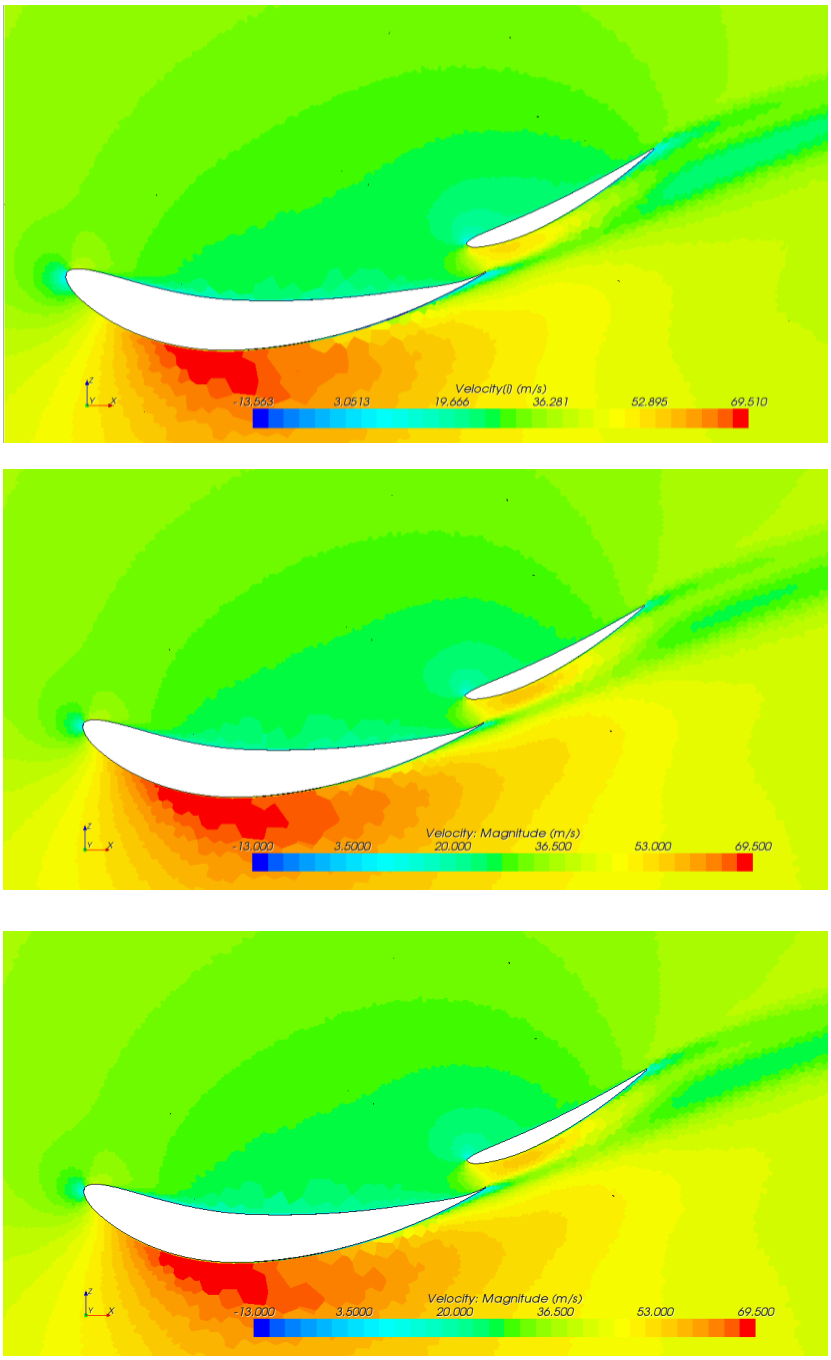

Fig 2.27- K-epsilon (top), Spalart-Allmaras (middle) and K-Omega (bottom) velocity flow field around the rear wing profile, centerline section.

Turbulence Model	Fx	Fz	L/D Ratio
K-Epsilon	68,57	429,7	6,266
K-Omega	68,62	429,8	6,263
Spalart-Allmaras	68,66	437,5	6,371

Table 2.14- Turbulence models output forces comparison

In the table above, Fx (drag) is nearly the same for all the turbulence models. However, Fz (downforce) is very different in the Spalart-Allmaras model. As a result, Spalart-Allmaras has a L/D Ratio of 6,37 quite far from K-Epsilon and K-Omega, which are around 6,26. Nevertheless, the higher time to reach the final solution leaves Spalart-Allmaras behind the other two turbulence models.

However, despite having the same values in this simplified model of a Formula One rear wing, the high precision needed for the optimization implies that K-Omega must be chosen, as it is better for high adverse pressure gradients, although it is slightly slower than K-Epsilon.

2.2.9-CFD software testing conclusions

Despite being like a videogame nowadays, CFD programming is not easy, and should not be used by inexperienced student without the supervision of an engineer. It is a really powerful tool, but the quantity of variables and decisions that must be taken into account (not only geometry, but also mesh quality and turbulence models) will definitely influence the final result. Nevertheless, even if everything is correct, wind tunnel validation is highly recommended before putting any new aerodynamic device on the track, if not mandatory. Currently, in 2010 & 2011 seasons, Virgin Racing F-1 team tries to fully develop its race car without wind tunnel, and they are still not being as competitive as the other teams. This is because CFD software is design to visualize correctly the flow, and to obtain some numbers, but they are not as accurate as the wind tunnel. Improvements in CFD will often be improvements in the real car, but to obtain real force and moment aerodynamic coefficients, wind tunnel is always the reference.

2.3- Optimization software

2.3.1- Introduction to the optimization process

For the improvement of the rear wing, a massive number of simulations should be scheduled. Moreover, new simulations, after studying the results must be decided in order to find the maximum performance. It means that the engineer should use Excel to study the influence between parameters, redesign in Catia V5 the new geometry and then import it and configure the CFD software StarCCM+.
Such a difficult and slow process can be totally automatic thanks to the optimization software Modefrontier, which will be used for the optimization of the rear wing. Consequently, a deep programming should be done to involve all the software without problems. However, the benefits are infinite: the engineer could leave a simulation during the time he is not in the office (at night, on the weekends… even in summer or Christmas) and the software will keep designing, testing, and improving the geometry. The power of this procedure in aerodynamics is absolutely astonishing.

The interface of this software is user-friendly. There is no need of thousands of lines of code to give him orders. Nevertheless, the communication between software, the quantity of actions involved, and the prevention of any error is a hard work to do.

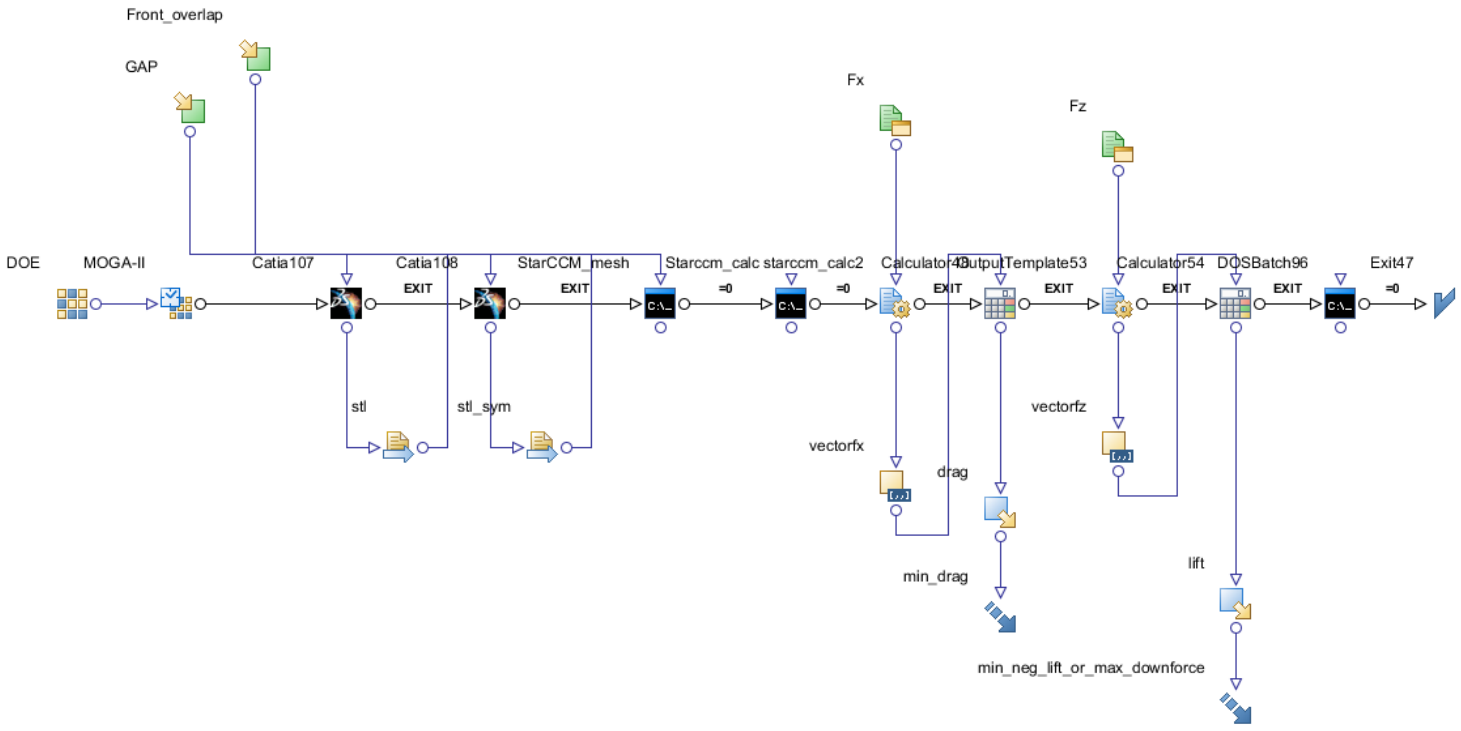

Fig 2.28 - Diagram of optimization for the Formula One Rear Wing with Modefrontier. Notice that the name of each node is on its upper left corner.

The software works with nodes (the small boxes with icons). This diagram is representative of the work being done with the rear wing, as it only requires small changes or modifications. In this example, Modefrontier modifies the main wing and flap positions, in the x direction (forward or rearward) and the z direction (up and down). The objectives are to minimize drag and maximize downforce (or minimize negative lift, as it is happening in the diagram).

Node Description:

DOE: Design Of Experiment, decides how many simulations are necessary to map the parameters, and also the values of this parameters to achieve a correct representation of the whole range. The most used are SOBOL and Random algorithms.

MOGA-II: Multi-Objective, Genetic Algorithm, is the node where the DOE results are evaluated in order to decide which new cases will be evaluated in order to maximize or minimize the variables chosen.

GAP/Front_overlap: Input variables, are variables defined by a central value, range and step.

Catia107/Catia106 nodes: they open a Part in Catia, modify them (and/or execute a macro if necessary). These nodes are totally integrated with Catia, and it is possible to keep it open to see what is happening during the modification. Geometrical modification should be done through parameters introduced previously in CATIA.

Stl/stl_sym: Transfer files, these are actions which links one software with another. In this case, Catia exports a file (in any format, in this case a .stl) to deliver it to StarCCM+.

StarCCM_mesh/StarCCMcalc: DOS nodes, they are NOT integrated. In this kind of files, the user has to program some lines like in the DOS operative system. It is useful to copy or delete files, and to execute non-integrated programs, like StarCCM+. The user can write the name of the software, the file which wants to open, macros (if used) and number of CPUs used.

Fx/Fz: Support files, they are .tab files which are exported by StarCCM+ externally. They contain the results of forces of the CFD simulation.

StarCCM_calc2//OutputTemplate53: They process support files, and tabulate them in a way that Modefrontier is capable to understand.

Vectorfx/vectorfz: Vector buffers, they get the data from the Output templates and convert them into a vector.

Calculators: They do mathematic operations with the variables, from sums to find maximums of standard deviations.

Drag/Lift: Output variables, they are numbers registered by Modefrontier to calculate objectives.

Min_drag/min_neg_lift_or_max_drag: Objectives, which consists in “Minimize” or “Maximize” an output variable.

DOSBatch96: Last DOS node, the same as StarCCM+ nodes, but this is to erase previously created files, to avoid repeating tests, or overwriting errors.

Exit 47: Termination process signal.

Names and numbers of each node are only to help the designer to understand processes are they doing. Double-clicking on them, a dialog box appears to configure it. They are very useful and user-friendly. However, one single mistake in any of them, and the simulation will not give the desired results. Or even worse, it will give wrong results which the user will not realize. Therefore, checklists are created to help the user not to make any mistakes, although it is highly unlikely to run for first time without errors.

This diagram represents a two step design/two step CFD simulation. There are two Catia nodes because it is needed to modify two CatParts, the Rear Wing and the Symmetry plane at the same time, to avoid non-manifold problems. The two DOS nodes (StarCCM+ process internally) are divided like this in order to mesh the geometry with 1 processor (because meshing with multi-processing techniques is still not available in the market), save the file to have a backup copy, and then calculate the CFD with 8 processors (the maximum of the computer). When the profile of the wing is also changed, two extra Excel nodes are included, which are modified by the Input variables, and returns its values to the Catia nodes.

The support files are tables with the lasts 500 iterations of the CFD calculation. They are not linked as “Transfer Files” from the DOS node because they are created externally by StarCCM+, thanks to a Macro programmed in Java to set up un run the simulation automatically.

Apart from this, the loop created in Modefrontier will need some macros to be programmed. Only Catia (and some other) software is integrated, so it will be necessary to create macros (for StarCCM+, Excel) to do the same operations as a user would do. And files must be ready in a directory specified in the nodes, and permissions for Catia/Excel/StarCCM+/etc. must be activated. To sum up, the whole set up of the loop is quite difficult and must be thoroughly done. However, once it is programmed correctly, the computer becomes a super-fast aerodynamicist, which will not do any mistakes.

To control all the process while calculating, there is a full menu when everything is logged, and the user can have real-time access.

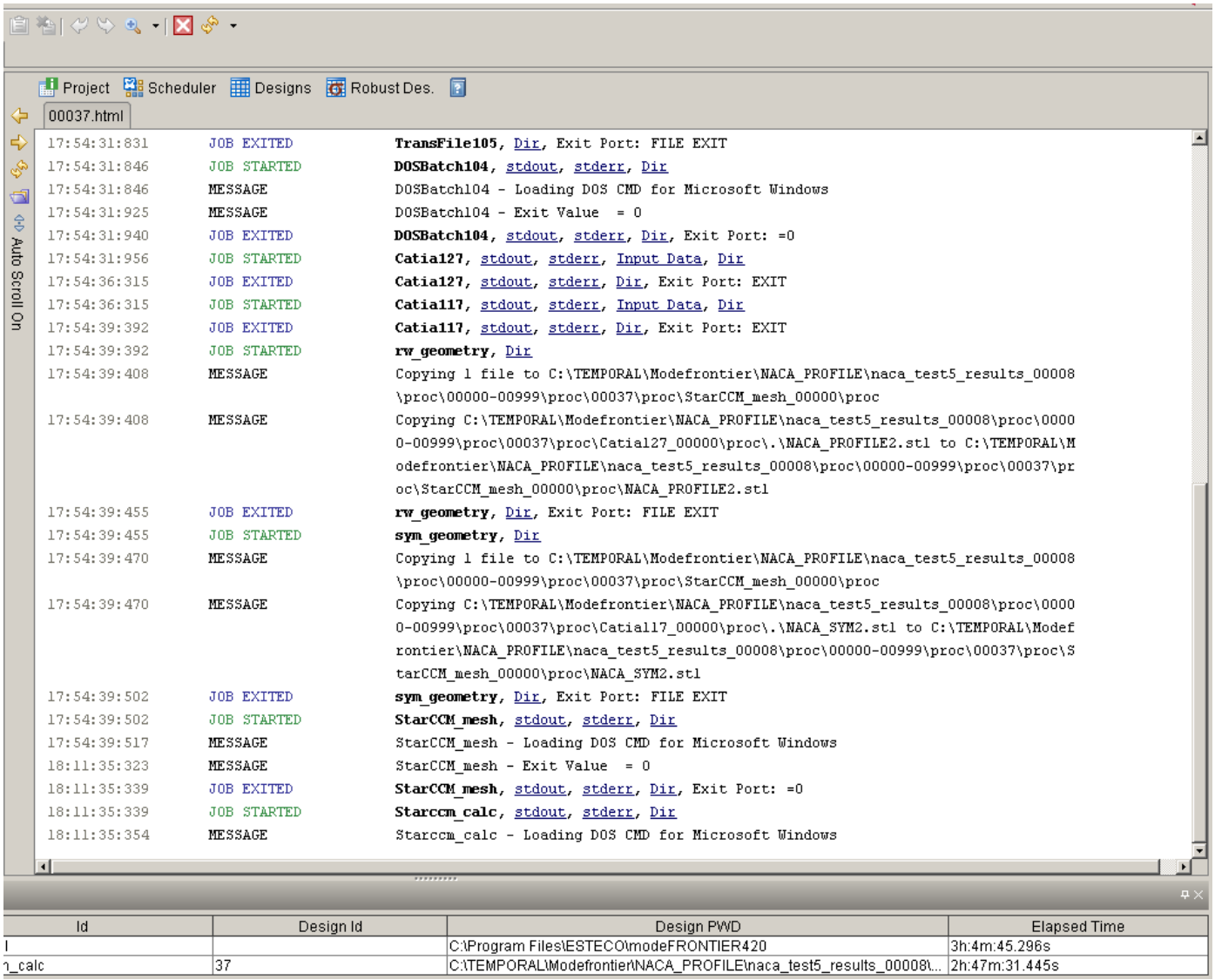

Fig 2.29- Real-time logging of a simulation in Modefrontier

2.3.2- Design Of Experiments algorithms

A design of experiments (DOE) algorithm is used to create a database of design configurations efficiently. DOE algorithms are used for the three following reasons:

-To get the **most relevant qualitative data**, with the **smallest possible number of experiments**.
-To create a database for a **response surface.**
-To create a **starting population** for optimization algorithms.

It is not difficult to imagine a simple problem, with a couple of variables, and with a hundred of different configurations. If each simulation is 1 one minute long, in a few minutes it is possible to obtain the optimum. However, in CFD engineering, simulations are more likely to run for a few hours. Then, if a project faces 20 variables with thousands of different configurations, it is clear than the key is to minimize the number of experiments to maximize performance. DOE Algorithms are in charge of selecting as few configurations as possible, avoiding correlation between input variables in order to obtain a representative population of the whole range.

In this project, the two DOE algorithms (space fillers) used are SOBOL and RANDOM. For a 2 variable problem, the representation of its behavior is the following:

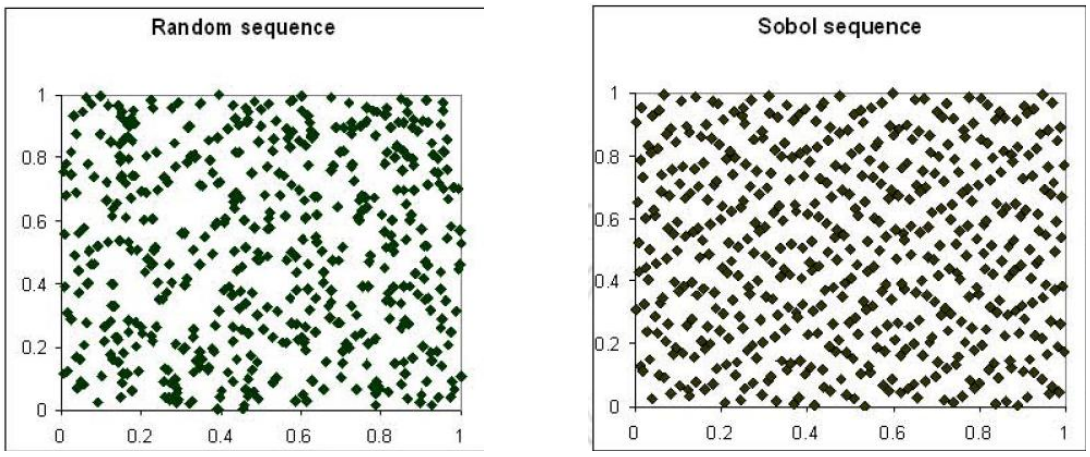

Fig 2.30 – RANDOM and SOBOL space filler algorithms **[3]**.

It is quite obvious that SOBOL covers the domain better, or more uniformly. However, for small sampling, sometimes RANDOM is slightly better. Moreover, depending on the optimization process (for instance using SIMPLEX), SOBOL is not recommended due to “diagonal” clusters (rhombus distributions can be seen looking thoroughly). As a result, both are used along the project.

2.3.3- Optimization process

There are some Multi-Objective algorithms which can be used in ModeFrontier. First of all, an aerodynamic optimization is always multi-objective, no matter if the optimization is considering drag, lift, downforce, lift to drag ratio, aerodynamic coefficients… there will always be a force in the vertical axis (downforce) and a consequence in horizontal axis (drag). However, depending on the criteria of optimization, two variables will be considered to discuss the best design. In the case of a Formula One rear wing, the objective is to achieve a certain level of downforce, enough to heat up tires and to achieve a cornering speed, decided by the chief aerodynamicist. Consequently, the main objective is downforce. However, it is not free, and the more the downforce, the higher the drag. Therefore, for a given target (for instance, 300 kg of load at "x" m/s), the second objective is to maximize is the efficiency, or "lift to drag ratio".

Once the optimization objectives are clear, the selection of the "optimal", or the best rear wing should be discussed. The optimization may find values which doesn't improve L/D ratio, but better in downforce. Therefore, two methods can be used to select the best design: mathematical or graphical approach.

- Mathematical approach: Weighing system – It consists in giving a value or percentage (weight) to each target (downforce and lift to drag ratio). Then, the optimization is:

$$\text{Max}\ (v\% \cdot \text{downforce} + w\% \cdot \text{lift\_to\_drag})$$

- Graphical approach: Pareto frontier – It is based on the graphical representation of two different outputs in an XY diagram. The pareto frontier is clearly visible, and is better as the number of experiments is increased. The optimization consists in finding new configurations outside the pareto frontier, thus modifying it.

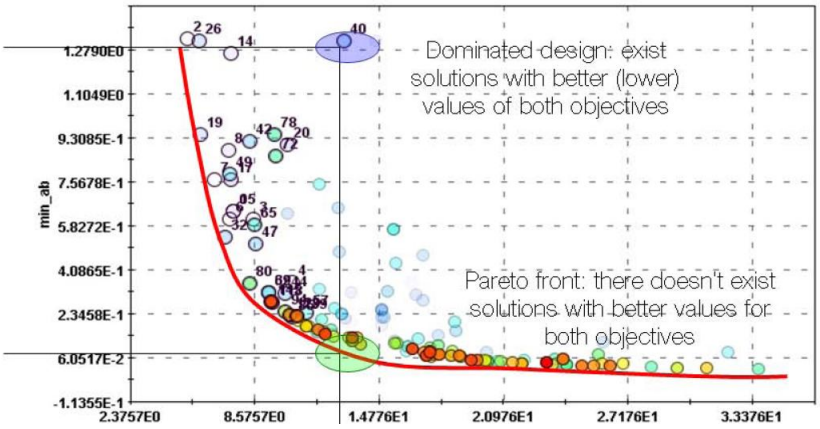

Fig 2.31- Example of Pareto Frontier (in red) **[3]**.

Both systems are valid if used properly. However, the mathematical approach is very sensitive to the “weight” assigned to each variable – and of course, should be chosen by an experienced aerodynamicist. It is very difficult to understand what is happening with the optimization, and it can also dismiss better solutions if the variable with less “weight” is improving a lot while the variable which weighs more is decreasing slightly. In contrast, the graphical approach with Pareto Frontier is a way better, as it shows all configurations which have surpassed the frontier. That is why in this project, the best configuration (or the one with more potential) will be chosen with the Pareto Frontier.

2.3.4 – Optimization algorithms

As explained before, the simulation will set a number of cases to represent the whole range of all variables, minimizing correlation between them, and then it will map the results to find the Pareto Frontier. But after finishing it, the computer has to make some decisions to calculate the new configurations to attempt to surpass the Pareto Frontier. That is when the optimization algorithms start to work.

Multi-Objective optimization algorithms are highly complex, and specially designed to work with hundreds or thousands of experiments. Therefore, their parameters remained unmodified.

-**DNA strings mutation ratios** show the ratio of parameters modified randomly/total number of parameters to avoid premature convergence;

-Directional cross-over is to configure different paths or directions to find optimums;

-Generations number is the quantity of times that the process of finding an optimal will be repeated.

And many other parameters can be changed. However, software developers highly recommend avoiding algorithm modification. This topic could perfectly be another totally different investigation project, so this project will not go into details about this.

Three different algorithms are used depending on the targets:

-MOGA-II (Multi-Objective Genetic Algorithm) – The standard one, which rapidly reaches the Pareto Frontier. The best solution is to leave default configuration, but it doesn’t work with continuous variables.

-NSGA-II (Non-dominated Sorting Genetic Algorithm) – A fast an elitist multi-objective algorithm. It is more advanced than MOGA-II (so more difficult to set up), but it can work with continuous variables.

-MACK (Multivariate Adaptive Crossvalidating Kriging) – It always samples the design space where the interpolation is less accurate. Used especially when the designer wants to explore the design space more than finding the optimum – Response Surface Method (Kriging), explained in the next chapter.

2.3.5- Response Surface Methodology

It is a statistical process to explore the relationship between several variables and one or more response variables. In this project, the statistical model for the RSM will be ordinary “Kriging”, which is the model to build a 3D surface. Therefore, Kriging will build an output surface with the 2 variables chosen (X and Y coordinate), and the Z coordinate will be the result expected (Drag, Downforce, Lift to Drag Ratio…), no matter how many variables have we used in the experiment. However, the more variables used, the more the “noise”, so the accuracy will diminish. It is an excellent way to find an “optimum” visually, after exploring the design space. Kriging is based in geostatistical techniques to interpolate values, so the typical graph presented is like a 2D topographical map with many colors, or the surface 3D with the contour lines drawn on top of it.

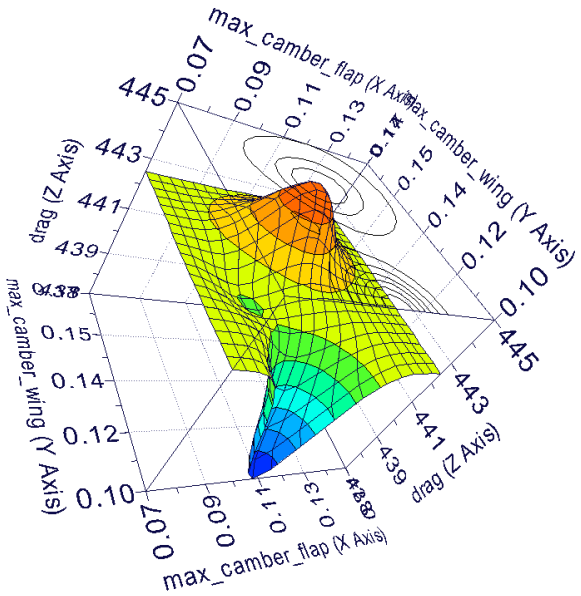

Fig 2.32- Typical Kriging 3D surface with the contour lines on top

2.4- CAD Parametric Design

2.4.1- Main plane and flap profiles parametric design

One of the most important parts of the project consists in the parametric design and its potential to be developed. Some parts of the car, like the endplates, are difficult to be designed with a parametric model, and the potential of it is not very high, nor the tenths of a second that is possible to gain improving it. Airflow visualization is necessary to constantly improve the shape, louvers, and cuttings. On the contrary, any wing profile is extremely sensitive to any change on its shape, and the visualization of the flow can improve its development, but in advanced stages of design. At first, it is very important to run a series of loops with different parameters, and when the best 2D profile is achieved, then some graphical tools are very useful to design the 3D shape, specially pressure contours, streamlines and “Oil flow” (it is like the wind tunnel tests, where the rear wing is painted with colored liquid), exactly the same as in the picture below of the RenaultF1.

Fig 2.33 - Typical “Oil flow” experiment during Abu Dhabi tests, RenaultF1 Team **[4]**, November 2010.

Before starting the loop, a number of parameters must be chosen, in order to set the number of loops and the number of experiments in each loop, to obtain a Master Plan and define

a date to deliver the final results. As any new project, different models were designed before starting the loop to evaluate its potential and time to be developed.

Main Plane and Flap profile – NACA 4-Digit adaptation

The NACA 4-Digit profile is very easy to control, as it is driven by 3 parameters:

-Camber (% Chord)

-X position of maximum camber (in tenths of chord)

-Thickness (% Chord)

Camber is the first digit, x position of maximum camber is the second digit, and thickness the last 2 digits. For example, a NACA 1212 is a wing profile with 1% of camber, with its maximum camber located at 20% of chord from the leading edge, with a thickness of 12% the chord length. However, in this project an Excel file is used to modify each parameter without any restriction (that is, with as many decimals as needed), with the equations already implemented. The Excel file is linked with CATIA with a Design Table, which is automatically updated. CATIA imports a cloud of points, which are automatically joined by two splines, obtaining the upper and lower surface of the wing or flap.

Finally, NACA 4-Digit adaptation requires a small adaptation for the main wing and flap. The trailing edge ends with a very thin trailing edge, but for a real model it has to be 1 mm thick due to composites department petition, so a small modification is made for the main plane. Moreover, the flap has a “gurney flap” which is implemented in the NACA profile, perpendicular to the lower surface end.

To sum up, it is a simple model, which creates very natural profiles, universally accepted in airfoil design, and extremely easy to configure with only 3 parameters.

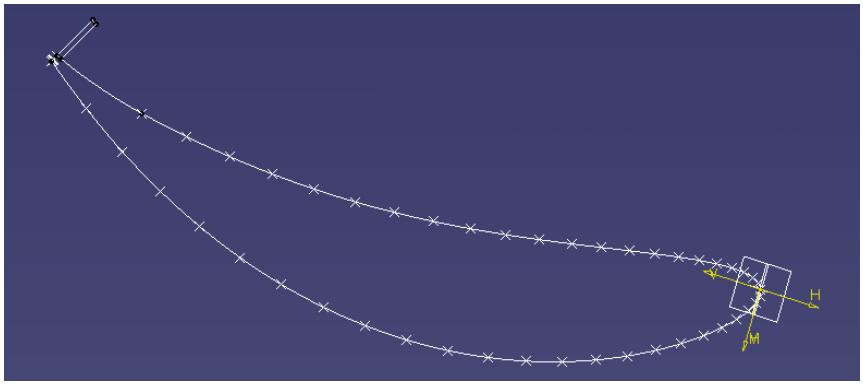

Fig 2.34- Wing profile generated in CATIA with a cloud of points imported from an Excel file.

Main Plane and Flap profile – Tangency-based design

Another design 100% integrated in CATIA was developed to have a higher number of variables, to have more control of the airfoil profile, thus having much more room for improvement, and more potential of development. This design consists in three splines, the upper & lower surface plus the camberline. The leading edge is generated with a circle of controlled radius, and the upper & lower surfaces are both controlled by a few points, and tangency tensions. The final list of used parameters is:

-X position of maximum camber

-Camber Maximum

-X position of maximum thickness

-Maximum thickness

-Profile Chord

-Leading edge circle radius

-Upper & lower tangency radius (contact point of the upper % lower splines with the leading edge circle).

-Upper & lower tangency tension (tension with the contact point of the leading edge circle).

-Tension 1,2 – Tangency tensions with intermediate control points of the upper spline.

-Tension 4,5 – Tangency tensions with intermediate control points of the lower spline.

-Tension 3 – Tangency tension of the camberline unique control point.

-Upper & Lower tangency end tension (trailing edge tangency tensions).

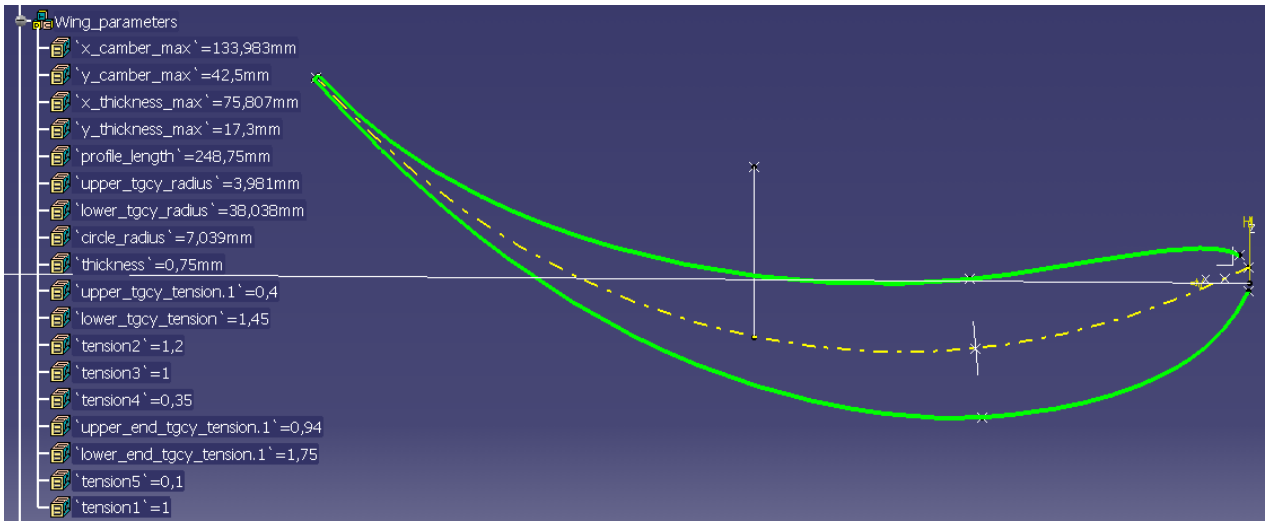

Fig 2.35 – CATIA integrated design of a parametric airfoil.

The total number of parameters controlled by a single wing profile is 17. But as the rear wing is formed by a main plane plus a flap, the number has to be multiplied by two. Moreover, some parameters like angle of attack, gap, overlap and others should also have to be taken into account, so the total number of parameters is close to 40 parameters. This obviously gives to the designer a better control of the rear wing, but an optimization with so many parameters would take twice time at least than the NACA based design. So finally, **despite having much more potential, for timetable issues, the chosen design for the optimization is the NACA 4-Digit adaptation**.

Positioning Parameters

Apart from the aforementioned profile parameters, the rear wing has a small regulation box, were a main plane and flap (with gurney) has to be fitted inside. This means that some extra parameters should be used for the positioning of both airfoils into the box:

-Gap: Minimum distance between main wing and flap. It is mandatory to be 15 mm or higher. If both wing and flap are well designed, it is the distance between the trailing edge of the main plane and the bottom surface of the flap. By well designed, it is understood that the overlapping zone where the air flows between the flap and the main wing should be convex, in order to accelerate the flow field in that zone, as it can be seen in the picture below.

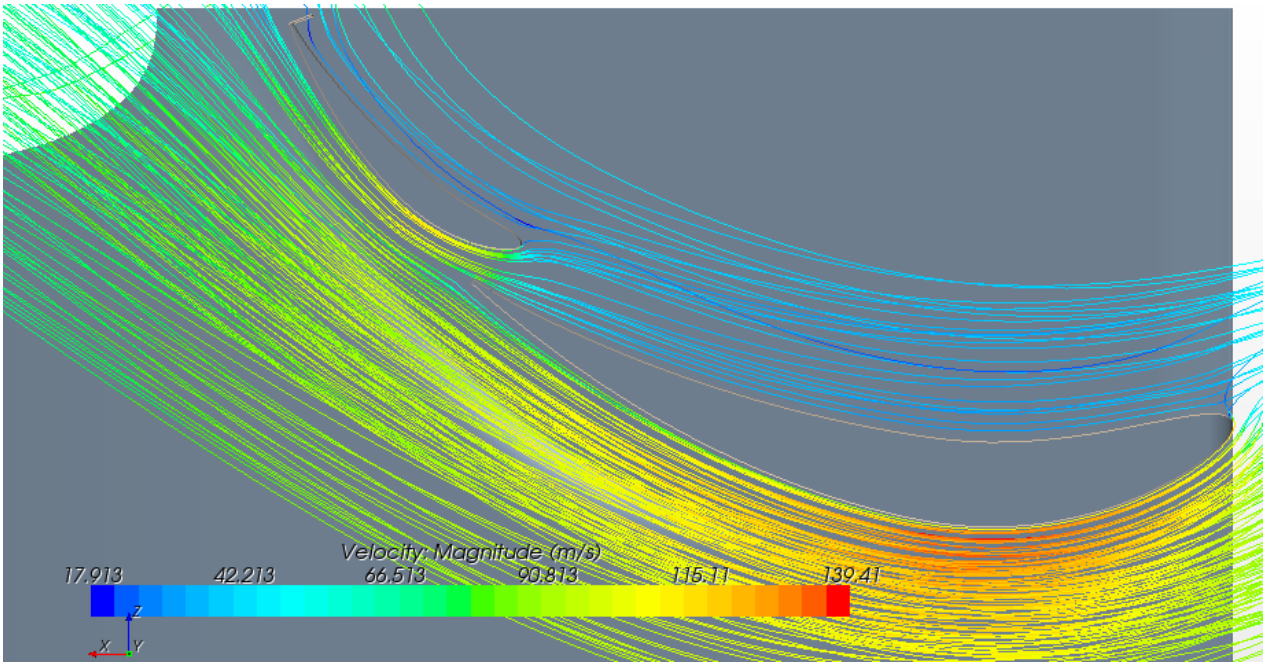

Fig 2.36 - Velocity streamlines, notice airflow acceleration in the main plane/flap overlapping area.

-Overlap: It is the distance between the most forward point of the flap and the trailing edge of the main wing on the horizontal plane. There are no restrictions on this parameter.

-Angle of Attack: It is the angle of the wings compared with the X axis of the car. As the design is totally controlled, it is only possible to control the angle of the flap, and the main wing angle is a result of all the other parameters and restrictions.

-Horizontal and Vertical position of the Main Plane: The main plane will always be situated in the bottom front corner. Depending on the track, the horizontal and vertical position can vary. For instance, in Monza, where maximum speed is required, the whole regulation box is not used, and the main plane is moved upwards and backwards. However, in the medium downforce tracks (more than 60 % of the championship) and for the high downforce tracks, the whole regulation box is used. Moreover, the bigger the main plane, the more the downforce that it will generate. Therefore, X and Y positions will be fixed with tangencies, that is, the most forward point of the main plane will be tangent to the regulation box, and the lowest point of the lower surface as well.

-Horizontal and Vertical position of the flap: It is always positioned depending on the trailing edge of the main plane, so the leading edge is positioned with the main plane. However, the trailing edge is positioned tangent to the most rearward part of the regulation box, to have the maximum chord possible. The same happens with the top of the regulation box, but as the "gurney" can be changed, a little margin of 6.5 mm is left from the top of the regulation box. Only the trailing edge of the flap is fixed during the whole process of optimization.

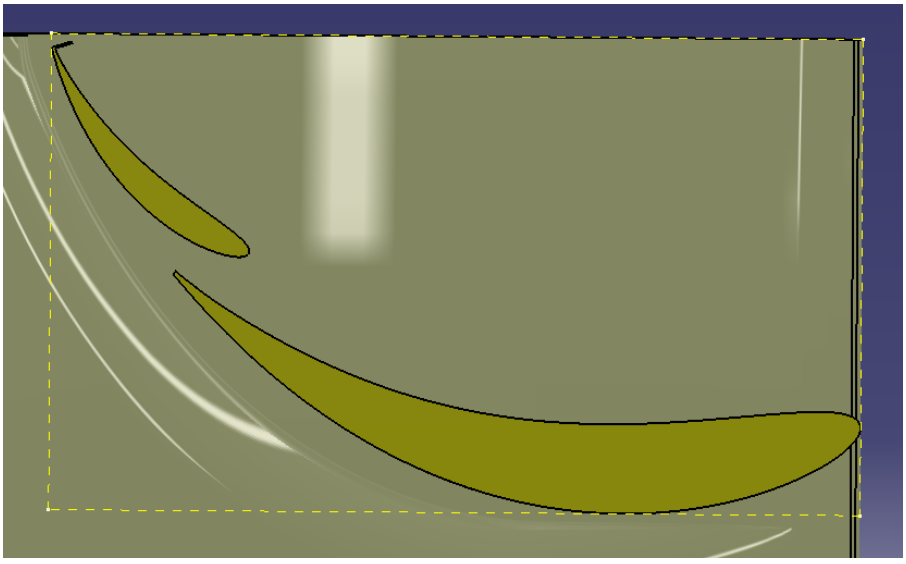

Fig 2.37 – Main plane and flap inside regulation box. Notice car longitudinal axis inclination of 0.407º.

2.4.2- Main Plane and Flap 3D parametric design

Once the optimization of the rear wing profile has been done, it is time to start modifying the 3D shape. In fact, the overall process is a 2D wing + flap design, run into a 3D CFD environment. So the best rear wing achieved is the one which is working better along the full span of the wing. However, due to the flow interaction with the bodywork (front wing, wheels, engine cover…), the direction of the air is not straight, so the optimum solution is far from being a simple straight extrusion of a single profile (actually, even for a simple, straight flow the best wing profile may not be a straight extrusion of a 2D profile).

To understand what is the wing demanding, graphical post-processing of the CFD simulations must be done. Here is where CFD unlocks all its potential, although not being capable to give close-to-reality force values, it is very accurate and powerful talking about flow visualization. In this situation, a post-processing method similar to the wind tunnel “oil flow” (like Fig. 2.54 at the beginning of this chapter) will be used to study the wing and flap profiles, called “constrained streamline”. This method shows the streamlines attached to the rear wing, showing the trajectory on the surface. It is very important to evaluate the stagnation point position on the leading edge zone (re-shaping the wing to put the leading edge closer to the stagnation point will reduce drag). Moreover, the streamlines of the lower pressure surface of both main plane and flap are very important to observe if the flow is detached from the surface, which indicates that the wing is stalled (which is destroying downforce and increasing drag as well).

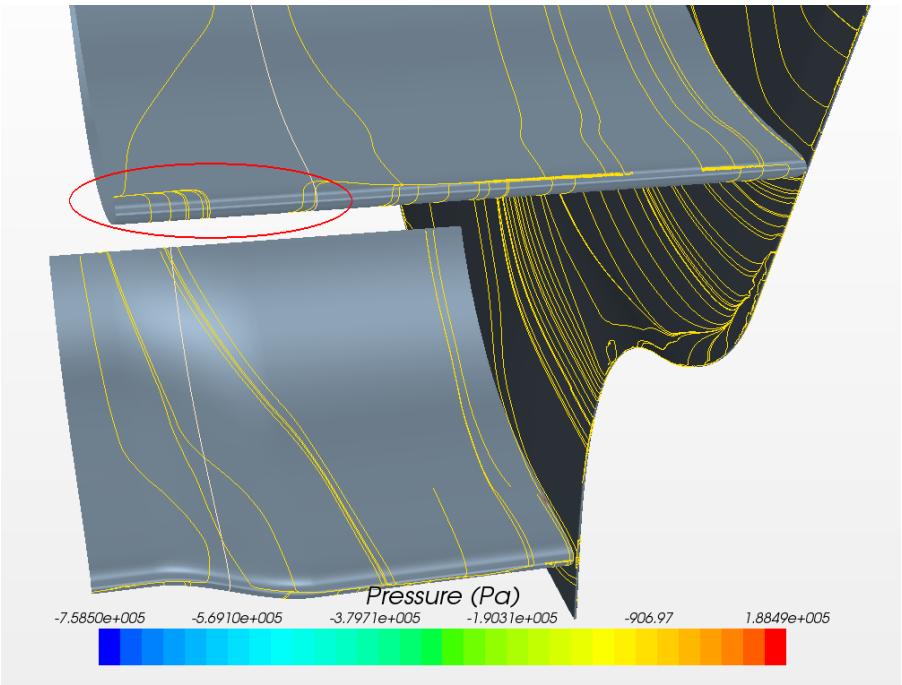

Fig. 2.38 – Constrained streamlines on the left half of the rear wing – notice the stagnation point going up in the central section of the main plane.

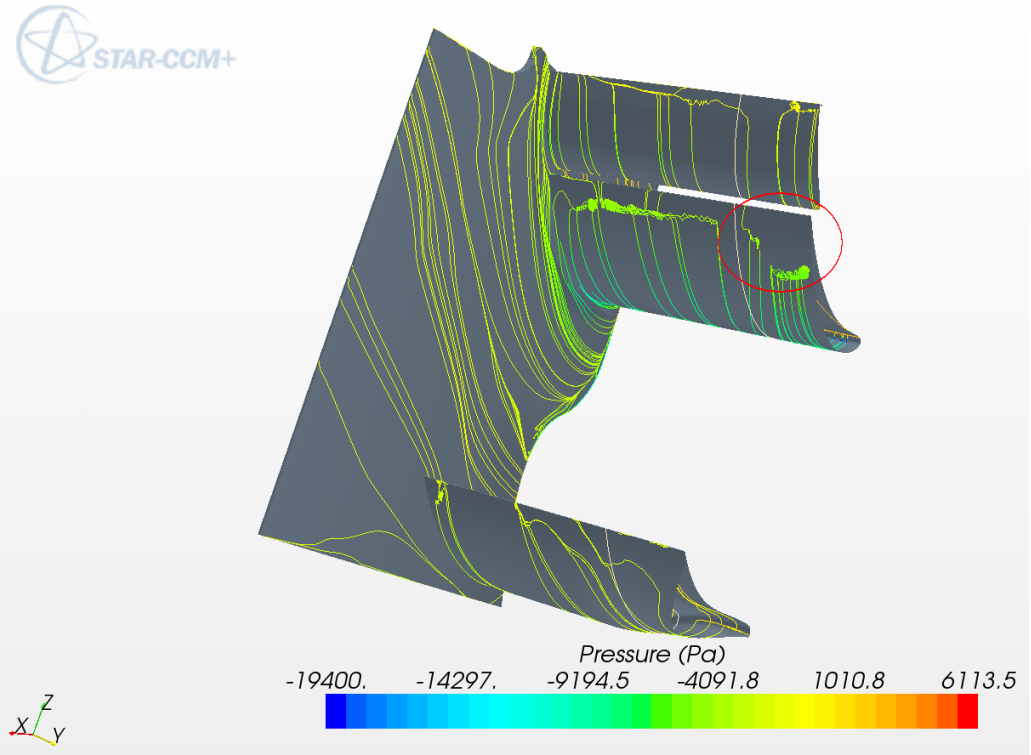

Fig 2.39 – Constrained streamlines on the lower surfaces of the rear wing – Notice premature detachment of the streamlines in the central section of the main plane.

Taking a look at the pictures of the constrained streamlines on the surface of the rear wing, the flow is working quite well, as the stagnation point is close to the leading edge, and the flow is attached in the main plane and the flap, except in the central section, where the stagnation point has been moved a few mm over the leading edge, and there is a slight detachment of the flow in the main plane. Therefore, the central section must be improved to reattach the flow, and the repositioning of the leading edge will probably help with this (it is not a simple coincidence that the stagnation movement and the detachment of the flow.

Following FIA Formula One 2011 rules, the rear wing (main plane + flap) must be enclosed by the regulation box. However, the central section, which is from the centerline of the car to +/- 75 mm, the regulation box is not applied, so the shape is completely free (this is the reason why the famous F-Duct was born), which means that the angle of attack can change, the chord, or even it is possible to add more elements, like many teams in high-downforce tracks. Nevertheless, the addition of an extra element (like Virgin or Lotus cars) is not efficient, but it is the last solution to increase downforce if it is necessary. However, other teams prefers to add a small slot (so simulating a third element in the central section), feeding the suction surface with more energized air thus being able to create more downforce.

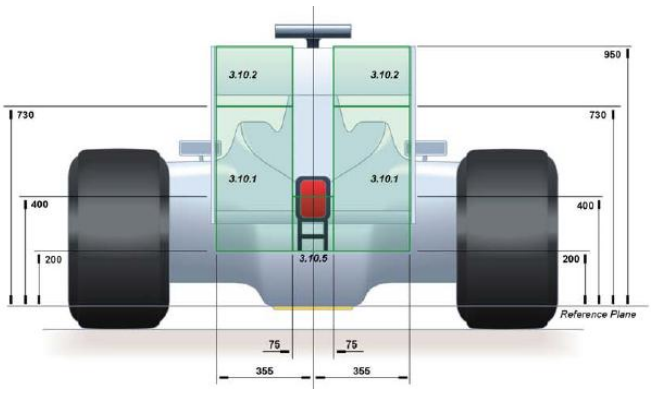

Fig 2.40 – Drawing 14a FIA Formula One 2010 regulations **[5]**, notice the regulation box area (3.10.2).

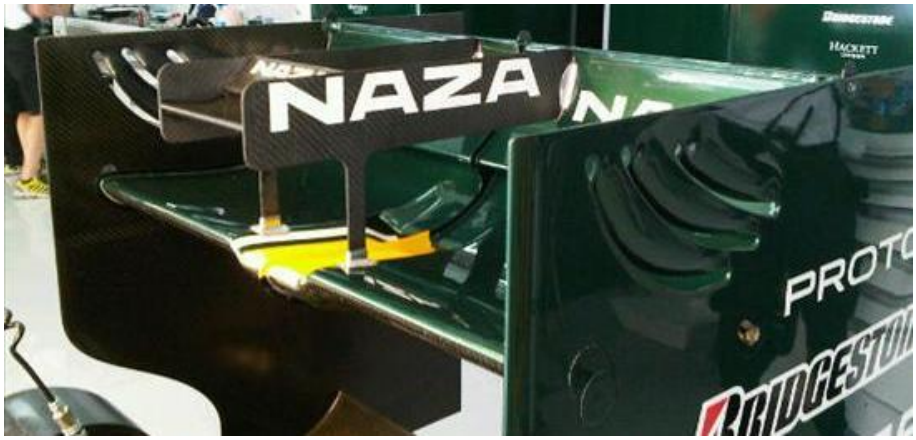

Fig. 2.41 – 2010 Lotus F1 rear wing **[6]**, with an extra element mounted on the central section (actually, it is a 2-element wing with their own endplates, so it is clear the freedom of design in this central section).

Fig. 2.42 – 2010 Ferrari F1 car **[6]**, with the slot positioned on the central section of the main plane.

Besides being proved as useful, the optimization process will continue developing the shape of a 2-element rear wing, as the introduction of the slot would present a big difficulty for the optimization process (apart from delaying the scheduled program, as the CAD should be re-designed). Therefore, different compromises should be studied in order to keep using a similar shape as the optimum selected, while modifying it enough to see any changes.

The rear wing is going to keep the same **"Positioning Parameters"** as in the 2D profile generation, in order to keep the same gap and overlap all along the span. However, the rear wing wil be divided into three different sections: Central, Intermediate and Endplate sections, with the following features:

-Central Section: Given that the freedom in this area is absolute, the geometrical construction of the 2D profile will be scaled (just by re-sizing the regulation box), to increase the plain area of the wings, thus generating more downforce. It will also be focused on re-positioning the stagnation point to decrease drag.

-Intermediate section: It will accomplish with the regulation box, trying to get the maximum with the given boundaries, so no changes respect the 2D optimization.

-Endplate section: It will also accomplish with the regulation box, but the chord of the overall wing will be reduced, and the angle of attack will be modified. As seen in many Formula One cars, the rear wing close to the endplates is not so aggressive (with reduced chord and/or lower angle of attack). **This is because on the tip of the wings, a vortex is created, which also enhances induced drag. Moreover, the induced drag will create a greater upwash (which reduces the effective angle of attack of the rear wing), so both downforce and drag will be worse.** Endplates are the main counter-action to avoid the wingtip vortex, but it still exists, so the next step is to reduce the pressure difference between upper and lower surfaces on t he wing tip to weaken the vortex. This method has been used for a long time in aeronautics, as the famous "Supermarine Spitfire" (Fig. 2.35), with an elliptical wing which reduced the pressure difference on the tip thus reducing the vortex and consequently induced drag.

Fig 2.43 – Supermarine Spitfire **[7]**, one of the most famous fighters during the World War II.

Therefore, to control the 3 different sections of the wing, 4 different profiles will be used. The second and the third profile will be equal, to keep a simple, straight shape in the “Intermediate” section, while the first and the fourth sections will be variable. In the following table, the different parameters are listed:

Parameter	Central Section	Intermediate Section	Endplate Section
Gap	Constant	Constant	Constant
Overlap	Constant	Constant	Constant
Flap/Main plane chord ratio	Constant	Constant	Constant
Total Chord	Variable	Constant (maximum)	Variable (reduced)
Main plane chord	Variable	Variable	Variable
Flap chord	Driven (by main plane)	Driven (by main plane)	Driven (by main plane)
Flap Angle of Attack	Variable	Variable	Variable
Main plane Angle of Attack	Driven (by flap)	Driven (by flap)	Driven (by flap)
2D Profile positioning (Y)	Y1=0 (Symmetry plane)	Y2, Y3 Variables	Y4 = 370 (Endplate)

Table 2.15 - Table of parameters for the 3D rear wing construction

With this model, once the 4 different profiles are decided, the development of the final 2D shape is done by CATIA V5. With the “Multi-Sections Surface” option, it is very easy to get a natural shape, but always keeping the first 2D profile surface tangent to the Y axis to have a smooth shape on the symmetry plane.

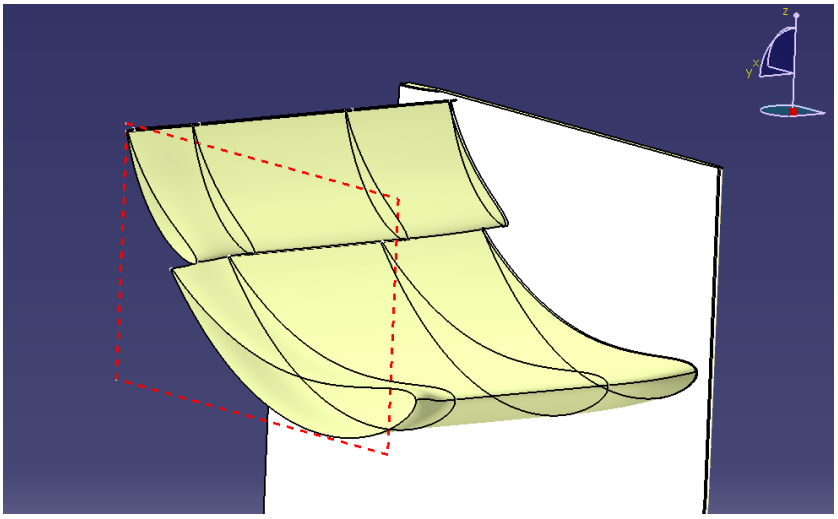

Fig. 2.44 – 3D Parametric wing construction, with the regulation box projected on the symmetry plane.

2.4.3- Beam wing parametric design

Parametric design of the beam wing is exactly the same as the rear wing with an extra restriction. The beam wing is attached to the back of the engine cover bodywork, and it cannot be modified due to structural reasons. The "virtual joint" between the bodywork and the beam wing must be respected, thus the initial profile of the beam wing. This leaves less room to play with profiles, either NACA profiles or different ones.

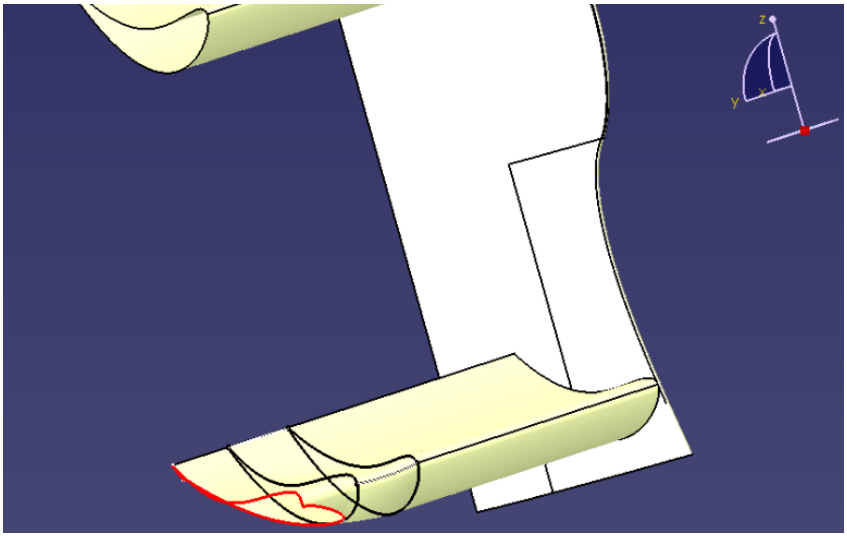

Fig 2.45 – Split rear wing from its symmetry plane. The beam wing joint with the bodywork which must be respected is marked in red.

Therefore, the same approach as in the rear wing will be adopted. One design of the beam wing will consist in a NACA profile extruded straight from the endplate, with its final section adapted to the joint with the bodywork. The other approach will be as the 3D parametric design of the rear wing, 4 sections will control the shape of the beam wing (apart from the joint with the bodywork, which is the 5th one).

Beam wing profile – NACA 4-Digit adaptation

The NACA 4-Digit profile is very easy to control, as it is driven by 3 parameters:

-Camber (% Chord)

-X position of maximum camber (in tenths of chord)

-Thickness (% Chord)

-Exactly the same profiles used in the upper part of the rear wing.

In this part, the NACA profile is extruded straight from the endplates (section 3 in the following picture). Section 2 is a sweep between the NACA profile in section 3, and the original profile extracted from the bodywork joint. Finally, section 1 is the bodywork joint with the beam wing.

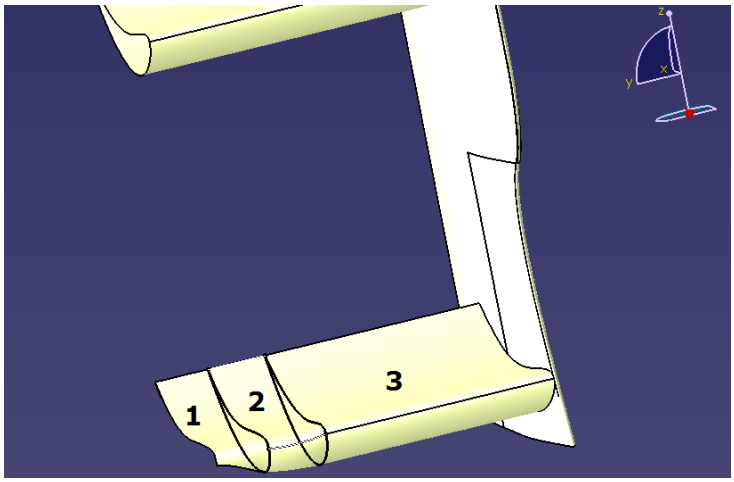

Fig 2.46 – NACA adaptation for the beam wing. Section 1 is the bodywork joint, section 2 is the transition between the joint and NACA profile, and section 3 is the straight extrusion of the NACA profile.

Beam wing profile – 3D parametric design

3D parametric design like in the rear wing method. Wing profile is the same as the original beam wing, but scaled and rotated appropriately in each section.

-Wing profile 1: fixed (bodywork joint)

-Wing profile 2, 3 & 4: Variable angle of attack and chord; profile 3 equal to profile 2.

-Control point for all profiles (fixed): trailing edge.

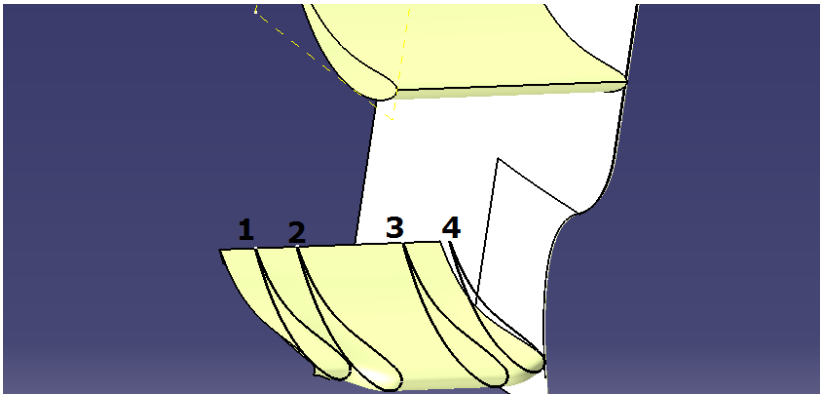

Fig 2.47 – Parametric 3D beam wing design, with joint profile (1) and free profiles (2, 3 & 4).

Although the restriction imposed by the structural function of the beam wing, rules concerning beam wing are less strict than in the upper part of the rear wing. The top, bottom and rear limits of the beam wing are restricting the rear of the wing, but the front profile is completely free. However, the engine cover is close to the beam wing, so a safety distance must be kept in order not to intersect the bodywork with the beam wing.

Again, the rule 3.10.1 from the FIA Formula One Rules 2011, (can be seen in the official Drawing 14a in the Main plane and Flap 3D parametric design section), the central section of the beam wing (+/- 75mm from the car centerline) is not under the regulation box, so it can have more than 1 profile and does not need to respect the regulation box size. Nevertheless, the joint with the bodywork implies a conservative design in the central section for this project (modifications of both engine cover bodywork and beam wing have much more potential, but also involves further work for the structural revision of the rear of the car, thus torsional stiffness of the car, so it is out of this project). Therefore, the optimization of the rear wing will be limited in this project, although the potential of this part is very high but demands a lot of resources and manpower.

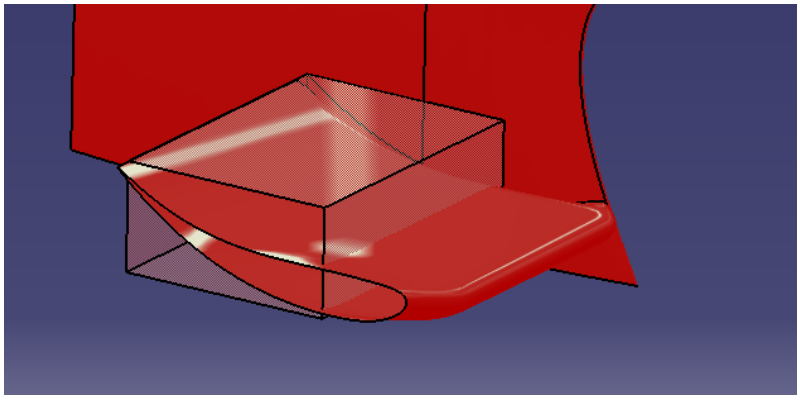

Fig 2.48 – Regulation box for the beam wing – Notice that the front of the wing is not under regulations.

2.5 - Track conditions simulation

2.5.1 – Car dynamic properties

The simulation of the CFD must be similar to a wind tunnel test environment, which is also trying to simulate the reality. Although flow is as real as in the race track (there are no equations involved), the fact that the model is scaled (50% of the real size), the belt simulating a rolling road and the blockage of air due to wind tunnel walls makes it only another test to simulate the reality. Finally, the truth is real track testing, but it is not possible to test every part of the car (due to logistical issues, cost, and the rules does not allow it). So, how can be defined the simulation of the physical environment and the dynamics of the race car in CFD?

Fig 2.49 – Epsilon Euskadi Wind Tunnel facilities **[8]**.

Wind tunnel is capable to test different wind speeds (so different car speed), different pitch, roll and yaw angle (so different longitudinal and lateral accelerations, different cornering speed. different corner radius…), as well as instantly change ride height (different set ups and suspension stiffness). Apparently, it is the ultimate tool for an aerodynamicist. However, it can only test one single configuration of the car. This means that a small change in a wing profile, sidepod, nose, etc. will require the manufacturing of moulds, carbon fiber laminating, and installation into the model, which can cost some hundreds (or some thousands) of Euros as well as many hours before entering the wind tunnel, while in a computer in a few hours can be designed and tested, with virtually no cost. Therefore, the connection and dependency between CFD and wind tunnel is obvious, as the wind tunnel can obtain the “aeromap” of the car and validate the CFD simulation

quickly, but a thorough development of each part should be done previously in CFD, testing thousands of small modifications to obtain the best parts. Having said that, notice the big difference between wind tunnel and CFD:

Wind Tunnel: 1 single model, many different dynamic positions tested.

CFD: hundreds of different models tested, but 1 dynamic position only.

This leads to the final critical decision of the exact dynamic position of the car for the CFD simulations. Firstly, multiple speeds optimization is dismissed, due to higher computing resources needed, although some Formula One teams are developing multiple-speed optimization, especially for the front wing. In the following Fig., an example of 2D multiple speed optimization data is shown, but notice that a 2D simulation is only done for preliminary approach to the development of the car, and it has nothing to do against a 3D simulation, as force values or coefficients cannot be extrapolated to a 3D wing working with a F1 car.

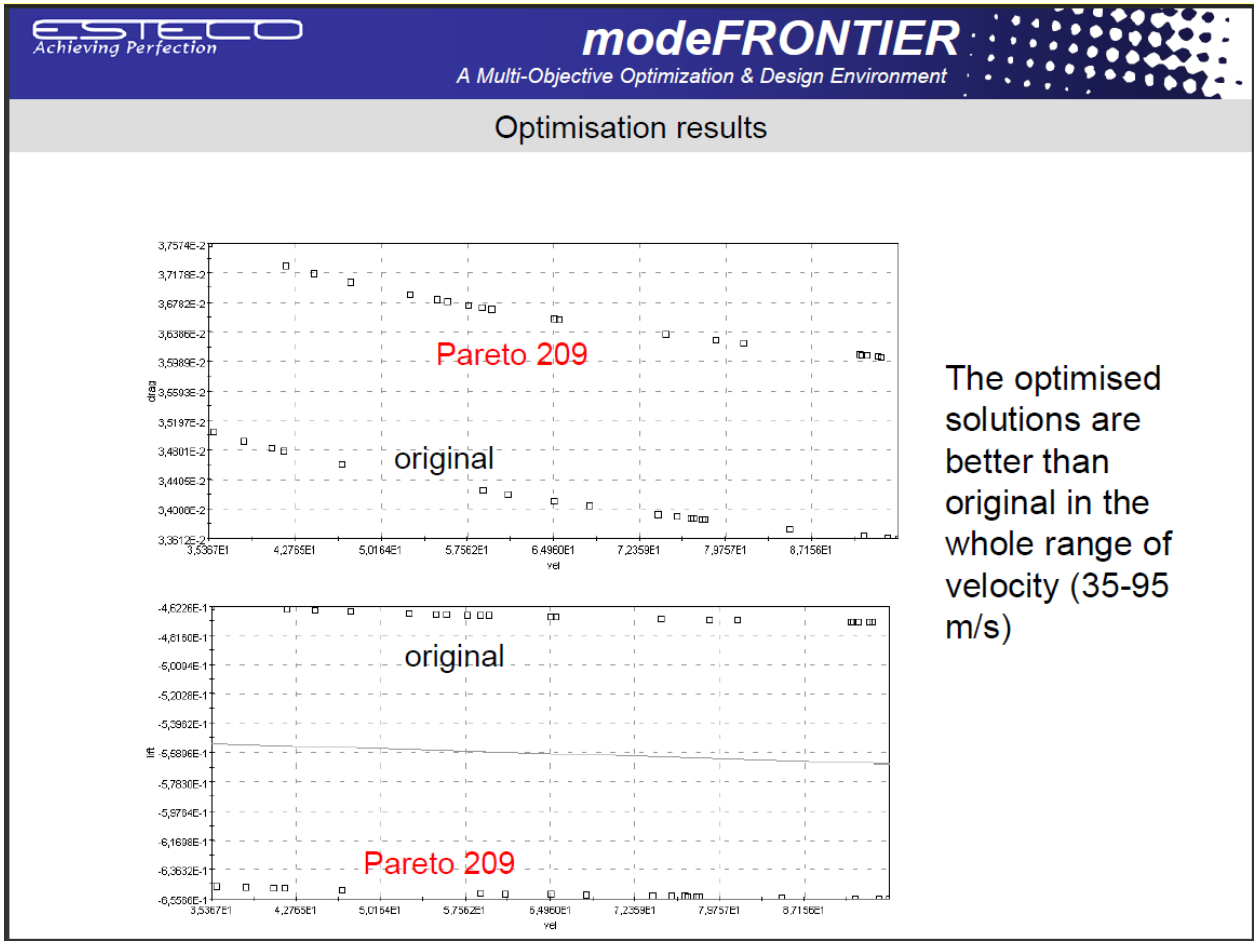

Fig 2.50- Multiple speed ModeFrontier optimization of a Formula One front wing **[9]**.

Once clarified the single speed simulation approach, it is time to define speed. Many people think that the optimization should be done at the maximum speed a F1 can reach (that is, around 350 km/h). But this is only for straight line, top speed testing. In this project, a rear wing is going to be optimized, so the conditions tested should reflect the car attitude which requires the maximum performance of the rear wing. Going back to basics, a rear wing is an aerodynamic element which generates downforce, in order to increase cornering speed in medium-high corners (not in slow corners, as aerodynamic elements are not very helpful under a certain speed). Therefore, the most representative speed is the one in the middle of high speed corners (290 km/h) and medium speed corners (210 km/h), so the average point of 250 km/h is easily found.

Moreover, a cornering state will imply a yaw angle (an angle between the airflow direction or car trajectory, and the car centerline or nose pointing direction), as well as roll angle produced by the lateral acceleration. However, none of them will be considered in the set up of the simulation, as they consequently require an asymmetric model, which means to double the mesh size of the model (the simulation will run with a longitudinal symmetry plane in order to reduce mesh size). Roll angle is hardly ever considered, due to super-high roll stiffness of current Formula One cars (around 0.5 deg/ lateral G, with typical corners of 3 Gs and maximum of 5 Gs in the current F1 Championship). Nevertheless, yaw is considered in Formula One full car CFD simulations, with values around 2 degrees of yaw, so this optimization will be validated with this angle as well, although not present in the reduced mesh model.

Finally, other details, like wheels position (as the car is turning, the wheels are also steered a certain degree) remains confidential, although it is also simulated in the CFD full car simulation. Ride height (this means, front and rear ground clearance) is decided by the chief aerodynamicist (which has been discussed with vehicle dynamicists and race engineers), and are modeled in both the full car mesh and reduced mesh simulations, but also remains as confidential information.

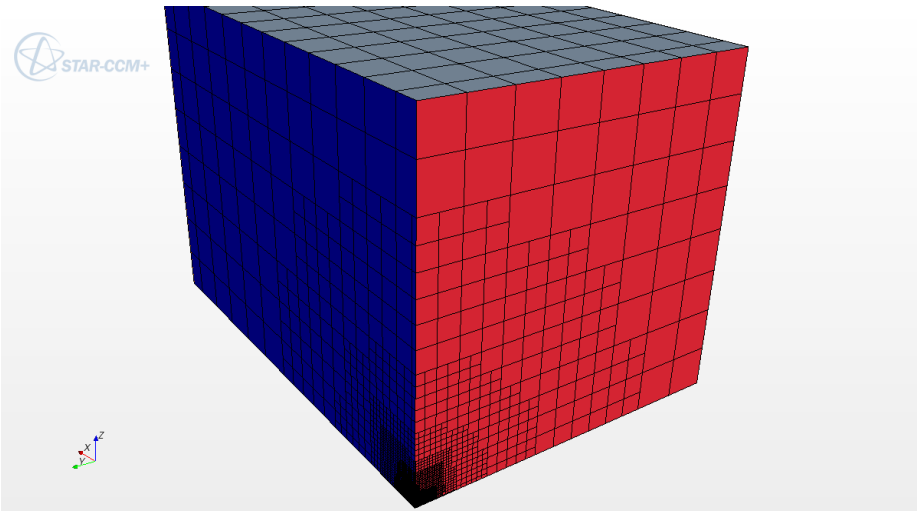

Fig. 2.51 - CFD boundary walls, or “virtual wind tunnel” – Notice the quarter car mesh in the bottom corner.

The physical environment is also represented without problems, like the rolling road (with the same speed as the airflow). Remember that the road is going at the same relative speed as the air (that is, absolute 0 Km/h speed, because it is static, the car is the element which is moving), so the CFD is actually simulating the wind tunnel rather than real track conditions. The air around the car is bounded by a big box (again, like the wind tunnel), with an inlet condition in front of the car, and an outlet condition at the back of the car. The remaining 4 faces of the box are the rolling ground (bottom), symmetry plane (left), and 2 frictionless walls on the top and the right of the car. Notice that it also has a slight blockage like the wind tunnel, but the fact that the walls are frictionless is helping a little. Moreover, the option in CFD to impose a velocity on the ground eliminates any problems of development of the boundary layer on the floor of the virtual wind tunnel, which is much more effective than current methods to eliminate the boundary layer in real wind tunnels.

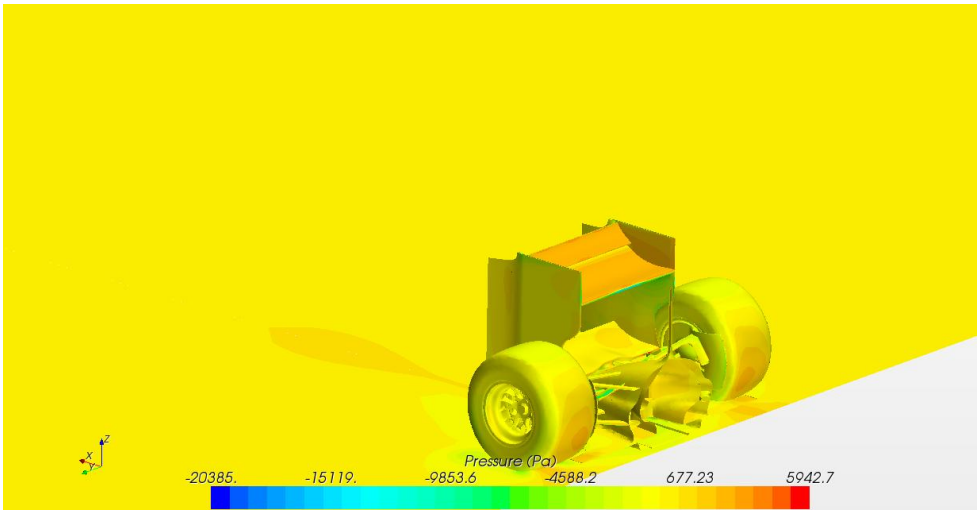

Fig 2.52 – Pressure contours of the rear of the car, inside the wind tunnel – Notice that a “visual” symmetry option is activated, so the whole rear of the car can be seen, although it is only calculated half of the rear part of the car.

Finally, the inlet and outlet conditions should be defined. The outlet condition is a “standard” pressure outlet, with a value of 0 relative pressure, which lets the flow to be developed around the “virtual wind tunnel” created by the boundaries, very far from the rear of the car to leave room for the turbulent wake. The inlet is also simple for full car simulation, as the initial speed of 250 km/h is the only parameter required. However, for the mesh reduction (deeply explained in the next section of the chapter), the car will be split by a transversal plane in order to calculate the mesh of the rear of the car (this means the whole rear wing and the bodywork which is affected by its upwash). This plane is carefully decided by the chief aerodynamicist, in order to keep all the flow details while reducing the mesh as much as possible. Therefore, the inlet will no longer be a single speed value, but it will be a much more complicated

procedure, which has been validated through many tests and airflow analysis. The process consist in generate the same cutting plane in the full car model, obtaining the values of the airflow through this plane. Air properties will be saved in different tables, which will contain the data of airflow speed, direction and turbulent viscosity ratio of each cell intersected by the cutting plane Then, the split geometry is imported in the reduced mesh simulation, and the tables are imported in order to have the appropriate inlet boundary conditions to simulate the flow passing through the front wing, front wheels and anything before the cutting plane. Moreover, the mesh of the inlet should be carefully designed in order to reproduce the original full car model mesh in the cutting plane area to avoid losing physical details of the flow.

The importance of the position of the cutting plane is due to the influence of the front of the car to the rear and vice versa. The shape of the wing generates an “upwash”, an influence to the flow in front of the rear wing, which must be taken into account. Moreover, as the optimization of the shape is being carried on, this “upwash” will be changed, so the flow in front of the rear wing will change, thus affecting areas in the forward part of the car. Therefore, if the cutting plane is too close to the rear wing, the inlet conditions will not be able to take into account this “upwash” generated by the rear wing, so the whole optimization would be wrong. **This means that ideally, while developing each part of the rear wing, a new simulation on the full car mesh must be done, in order to update the data from the cutting plane of the full car for the inlet conditions of the reduced mesh simulation**. Notice in the following picture, the pressure contour on the symmetry plane in the upper part of the rear wing, which is finished just before contacting the inlet boundary wall.

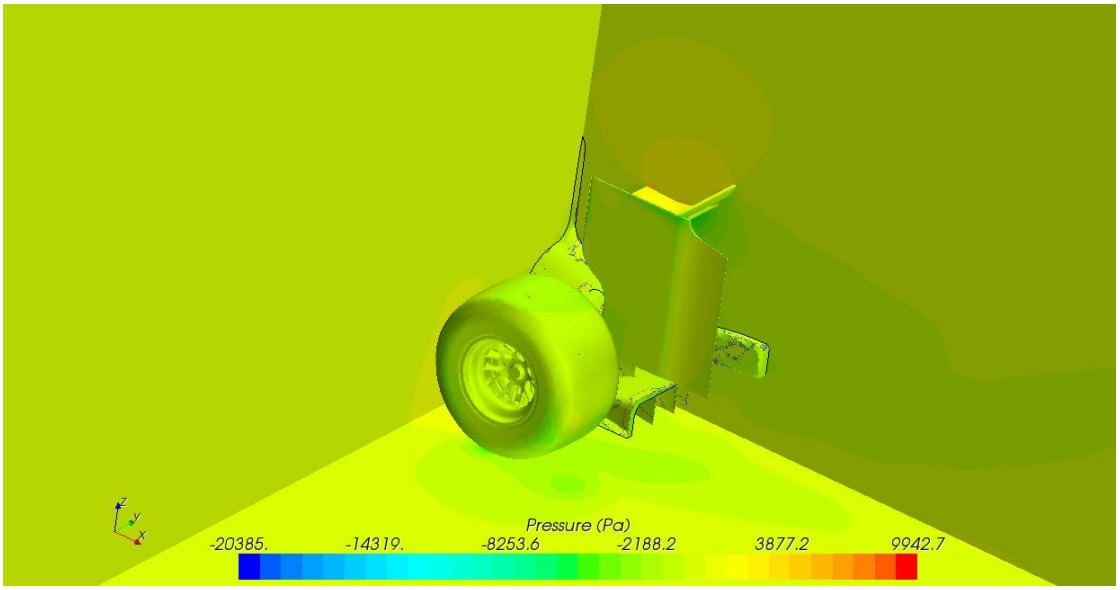

Fig. 2.53 – Pressure contours on the rear wing – Notice on the symmetry plane, the pressure contour over the rear wing in yellow, just finishing before touching the inlet boundary wall.

So to sum up, the main common features and differences which must be taken into account while doing this process of optimization are the following ones:

Concept	FULL CAR SIMULATION	PARTIAL CAR SIMULATION
Geometry	Full car	Rear part of the car
Inlet conditions	Inlet speed, 250 km/h	Flow properties on cutting plane
Outlet conditions	Pressure outlet, 0 Pa	Pressure Outlet, 0 Pa
Yaw angle	Yes	No
Roll angle	No	No
Pitch angle (ride heights)	Yes	Yes
Symmetry plane calculation	No	Yes
Rotating wheels, moving road	Yes	Yes
Steered wheels	Yes	No
Correlation	With wind tunnel	With full car simulation

Table 2.16- Comparison between full car simulation and a partial car simulation

2.6- Rear wing optimization

2.6.1- Introduction to Rear wing optimization

Four different software are involved in the optimization loop: ModeFrontier optimizer, CATIA v5 CAD, StarCCM+ CFD software and Excel database for NACA profile generation. ModeFrontier executes the whole loop and process the data within a few minutes, CATIA v5 CAD software needs a few seconds to update the geometry, and Excel files are modified instantly. So, apart from the Modefrontier algorithms behavior (which is quite quick to set up), and the different optimizations paths proposed by the Chief Aerodynamicist, the biggest amount of work is in StarCCM+. Mainly:

-Turbulence Model – Chosen by the Aero department due to correlation with full Formula 1.
-Boundary conditions (inlet, outlet, use of symmetry planes, and geometry involved in CFD).
-Mesh size, which is directly proportional to the amount of time required for the simulation.

Targets should be set in order to start reducing mesh size, and deciding the model geometry. As any optimization process in CFD, the priority is to launch as many simulations as possible to understand the influence of each parameter in downforce and drag. With the help of Modefrontier, “human working time” is extremely reduced, but it is not enough due to the size of the CFD simulation. Therefore, the only option which is feasible is to combine both Modefrontier power with StarCCM+ mesh reduction to achieve success. In the following charts, **the comparison of the current Formula One model without using Modefrontier is done versus the use of Modefrontier and StarCCM+ mesh reduction to around 2 million cells**, which is successfully achieved, reducing the mesh up to 1.7 million cells and with a satisfactory implementation of ModeFrontier. In the following graphs, it can be seen the difference between the distribution of time on the full model simulation and the reduced mesh model and the difference using Modefrontier, which automatically makes the set up (configuration) of each case like a macro. Notice the reduction in time in the simplified mesh model with the automatic set up process.

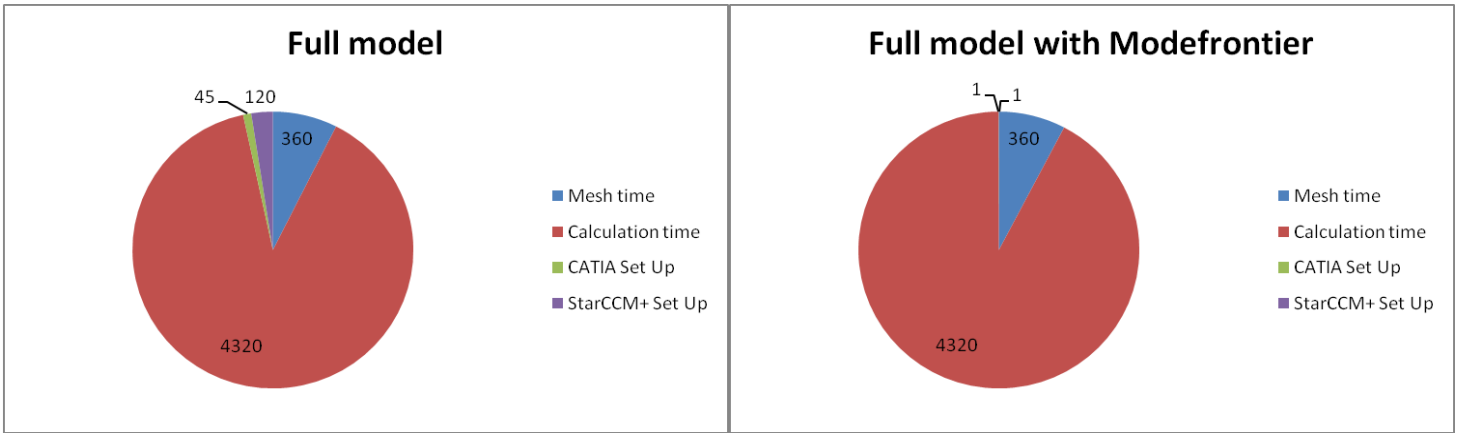

Fig 2.61- Pie chart of time spent (in minutes) on the full mesh model with and without Modefrontier

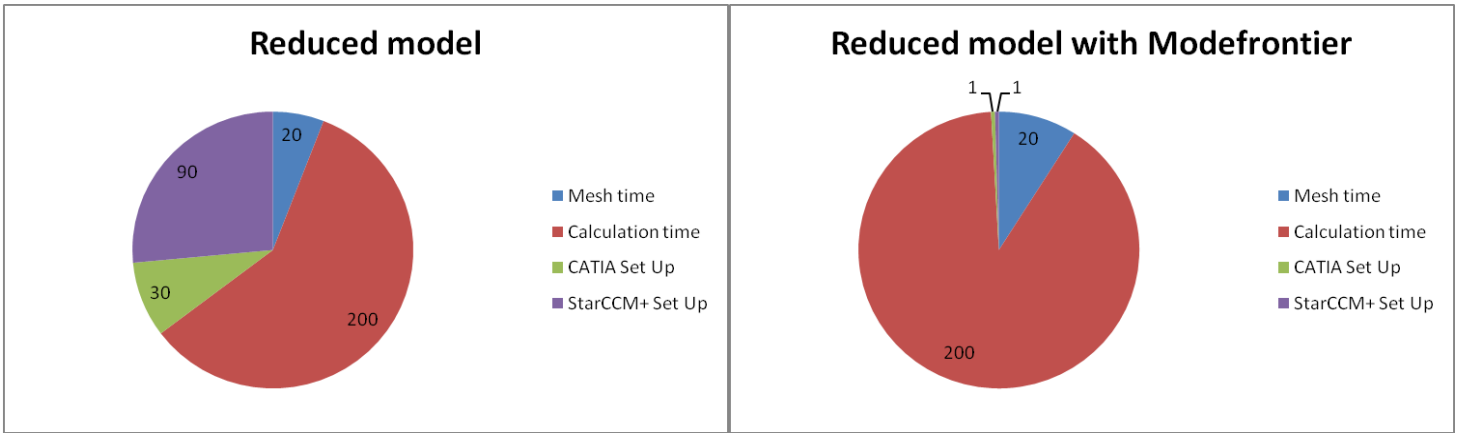

Fig 2.62- Pie chart of time spent (in minutes) on the reduced mesh model with and without Modefrontier

The original model of the Formula One car is around 60 million cells. It does not have any symmetry plane, because the car is usually tested in yaw (as the downforce is desired while cornering, not in straight line, which means yaw angle). Yaw angle means that the car longitudinal axis is not parallel to the flow direction, and it is an unavoidable dynamic result when cornering. Therefore, in order to reduce the mesh, the **first idea was to use a symmetry plane to cut by 50% mesh size, so the rear wing is always simulated in straight line without yaw.** This decision is critical, because the correlation should involve two different steps, one with the 60 million model in straight line, and another with yaw (where downforce is needed).

30 million cells are far from being enough. **The second critical decision was to cut part of the geometry to continue reducing mesh size, thus reducing it by 65%.** Therefore, a resulting mesh of 10 million cells is achieved. However, a very important compromise is being done cutting the car. This means that the virtual wind tunnel used will have its input in the middle of the car, in a plane after the helmet of the

driver, intake manifold and the exhaust, just having the end of the bodywork (that is the rear wing, the rear wheel assembly and the diffuser). So, the input boundary condition will no longer be a standard airflow velocity perpendicular to the inlet. Now, **a plane in the full Formula One simulation will get the data of the flow properties (Flow direction, flow speed and turbulence viscosity ratio) to be imported by the new reduced simulation as input boundary conditions.**

This risky approach should be tested and correlated with the whole car. The solution of importing flow properties from full car model is acceptable, but a rear wing always create an “upwash”, which means that the flow in front of the rear wing is affected by the rear wing, so the new flow field while changing the geometry during the optimization may not be realistic. However, to compare this new aggressive approach, the numbers of downforce or drag are not as important as the flow visualization. Vortex, pressure peaks, and low pressure areas should be created in exactly the same place in both models. Finally, after a few tests (data and graphs from the full Formula One car is confidential, so cannot be revealed), the correlation was approved and the reduced mesh had green light. But anyway, it was still far from the desired mesh of 2 million cells.

After analyzing mesh properties, the department reached the conclusion that **mesh size could be highly reduced in some areas far from the rear wing, which can affect the overall flow, but are not reflected on the rear wing, so correlation could still be done**. This areas are mainly the rear wheel internals (disc, caliper, rim) and underfloor plus diffuser. This doesn’t mean that we lose information about these parts, but an important mesh reduction can be achieved without sensitivity on the rear wing, and with nearly the same results of drag and downforce on wheels and diffuser. The whole bodywork, wishbones, etc. had also slight mesh size reductions (except rear wing profiles and endplates), and the whole reduction reached 5 million cells (50%). **So not being enough, a more aggressive reduction reached 1.7 million cells, which became the initial model after correlation tests**. Afterwards, the iterations needed by the flow to converge were reduced, as the case became much simpler with a lighter mesh, and testing of the influence on the number of iterations combined with the reduction of mesh size was also done. The only example which can be published due to confidential issues is the following table:

Filename	Mesh Size (cells)	Iterations	Fx	Fz	L/D
BSL00	10 million	1500	451.29	1493.93	3,3104
BSL00	10 million	4000	442.47	1483.42	3,3526
BSL00_5M	5 million	1500	453.09	1505.46	3,3227
BSL00_5M	5 million	4000	456.55	1521.22	3,3320
BSL00_1.7M	1.7 million	1500	452.19	1499.7	3,3165

Table 2.17- Table of results of mesh size/iterations correlation test.

epsilon EUSKADI

With this reduction on the number of iterations, not only the **mesh size was reduced by more than 30 times** the original one, but the **original simulation which took days in a Cluster was reduced to 4 hours in a 6 CPUs computer, as less iteration are needed to converge.** As it can be seen in the table of results, Fx and Fz are drag and downforce corresponding to the rear wing only, and the values are similar with the mesh reduction at 1500 iterations, **so the mesh size reduction of both wheels and diffuser is not affecting the rear wing.**

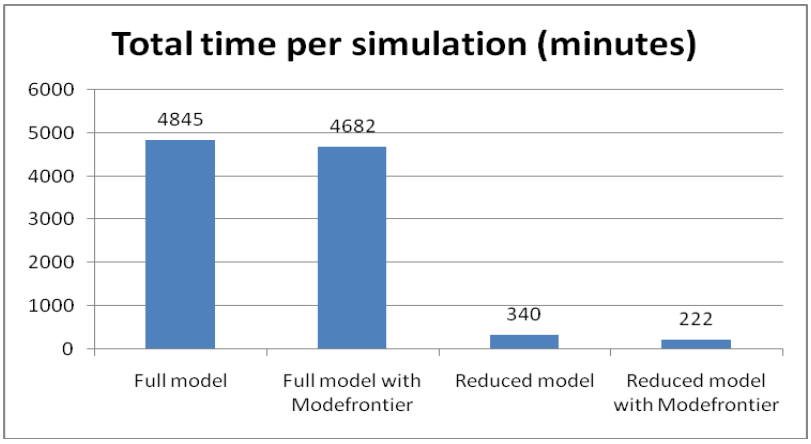

Fig 2.63- Simulation time chart with the full/reduced model and with or without Modefrontier.

However, the number of iterations is clearly influencing drag and downforce values (as mentioned on chapter 2.2-CFD Software testing). So a new compromise is taken, but the number of iterations is directly proportional with the time spend on each simulation, so it was not possible to increase this number with the time given for this project. However, the most important thing is that each configuration of the rear wing is better or worse than others independently of the number of iterations calculated. This was controlled during the whole process, and a small example of one loop is presented in 2.5.2 chapter, to demonstrate that the compromise taken was a very good choice.

2.6.2- Convergence time optimization (number of iterations)

For a given test of 2 parameters (no matter if they are camber, angle of attack, or any other), with the simplified mesh of 1.7 million cells, different configurations have been tested, but the results of drag and downforce have been collected for 1500, 2000 and 2500 iterations, to check the decision of stopping the simulation at 1500 iterations to save time. The objective of this control tables is to demonstrate that, despite having demonstrated that drag and lift depend on the number of iterations, the best design of a group of experiments will continue as the best result, no matter if the simulation was stopped at 1500, 2000

or 2500 iterations, and also that the variation of the results is really small, as the flow at 1500 iterations is not far from converged.

10 different configurations will be tested, and the drag, downforce and lift to drag ratio of all them will be registered. Two candidates to be the “optimum” wing will be decided after the first 1500 iterations (which is the default number of iterations for each CFD simulation). The optimum selection criteria will be the configuration which is further from a simplified and hypothetical “Pareto frontier”, which will be drawn as a straight line approximately representing the typical behavior of the frontier in this project.

Iteration	Fx	Fz	L/D
1500	437,8	1505,3	3,4383
"	438,89	1514	3,4496
"	439,03	1508,9	3,4369
"	444,42	1520,3	3,4209
"	422,3	1471,7	3,4850
"	451,63	1548,9	3,4296
"	436,42	1500,5	3,4382
"	450,95	1543,4	3,4226
"	431,32	1490,2	3,4550
"	448,24	1527,5	3,4078

Table 2.18 - Table of results of drag and downforce for 2 random variables configuration

As we can see in the table of results, two candidates are selected, the green and the orange one. With an XY plot, it is clearly seen that they are the separated from the others, with a good amount of downforce and a considerable efficiency (lift to drag ratio). The hypothetical “Pareto” frontier is the blue line, and the red lines are isodrag lines (constant drag). A typical objective is to keep the drag constant while increasing the downforce, thus increasing lift to drag ratio, so if the evolution of the “optimum” rear wing follows an isodrag curve, the optimization is going in the right direction.

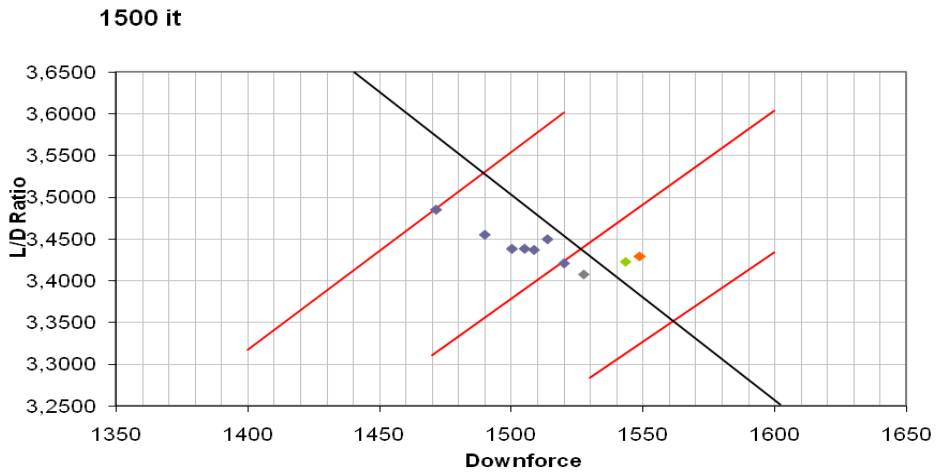

Fig 2.64 - XY plot (Downforce Vs L/D ratio) for 10 experiments with the simulation @ 1500 iterations.

Notice the green and orange candidates far from the rest of experiments. The decision between them will be done after looking at the plots for 2000 and 2500 iterations, although the relative position of the rest of points will also be observed. Although they are close, following an imaginary isodrag passing over the green point, the orange candidate is slightly better situated to be the “optimum” rear wing.

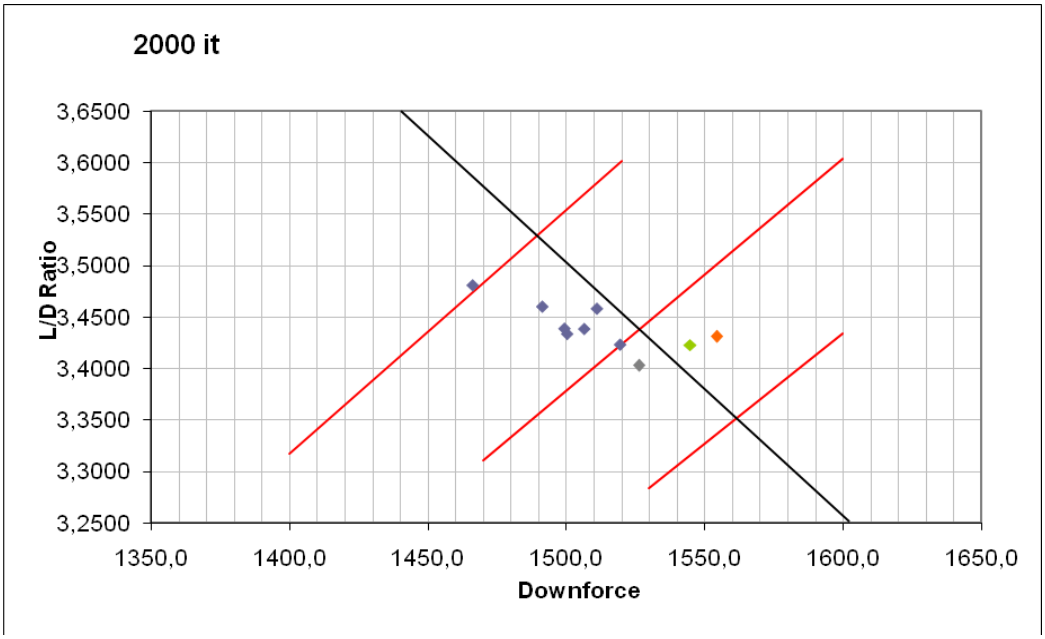

Fig 2.65 - XY plot (Downforce Vs L/D ratio) for 10 experiments with the simulation @ 2000 iterations.

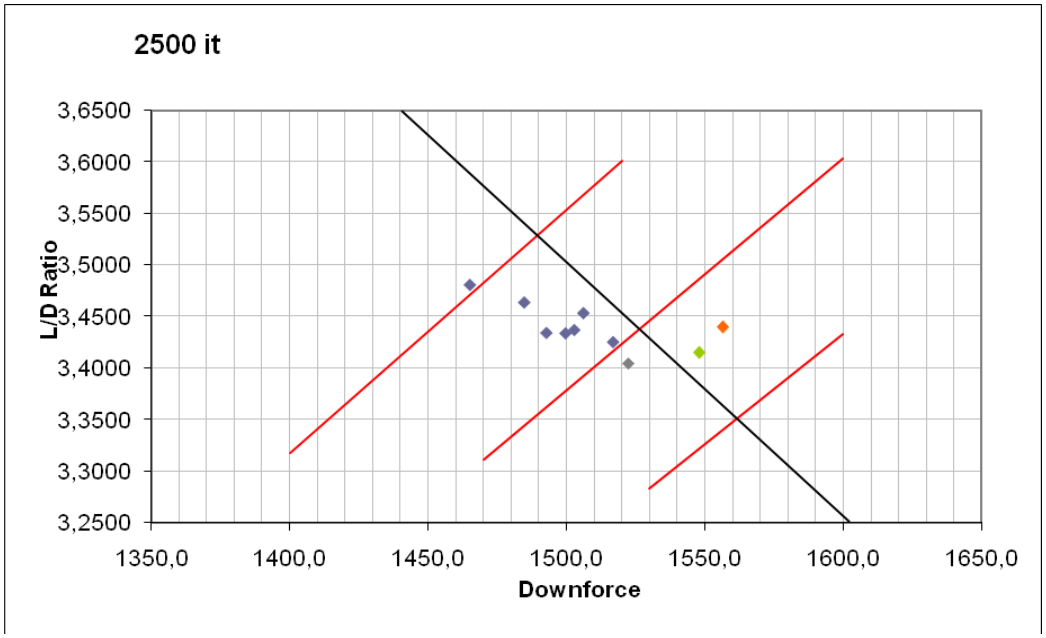

Fig 2.66 - XY plot (Downforce Vs L/D ratio) for 10 experiments with the simulation @ 2500 iterations.

At 2000 iterations, the results are more or less the same, with the same positioning as before for all the results, although the orange candidate has improved its downforce slightly. At 2500 iterations, all the points remain in a similar place relative to the other, although the orange one has improved slightly its lift to drag ratio, so it is confirmed as the best candidate to be the optimum rear wing. Therefore, the same candidate would be chosen at 1500 iterations, but with around 60% of the time spent to arrive at 2500 iterations. Actually, it means that at 1500 iterations the number of experiments per day can be roughly doubled. So, despite not being 100% sure that the best candidate will be the optimum rear wing (in fact with 2500 iterations it is still not possible to say it with 100% confidence), the possibility of doing nearly twice experiments is much better. Taking a closer look at each configuration, forces depends on the number of iterations, but the difference is not big enough to change their position relative to the other experiments (it can happen in particular situations that the best candidate is not the optimum, but it will not be very far from it). Anyway, in case of two or three candidates which are very close, there is always the possibility to run up to 2500 iterations to check the best optimum, with many more candidates already dismissed, and each selected candidate performing much better than the rest of dismissed candidates.

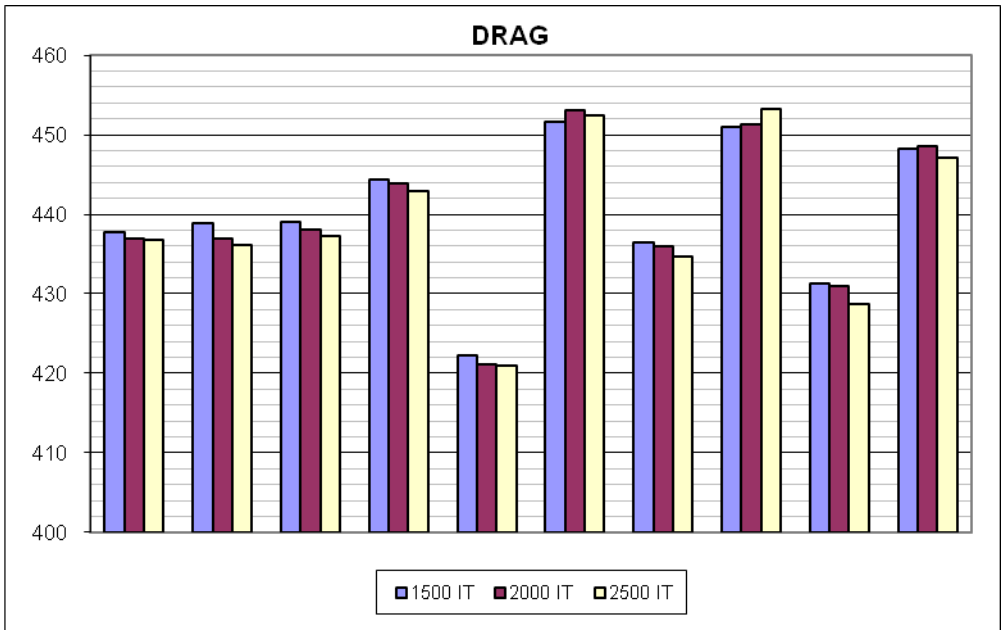

Fig 2.67 – Drag column chart for 10 different configurations at 1500, 2000 and 2500 iterations.

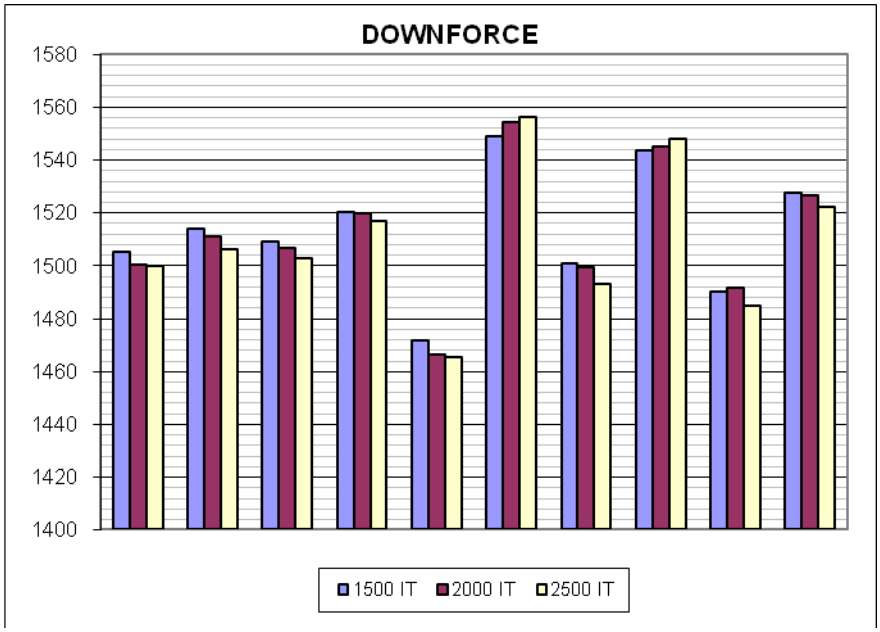

Fig 2.68 – Downforce column chart for 10 different configurations at 1500, 2000 and 2500 iterations

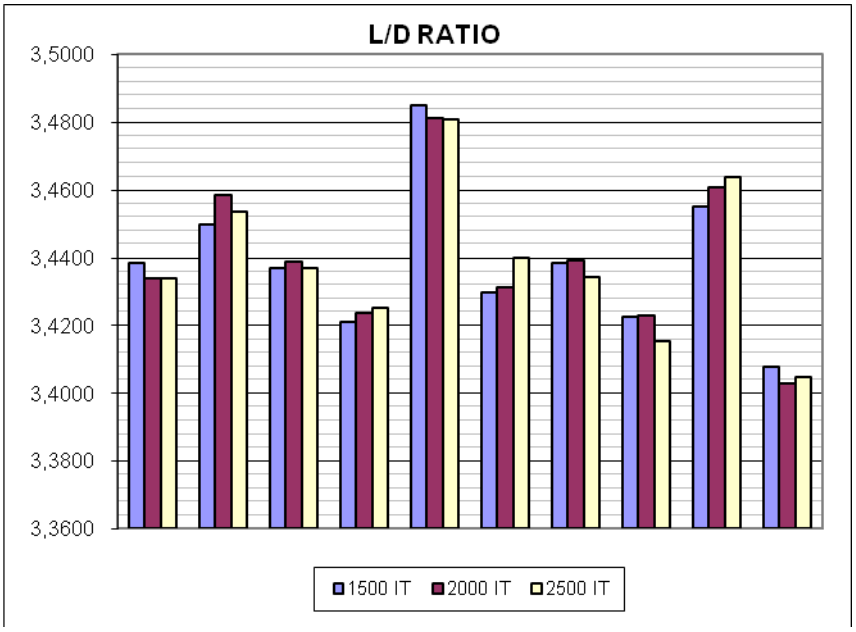

Fig 2.69 – Lift to drag column chart for 10 different configurations at 1500, 2000 and 2500 iterations.

Notice that the difference between configurations is clearly seen in each chart and the relative positions between them is not changing due to the number of iteration – the best case is still the best, and the worst case, the worst. To sum up, the compromise taken is absolutely justified.

2.6.3- Optimization scheduling

Once the parametric CATIA rear wing is ready, StarCCM+ mesh & geometry, and the Excel files needed to create the NACA 4-Digit profile, the optimization is scheduled with Modefrontier. At this point, the sequence of different optimizations must be decided by the Chief Aerodynamicist to develop the rear wing. There are many variables, and they cannot be tested all at once, because it would require a really big design of experiments, taking up to a few weeks of calculations for a 10 variables experiment, which is too risky. The simulation can crash (and with the consequent loose of data), or it can be done wrong (either the objectives or the results), and a few weeks without any results to process is not interesting for any Aerodynamics Department. Moreover, a simulation with so many variables would create Kriging surfaces with a lot of "noise", so it would not be helpful.

Therefore, a plan needs to be done. Each of the scheduled Modefrontier simulation is known as a **"loop".** For the main plane + flap of the rear wing, 4 different loops will be done:

-1st loop: Flap Angle of attack, Flap chord, flap camber and Main plane camber.

-2nd loop: X position of maximum camber (for flap & main plane), thickness for flap and main wing as well.

-3rd loop: Gap and Overlap.

-4th loop: 3D shape of the main plane + flap assembly (different angle of attack and chord on different sections along the rear wing).

Finally, 10 variables are studied within the 3 initial loops, having 4, 4 and 2 variables respectively. This is to avoid too much "noise" when studying Kriging surfaces and to evaluate each parameter minimizing influence of other input variables. It will also permit to reduce the number of experiments per simulation, and a better behavior for the optimization algorithm. The 4th loop, as it requires a different approach (flow visualization to take decisions), will be explained later in this chapter.

Once the third loop is finished, correlation of the best rear wing introduced into the complete Formula One car of 60 million cells (compared to the simplified simulation of 1.7 million cells) will start. Not only it is a much bigger model, but also much more complicated, as the full car is usually tested in yaw (an angle between car centerline and flow direction). Then, if the selected rear wing after the optimization process is better that the former one, it becomes the new baseline of the car. Improvements in the 4th loop will be evaluated later, after validating the previous three loops. It is easy to understand that a bigger design of experiments with the 4 loops together would have more potential of development. However, time and resources needed were not available. Moreover, having 4 loops will allow to "understand" how each parameter is affecting the whole rear wing, so further development can also be done based on this data.

2.6.4- 1st loop – Flap angle of attack, chord, camber and Main plane camber.

This first loop will consist in a design of experiments of 9 different configurations of the aforementioned parameters for the first loop, automatically decided by the SOBOL algorithm, with one generation of MOGA-II optimization (which means, 9 more configurations to try to find the optimum values, evaluating the previous SOBOL exploration results). The whole process time took around 68 hours, so less than four hours per simulation, with a computer running 6 CPUs @3 GHz and 16 GB of RAM (notice that for the calculation the most important parameter is the CPU power). The results are the following ones:

Fx(N)	Fz(N)	L/D	Configuration	
444,41	**1521,3**	**3,4232**	BSL_t2	AoA_Flap 43.5; Chord 140; camber flap 10.5%; camber wing 14%
447,96	**1507,8**	**3,3659**	BSL_t2	AoA_Flap 46.8; Chord 160; camber_flap 12.75%; camber wing 16%
422,48	**1483,4**	**3,5112**	BSL_t2	AoA_Flap 40.2; Chord 120; camber_flap 8.25%; camber_wing 12%
439,82	**1513,1**	**3,4403**	BSL_t2	AoA_Flap 41.9; Chord 150; camber_flap 9.35%; camber_wing 13%
471,18	**1564,1**	**3,3195**	BSL_t2	AoA_Flap 48.4; Chord 110; camber_flap 13.9&; camber_wing 17%
418,91	**1469,8**	**3,5086**	BSL_t2	AoA_Flap 38.6; Chord 170; camber_flap 7.1%; camber_wing 11%
455,15	**1537,5**	**3,3780**	BSL_t2	AoA_Flap 45.1; Chord 130; camber_flap 11.65; camber_wing 15%
437,84	**1489,4**	**3,4017**	BSL_t2	AoA_Flap 41.0; Chord 175; camber_flap 14.45%; camber_wing 14.5%
441,71	**1520,1**	**3,4414**	BSL_t2	AoA_Flap 46.6; Chord 120; camber_flap 8,2%; camber_wing 12%
451,41	**1522,6**	**3,3730**	BSL_t2	AoA_Flap 45.7; Chord 144.5; camber_flap 10.4%; camber_wing 14.367%
434,28	**1491,1**	**3,4335**	BSL_t2	AoA_Flap 38.8; Chord 170; camber_flap 13.5%;camber_wing 16%
443,63	**1503,4**	**3,3889**	BSL_t2	AoA_Flap 43; Chord 170; camber_flap 13.5%; camber_wing 14,533%
445,43	**1511,1**	**3,3925**	BSL_t2	AoA_Flap 48.4; Chord 150; camber_flap 9.35%; camber_wing 13%
444,44	**1527,3**	**3,4365**	BSL_t2	AoA_Flap 43.0; Chord 136; camber_flap 10,3%; camber_wing 14,533%
460,79	**1549,7**	**3,3631**	BSL_t2	AoA_Flap 46.6; Chord 110; camber_flap 12.7%; camber_wing 14%
435,46	**1488,9**	**3,4191**	BSL_t2	AoA_Flap 41; Chord 170; camber_flap 14.4%; camber_Wing 14%
436,94	**1510,7**	**3,4575**	BSL_t2	AoA_Flap 43.5; Chord 140; camber_flap 10.55%; camber_wing 10.233%
434,67	**1486,2**	**3,4191**	BSL_t2	AoA_Flap 41; Chord 174; camber_flap 14.45%; camber_wing 14.767%

Table 2.19 - Results of the first loop – Notice that colors are used to highlight best candidates.

The selection of “best candidates” to become the new baseline (the new basic configuration) for the following loop is always done in a meeting, where a group of aerodynamicists discuss about the best candidates, and depending on the experience and the potential that they have, the optimum is decided. Different tools are used, and as a new approach to rear wing development, tools to find the optimum rear wing are constantly improved. However, the XY graph of Downforce Vs L/D Ratio is always the first thing to look at in order to take the right decision. Other XY graphs are considered like 4D Bubble graph, and finally Kriging surface is also studied in order to identify more candidates, although it is not easy to identify them with a few simulations, as each new simulation can make the whole surface change notably, so many simulations are needed to have a “stable” surface. A few examples of the graphical tools to help taking decisions, and its evolution as the whole loops gives new results are presented below:

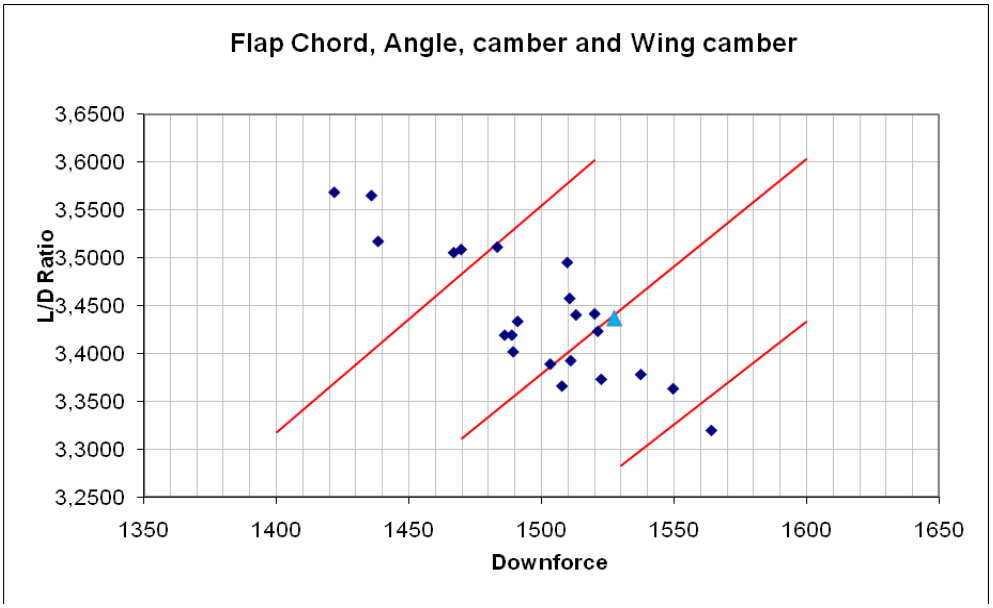

Fig. 2.70- XY graph of Downforce Vs L/D Ratio. Selected candidate is the blue triangle.

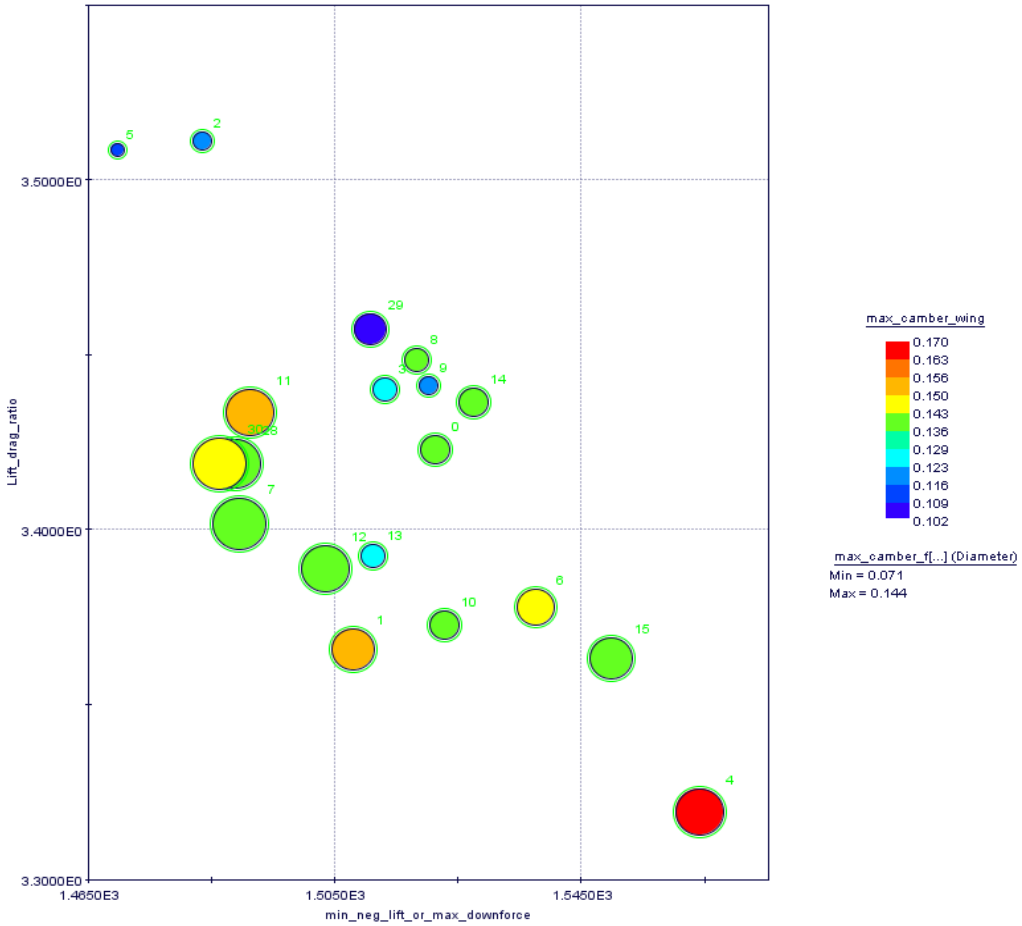

Fig 2.71- 4D Bubble chart, X axis represents downforce; Y axis L/D Ratio; Wing camber is represented with colors and flap camber is represented by bubble size.

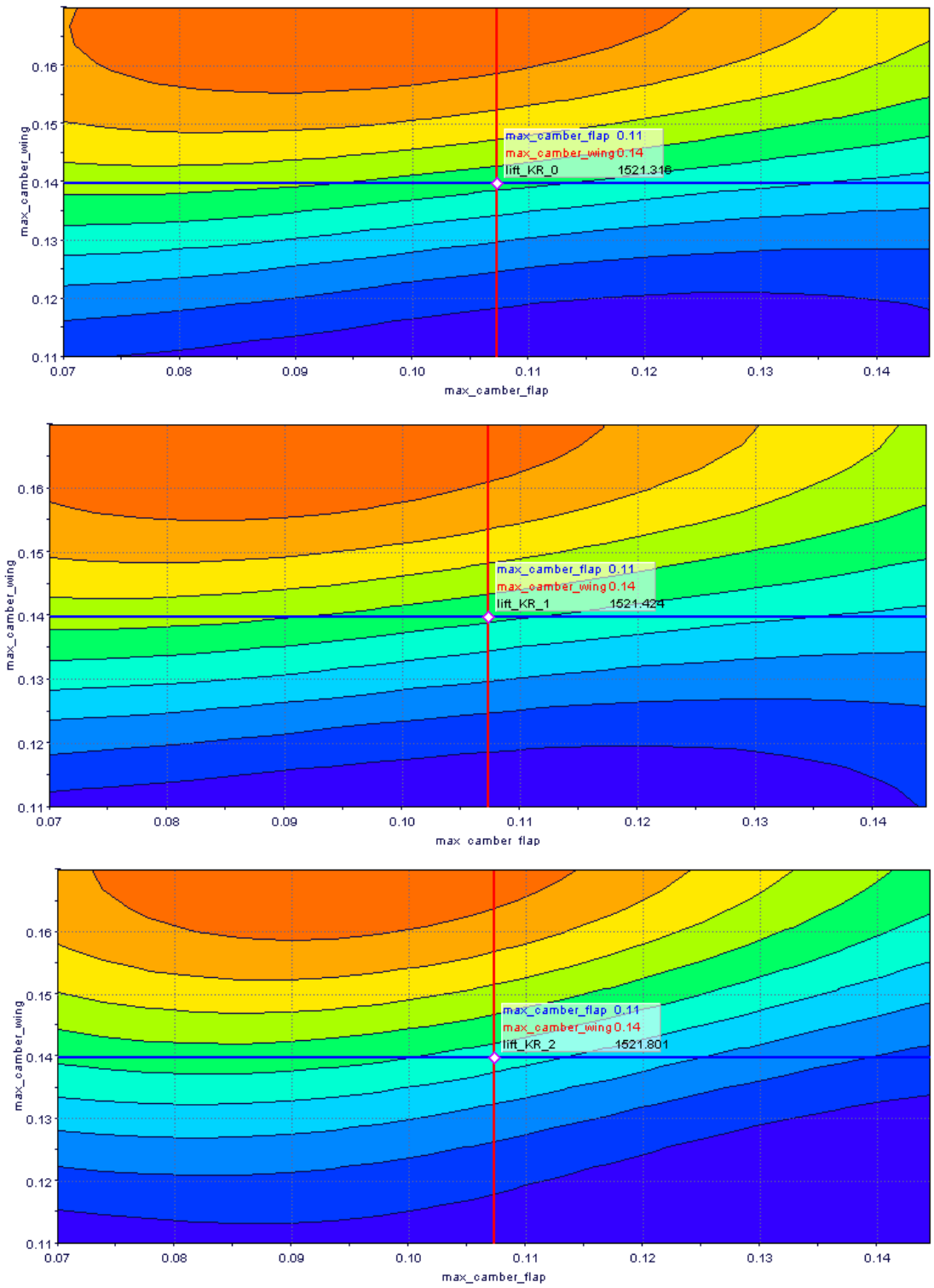

Fig. 2.72 - Kriging surface evolution (top view), from 14 to 15 to 16 points (experiments). X axis represents flap camber; Y axis main plane camber, and colors are dowforce. The maximum downforce is in the orange area, so it is the desired configuration.

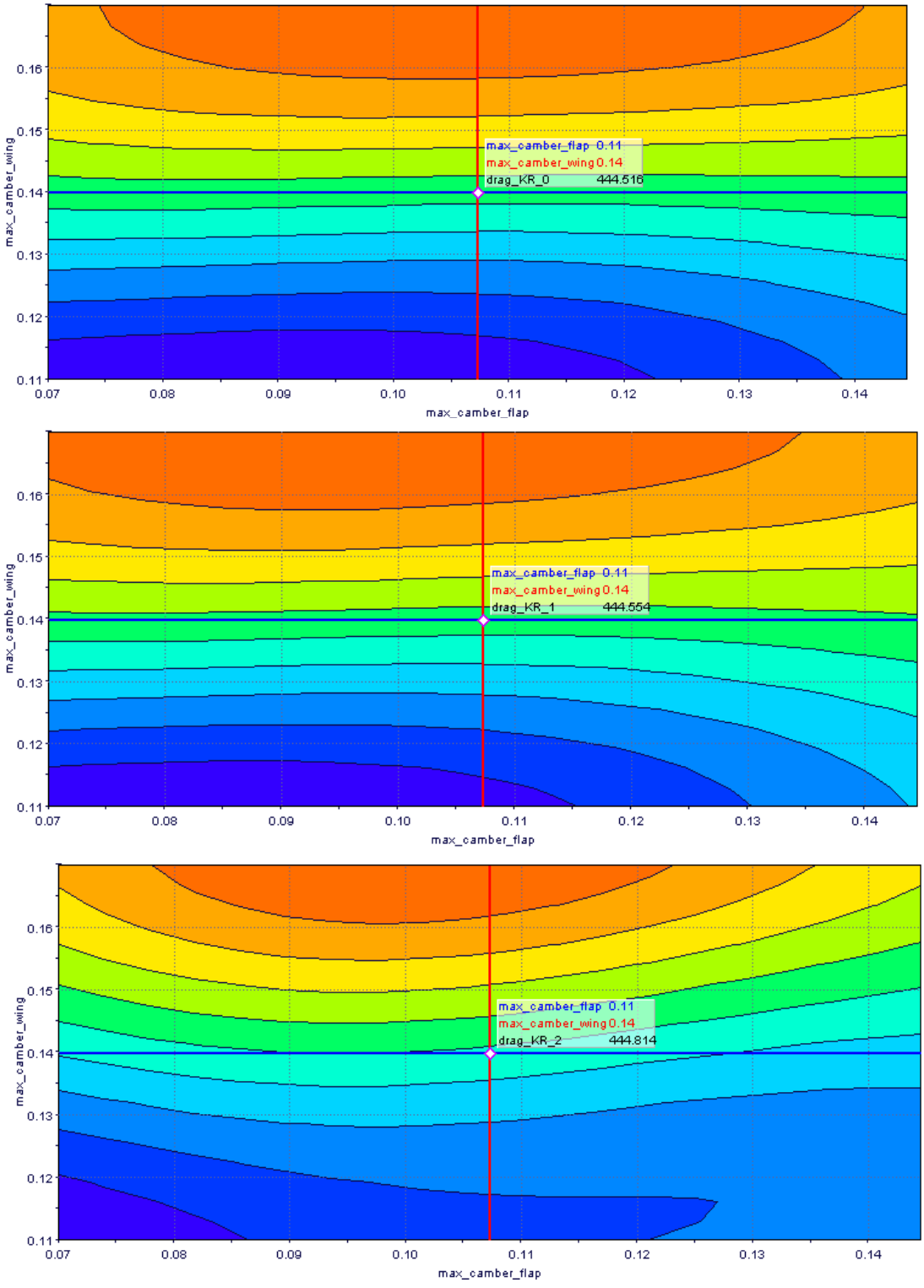

Fig. 2.73 - Kriging surface evolution (top view), from 14 to 15 to 16 points (experiments). X axis represents flap camber; Y axis Main plane camber; colors are drag. High drag is orange color, so it is desired to be in the dark blue zone. Notice the similarities between lift and drag surfaces, although they are slightly different, and the target areas are the opposite ones.

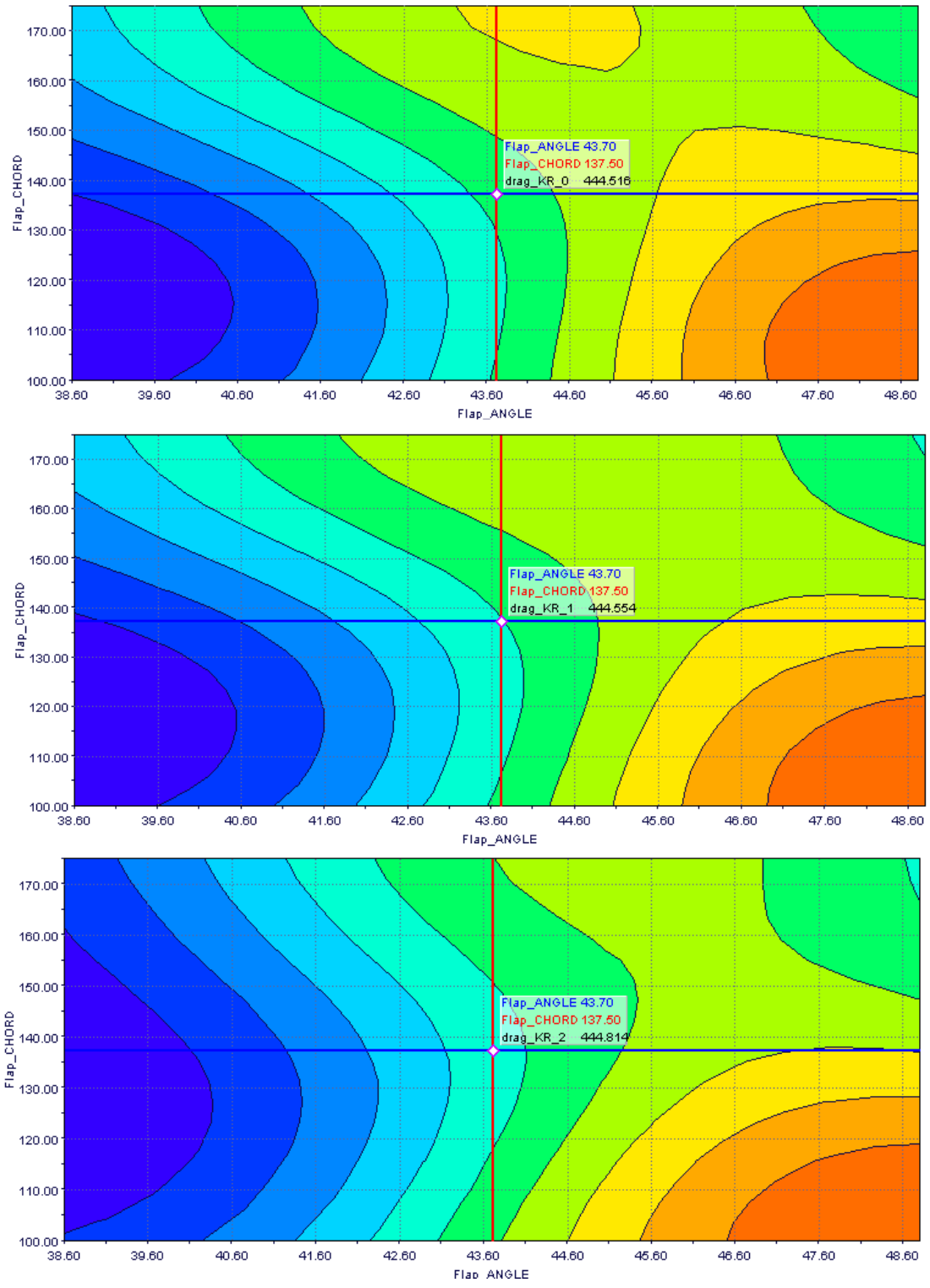

Fig. 2.74 - Kriging surface evolution (top view), from 14 to 15 to 16 points (experiments). X axis represents flap angle; Y axis flap chord; colors are drag. High drag is orange color, so it is desired to be in the dark blue zone. Notice the shape of the color distribution, completely different from the camber Kriging.

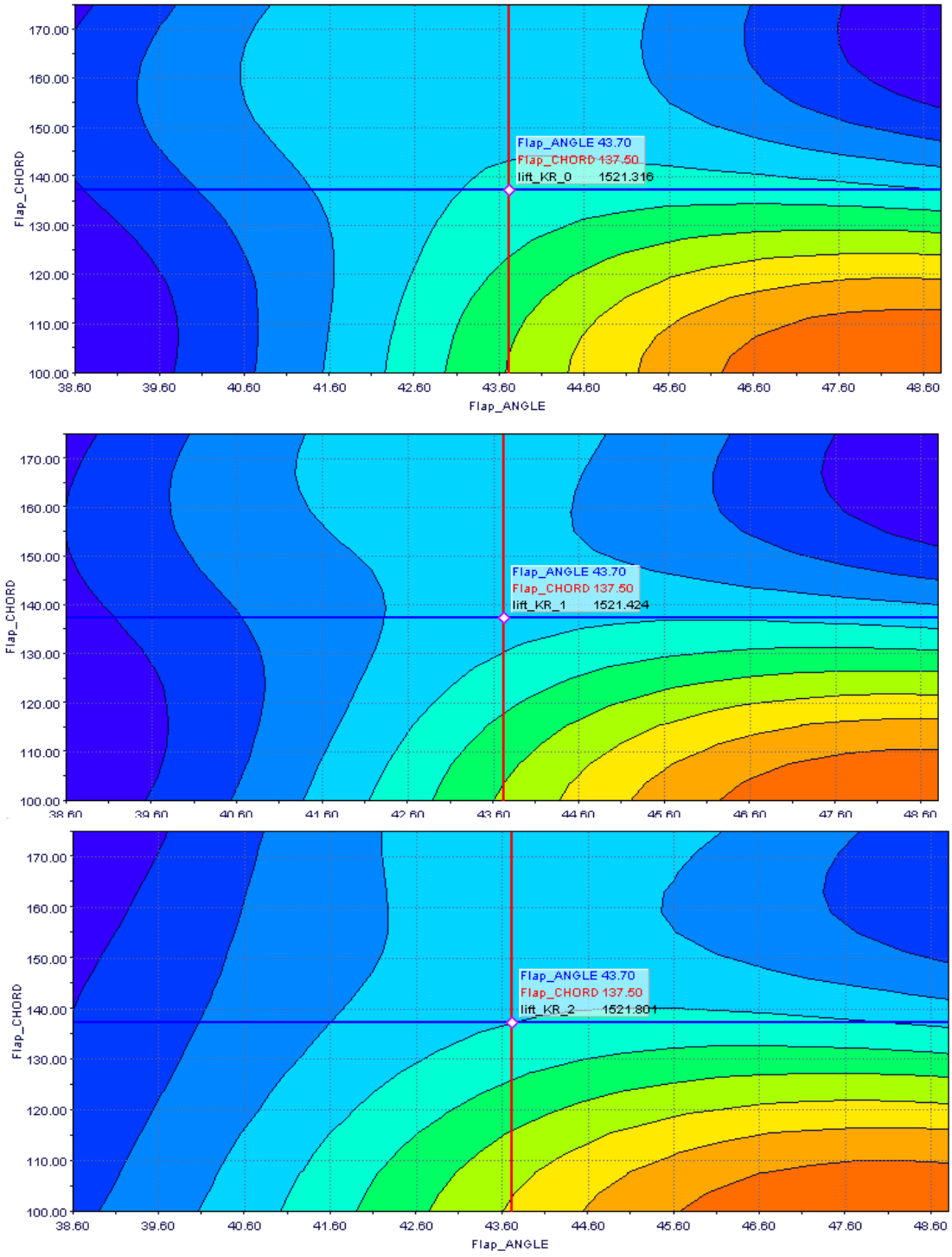

Fig. 2.75 - Kriging surface evolution (top view), from 14 to 15 to 16 points (experiments). X axis represents flap angle; Y axis flap chord; colors are downforce. High downforce is the orange color, so it is desired to be in there. Notice again the similarities between downforce and drag surfaces, although they are slightly different, and the target areas are the opposite ones. The target is to achieve maximum downforce area, while trying to avoid maximum drag peaks.

Not only is important to take decisions about the “best candidates”, but also to learn through the process. Each loop has different results and a different tendency, and the correlation between variables is very important, to understand how is each variable affecting each output of the design of the rear wing individually. This could be interesting for future developments of the rear wing, for instance an adaptation for a medium-low downforce track, or a super-high downforce track (like Monaco). The key is to understand which parameter can be changed to obtain a given target. For this reason, the “Correlation Matrix” is used, where the correlation between all parameters (inputs and outputs) can be seen, and it contains the R squared factor, which indicates the strength of the correlation. If it is close to 1, it means that if you increase the parameter X, the parameter Y will be increased (for -1, the parameters Y will decrease), with a very high confidence. If it is between 0.6 and 0.8 (or -0.6 to -0.8), the link between them is probable, but the degree of confidence is lower. For values between -0.6 and 0.6, a relation between both values can exist, but for experiments should be done in order to confirm it (going to +1 or -1) or dismiss it (going closer to 0).

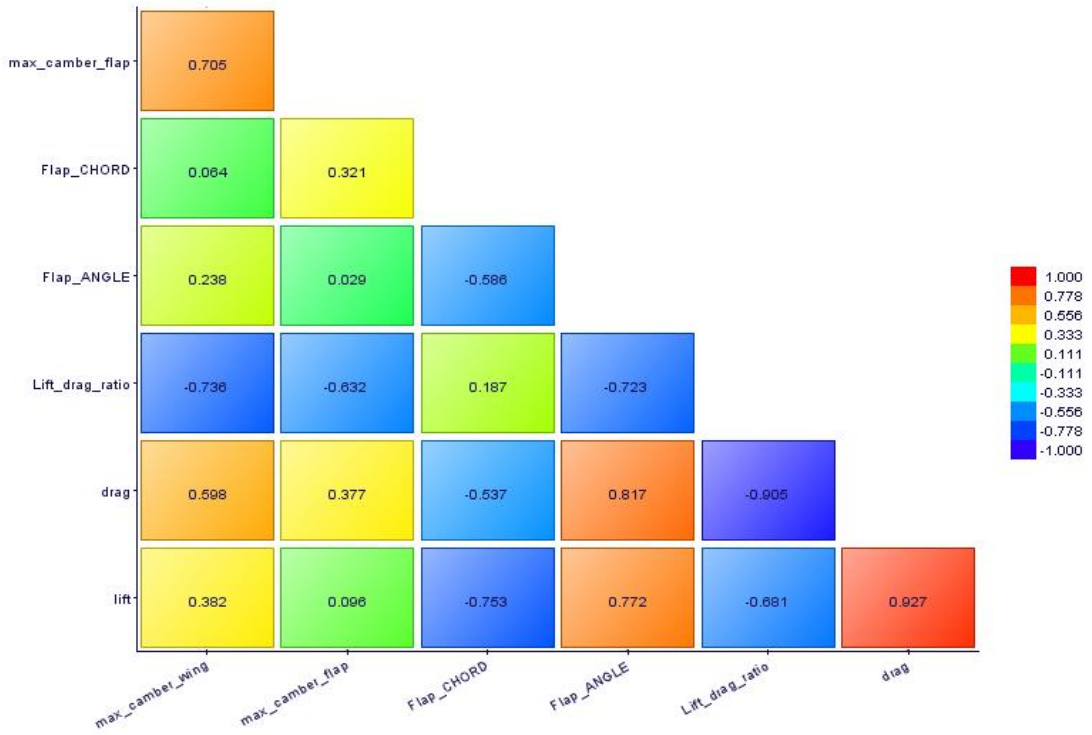

Fig. 2.76 – Correlation Matrix. Top values on Y axis are input variables, and bottom values are output results (lift to drag ratio, lift and drag). Notice the R squared number inside.

1st loop conclusions

Finally, the blue triangle **(Fig. 2.70)** is selected as the "best candidate" to be the optimum rear wing. It is situated in the middle of the cloud of points, it is better than all its neighbors, and it has slightly more downforce than the current Formula One baseline. So the new baseline parameters are:

Flap chord: 136mm
Flap Angle of attack: 43º
Flap camber: 10.3% of chord length
Main plane camber: 14,533% of chord length

Moreover, two conclusions can be obtained from this data, especially from the correlation matix:

-Longer flap chord decrease lift and drag, but it is not affecting the efficiency. However, increasing flap angle of attack increases downforce and lift (as the theory of wings says), but is making the rear wing less efficient.

- Both cambers don't have the same importance as flap angle of flap chord. However, increasing them will probably increase more drag than downforce, thus reducing efficiency. Therefore, they will be very low (10 % for the flap and 14.5 % for camber).

2.6.5- 2nd loop – Position maximum camber and thickness for Main plane & Flap

The same computing resources and algorithms as first loop are used. As the past loop was quite good with only the SOBOL algorithm exploration, this new experiment will consist in 9 (plus the baseline) points for the exploration and mapping for Kriging surface, and only 5 MOGA-II proposed designs for the optimization, thus having 15 designs to evaluate this loop.

epsilon EUSKADI

Fx	Fz	L/D	Configuration	
431,98	**1509,8**	**3,4951**	BSL01_t3	X_camber_wing 4; X_camber_flap 4; thk_wing 10%; thk_flap 10%
453,40	**1527,1**	**3,3681**	BSL01_t3	X_camber_wing 6; X_camber_flap 6; thk_wing 15%; thk_flap 15%
459,40	**1530,1**	**3,3306**	BSL01_t3	X_camber_wing 5.2; X_camber_flap 6; thk_wing 15%; thk_flap 15%
432,96	**1504,7**	**3,4754**	BSL01_t3	X_camber_wing 3.7; X_camber_flap 3.7; thk_wing 9%; thk_flap 8%
445,15	**1525,7**	**3,4274**	BSL01_t3	X_camber_wing 4.5; X_camber_flap 3.7; thk_wing 9%; thk_flap 12%
433,13	**1509,3**	**3,4846**	BSL01_t3	X_camber_wing 4; X_camber_flap 4.2; thk_wing 12%; thk_flap 9%
440,85	**1518,3**	**3,4440**	BSL01_t3	X_camber_wing 4.3; X_camber_flap 4.3; thk_wing 9%; thk_flap 12%
422,45	**1487,2**	**3,5204**	BSL01_t3	X_camber_wing 3.8; X_camber_flap 4.2; thk_wing 15%; thk_flap 12%
427,97	**1496,2**	**3,4960**	BSL01_t3	X_camber_wing 4; X_camber_flap 4; thk_wing 15%; thk_flap 12%
428,44	**1498,7**	**3,4980**	BSL01_t3	X_camber_wing 3.8; X_camber_flap 3.8; thk_wing 11%; thk_flap 11%
433,55	**1506,1**	**3,4739**	BSL01_t3	X_camber_wing 4.5; X_camber_flap 4; thk_wing 14%; thk_flap 10%
440,11	**1520,6**	**3,4550**	BSL01_t3	X_camber_wing 4; X_camber_flap 4.5; thk_wing 10%; thk_flap 14%
450,37	**1527,9**	**3,3925**	BSL01_t3	X_camber_wing 5.5; X_camber_flap 5.5; thk_wing 12%; thk_flap 12%
444,44	**1527,3**	**3,4365**	BSL_t2	X_camber_wing 5; X_camber_flap 5; thk_wing 12%; thk_flap 12%

Table 2.20 - Results of the second loop – Notice that colors are used to highlight best candidates.

The highlighted blue results are for the previous baseline, and the yellow is another candidate to be selected as the optimum. It is very interesting to observe the evolution of the loop, which is gaining efficiency while losing downforce (perpendicular to the isodrag red lines). However, it cannot increase its downforce, so the efficiency is falling dramatically after the former baseline configuration.

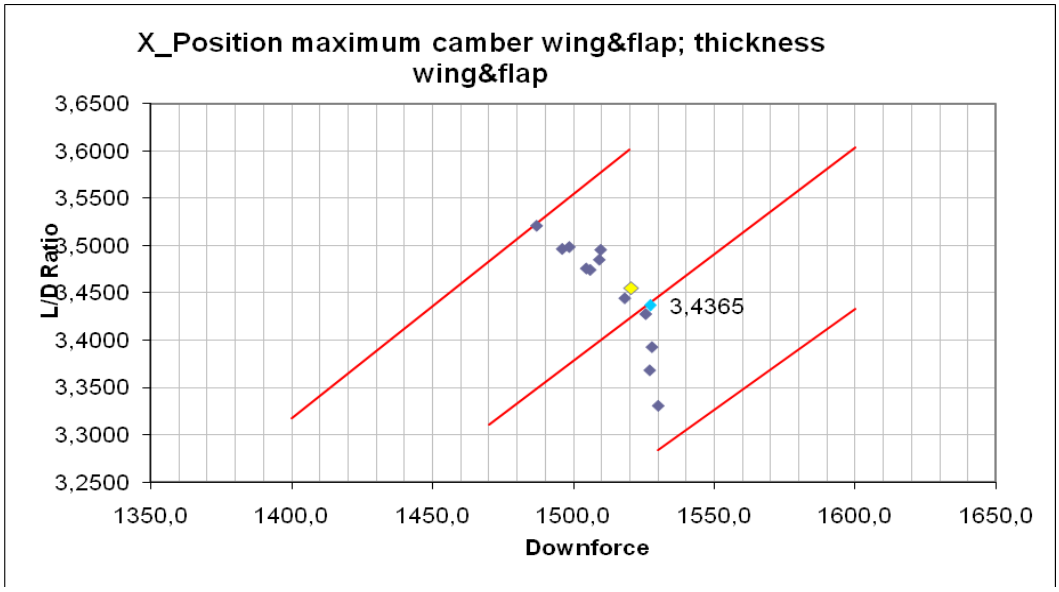

Fig. 2.77- XY graph of downforce Vs L/D Ratio. Notice the two highlighted candidates.

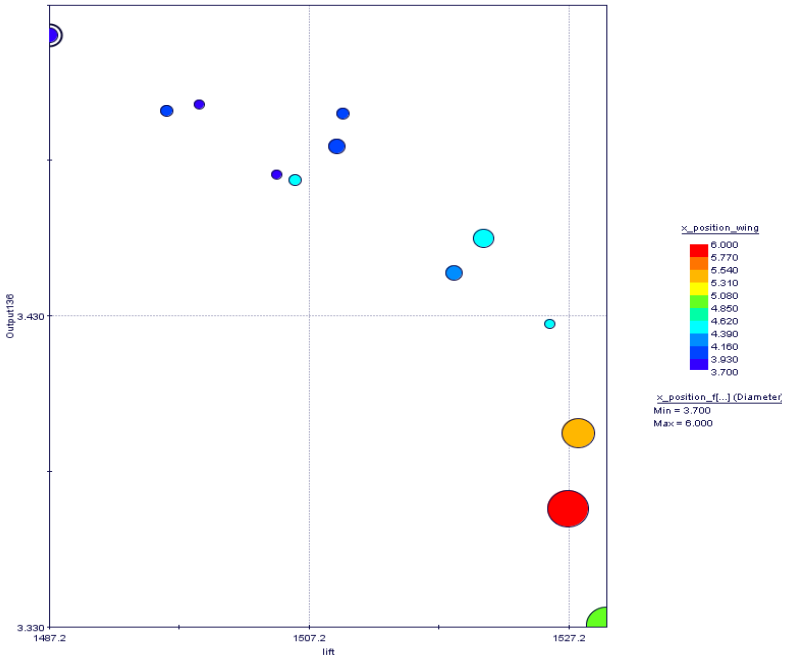

Fig 2.77b- 4D Bubble chart of position of maximum camber along the chord of the flap Vs position of maximum camber along the chord of the main plane.

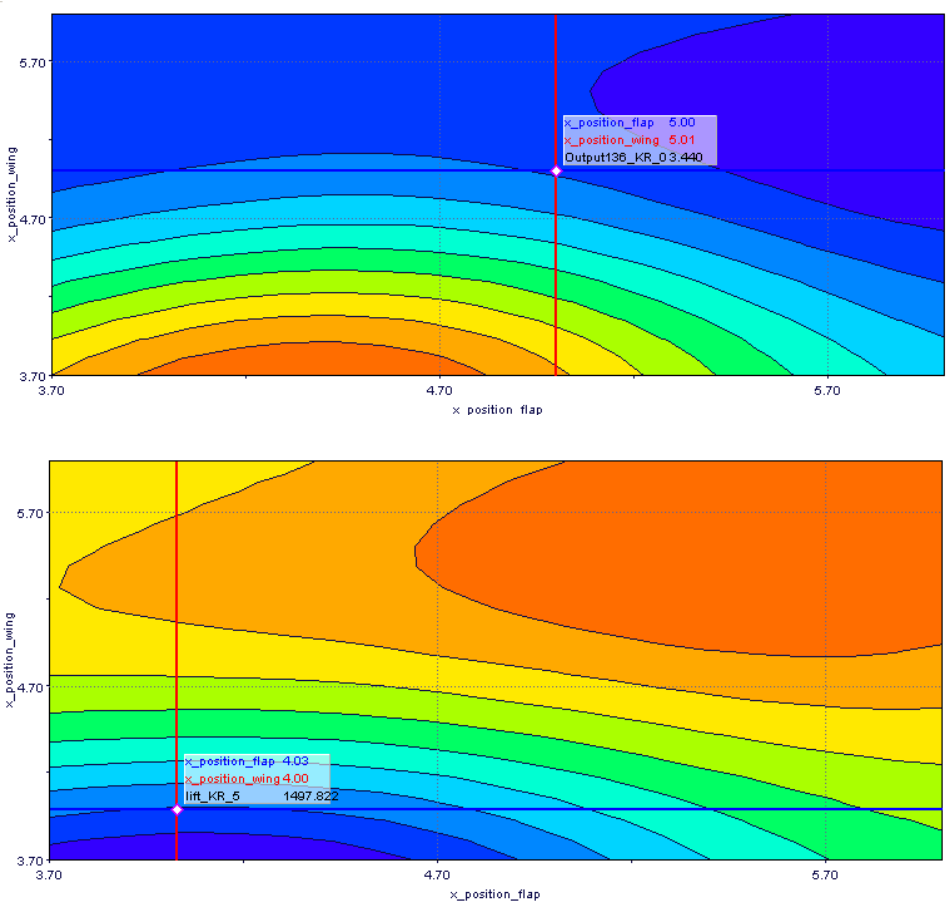

Fig 2.78 & 2.79- Lift to drag ratio (top) and downforce (bottom) Kriging surfaces. X axis represents the maximum camber position along the flap (in tenths of the chord), and Y axis the same for the main plane.

Unlike the first loop, here the comparison is between the Lift to drag ratio and downforce. This change is due the difficulty of comparing downforce and drag without knowing the efficiency of the wing. However, with downforce and lift to drag ratio, it is possible to think about the drag, because the lift to drag ratio has implicitly the drag value as the denominator.

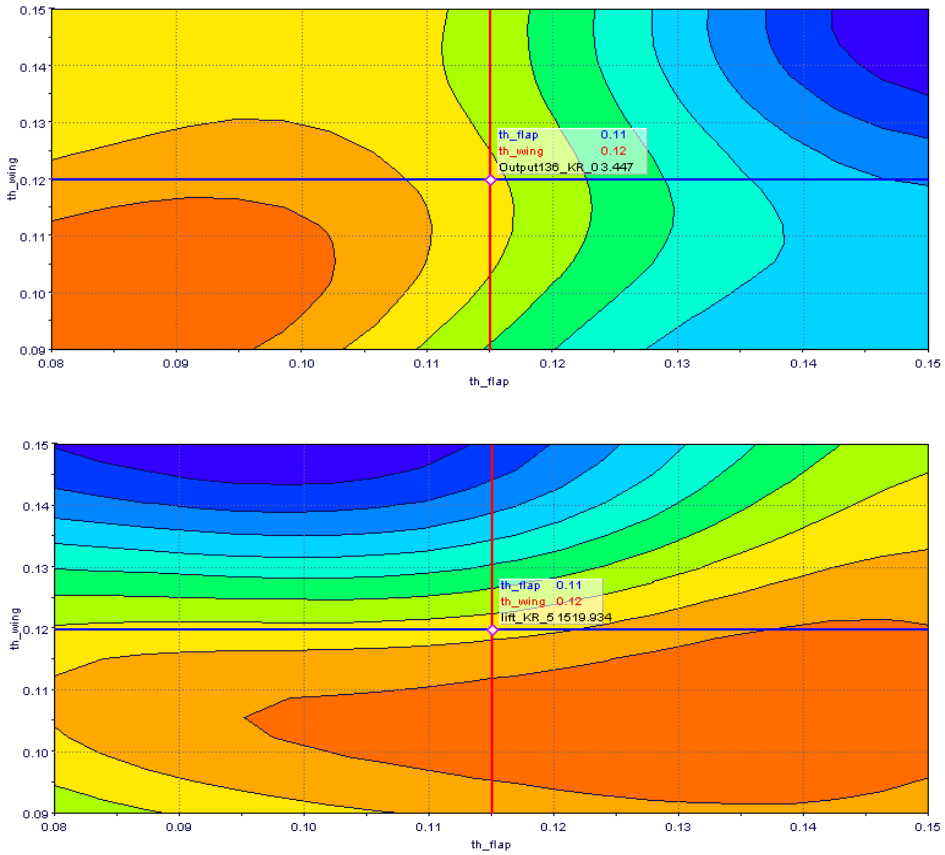

Fig 2.80 & 2.81 – Lift to drag ratio (top) and downforce (bottom) Kriging surfaces. X axis represents the thickness of the flap, and Y axis the thickness of the main plane. Notice the different shapes of each surface, so lower values (10-12% of chord) for both can easily reach a peak in downforce and efficiency.

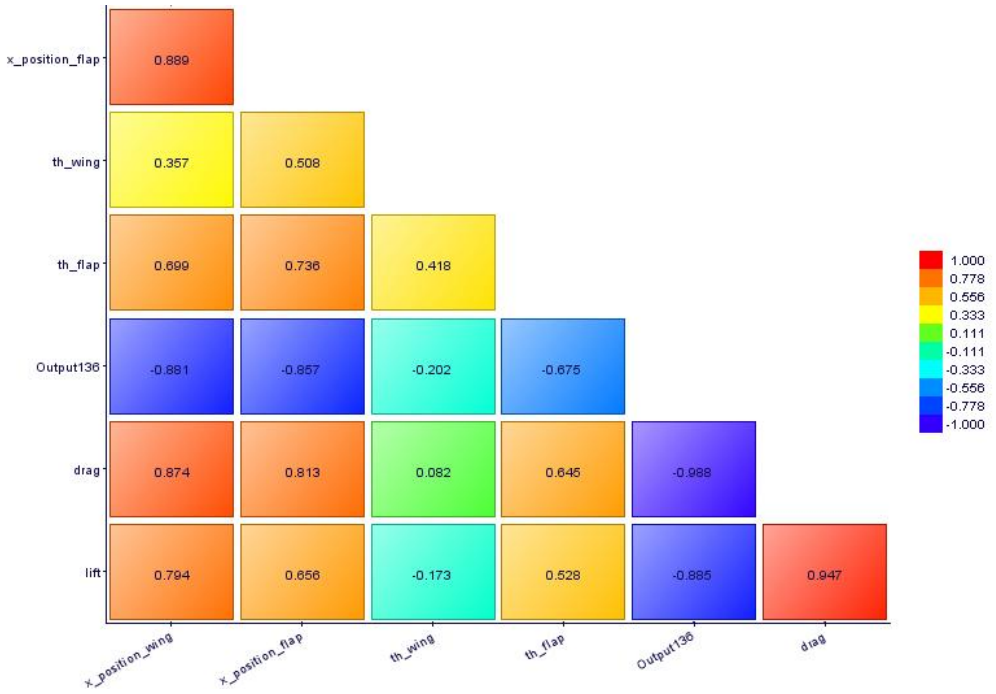

Fig. 2.82 – Correlation matrix for the second loop. Notice that “Output136” is the efficiency value.

2nd loop conclusions

It is very important to take into account that some Kriging surface can be very smooth and realistic; however, if the correlation matrix doesn’t give enough confidence for the correlation between values, it means that the optimum is being searched in a surface which is not reliable (which happens with the thickness surface). However, the position of the camber on the flap and the main plane is quite reliable. Moving backwards (increase x camber position) either the main plane or the flap will produce and increase on downforce and drag, but it will reduce the efficiency. So after considering the different candidates, it is decided to continue with the former baseline selected in loop 1, with the following values:

-Camber X position main plane: 5 (tenths of chord)
-Camber X position flap: 5 (tenths of chord)
-Main plane thickness: 12% (of chord length)
-Flap thickness: 12% (of chord length)

However, the yellow candidate will be considered if the evolution of this rear wing profile is not successful in the following loops, so it remains as the “alternative” candidate.

epsilon EUSKADI

2.6.6- 3rd loop – Gap and overlap

The same computing resources as the 1st and 2nd loop are used for the gap and overlap optimization. However, as a simple 2 variable optimization, it will only be done SOBOL exploration of the design space, with 10 new designs to be evaluated (apart from the former baseline already calculated).

Fx	Fz	L/D	Configuration				
437.8	1505.3	3.4383	BSL01_tgap	Gap	18,00	Overlap	25,00
438.89	1514	3.4496	BSL01_tgap	Gap	16,50	Overlap	17,5
439.03	1508.9	3.4369	BSL01_tgap	Gap	19,50	Overlap	32,50
444.42	1520.3	3.4209	BSL01_tgap	Gap	17,25	Overlap	28,75
422.3	1471.7	3.4850	BSL01_tgap	Gap	20,25	Overlap	13,75
451.63	1548.9	3.4296	BSL01_tgap	Gap	15,75	Overlap	36,25
436.42	1500.5	3.4382	BSL01_tgap	Gap	18,75	Overlap	21,25
450.95	1543.4	3.4226	BSL01_tgap	Gap	16,85	Overlap	38,125
431.32	1490.2	3.4550	BSL01_tgap	Gap	19,90	Overlap	23,125
448.24	1527.5	3.4078	BSL01_tgap	Gap	15,35	Overlap	30,625
444.44	1527.3	3.4365	BSL_t2	Gap	15,00	Overlap	20,00

Table 2.21 - Results of the third loop – Notice that colors are used to highlight best candidates. Best configuration of 2nd loop is highlighted in blue.

Remember that in Formula 1, minimum gap allowed are 15mm. Looking at the candidates and the X/Y graph, it is clearly seen that a combinaion of small gap (close to 15 mm) and a big overlap is the best combination, thus giving a lot of downforce keeping nearly the same efficiency. Notice the “hypothetical” pareto frontiers in violet, the former one over the blue candidate, and the new one over the orange one.

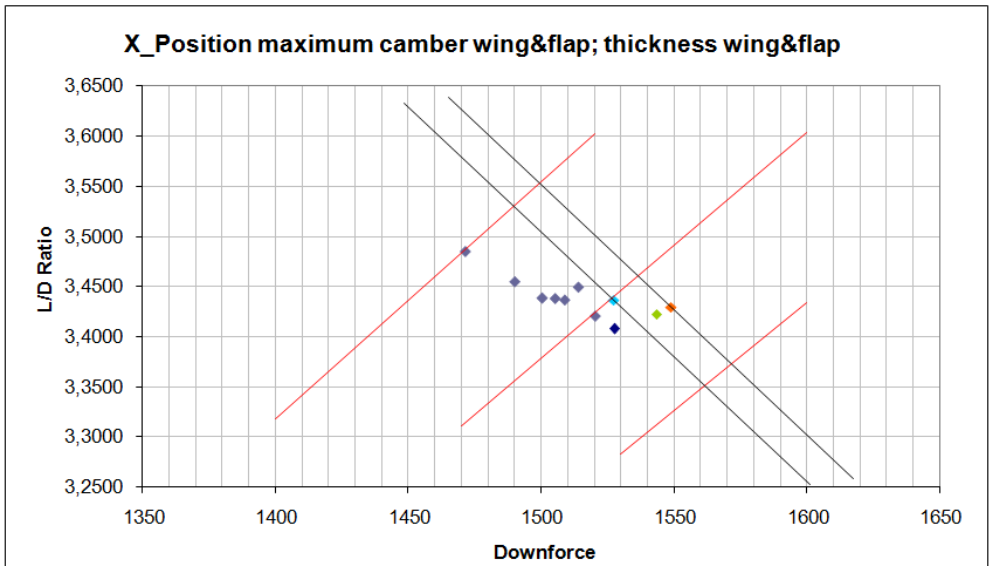

Fig. 2.83- XY graph of downforce Vs L/D Ratio. Notice the green and orange highlighted candidates.

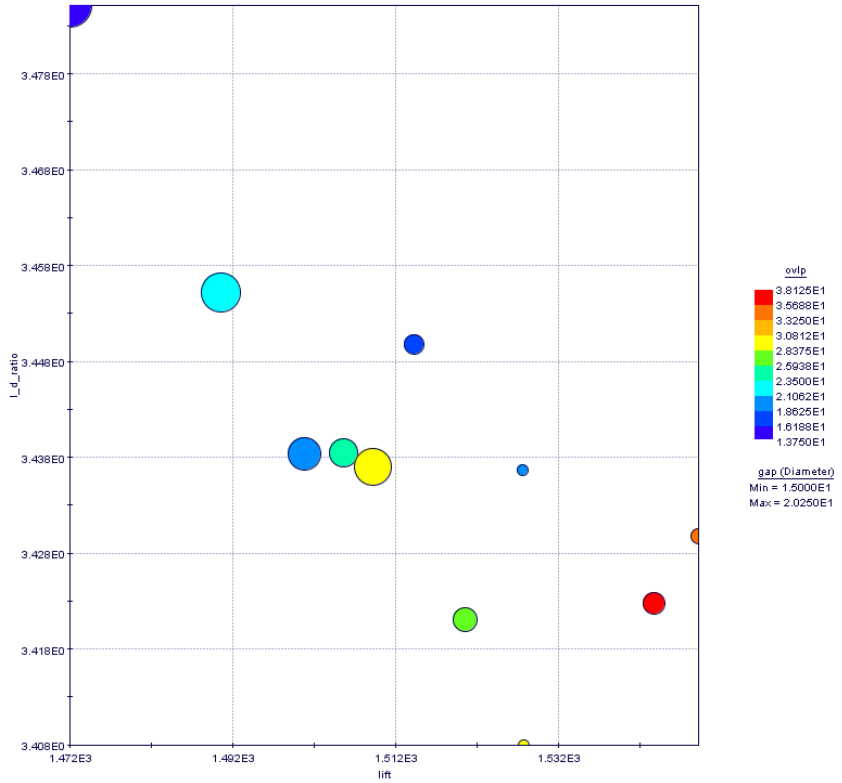

Fig 2.84 – 4D Bubble chart, Lift vs L/D Ratio, colors are overlap size and bubble diameter are gap size.

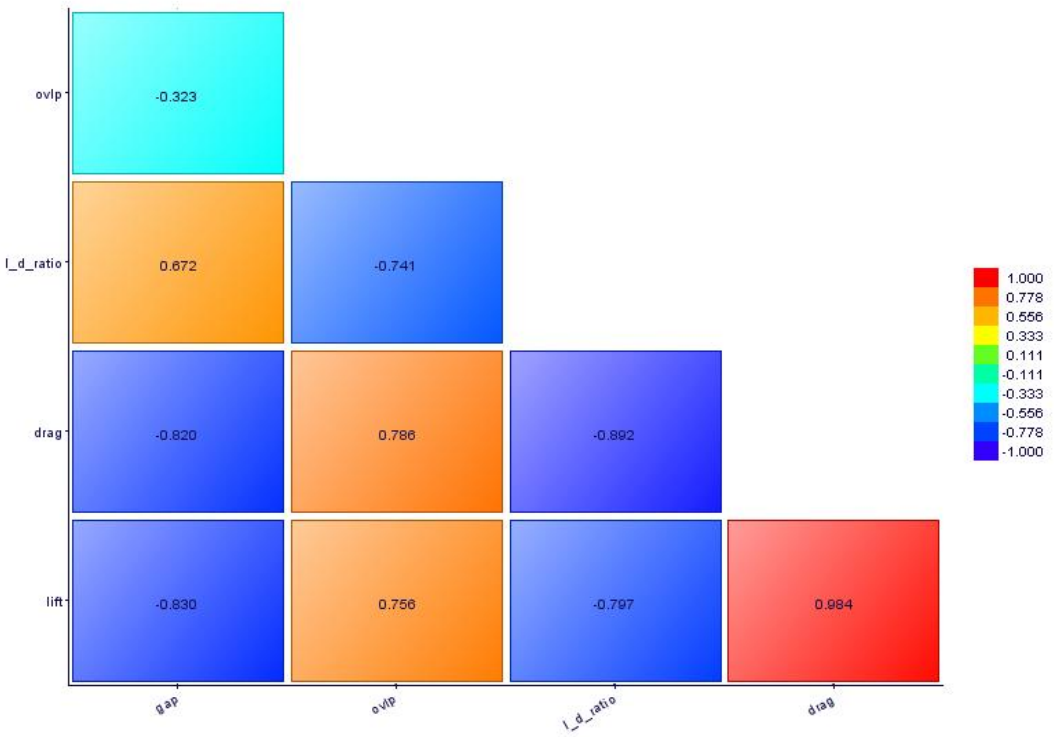

Fig 2.85 – Correlation matrix. Notice very strong colors, which shows a strong correlation of gap & overlap with drag & downforce.

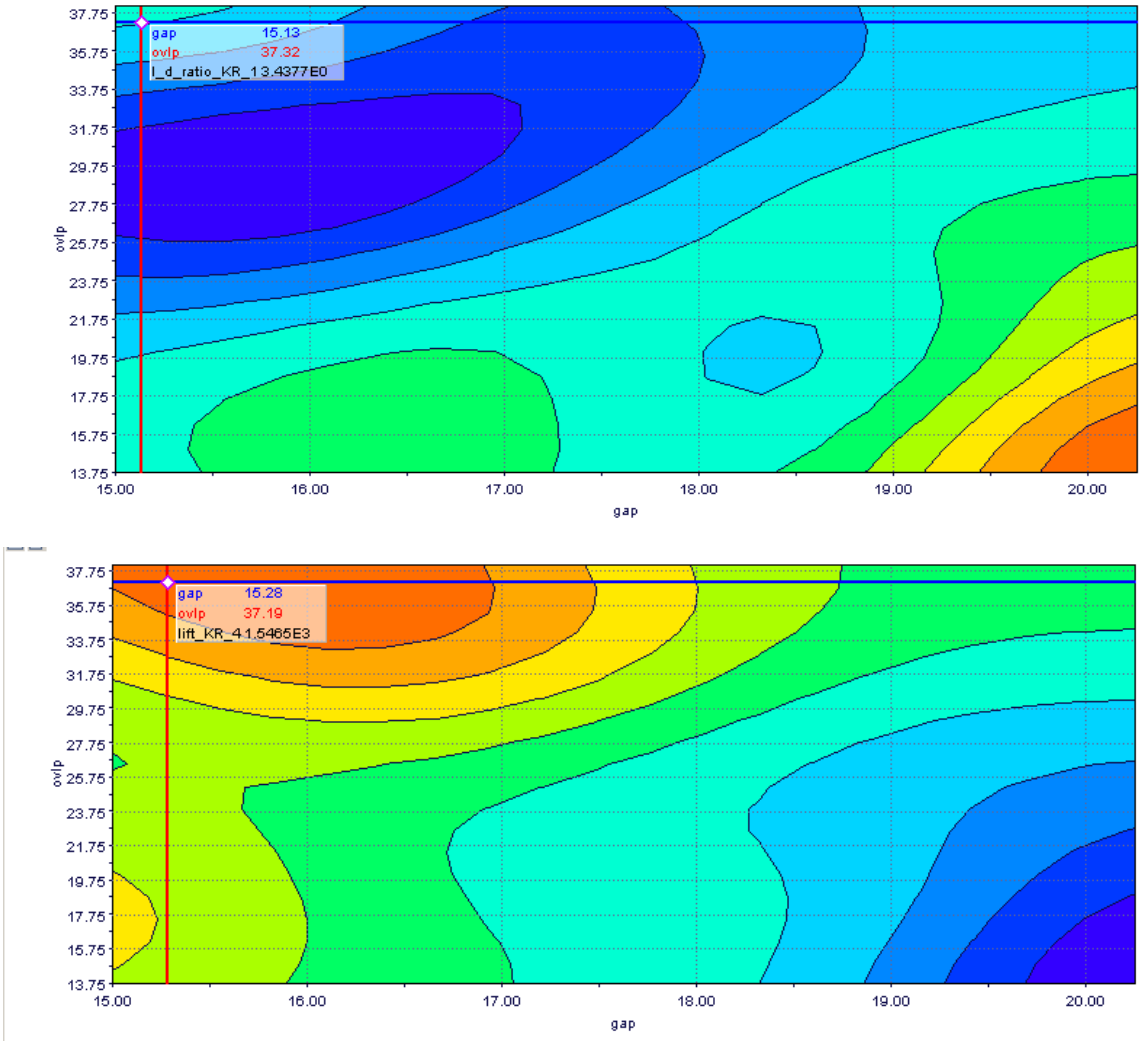

Fig 2.86 & 2.87 – Lift to drag ratio (top) and downforce (bottom) Kriging surfaces. X axis represents the gap (minimum distance between the main plane and flap), and Y axis represents overlap (superposition in top view of the flap over the main plane). Notice the different shapes of each surface, although bottom right corner is similar (bigger gap and smaller overlap is very efficient but does not produce enough downforce), the top left corner is slightly different, having the peak of dowforce, but not the minimum efficiency, thus having bigger overlap and smaller gap as the best compromise.

3rd loop conclusions

The simplest loop is giving very interesting information of the relative position of the main plane and flap to improve its performance. However, it is essential to remember that a two-element wing must be designed together, which means that this experiment can lead to wrong conclusions. For this profile of main plane and flap, a small gap (close to the limits of the rules) and a big overlap gives the best amount of

downforce while keeping the same lift to drag ratio (efficiency). It is good information for this rear wing, but cannot be extrapolated, as different profiles of main plane and flap may be less sensitive to overlap or gap, or both. The trailing edge of the main flap must be designed in order to redirect the flow to the lower surface of the flap, and the overlap must be designed in order to accelerate the flow between both elements. Therefore, for this configuration of main wing and flap, the best candidate to become the new baseline is the orange one, which has 0.2% less efficiency but 1.62% more downforce:

BASELINE_02

-New Gap: 15,75mm

-New Overlap: 36,25mm

However, to obtain the maximum potential of a loop with different gap & overlap values, other parameters should be considered, like maximum camber or camber x position along the chord of the main plane, and/or thickness of the main plane, to combine gap and overlap potential with a good design of the trailing edge of the main plane to maximize the performance of the flap, which could not be calculated in this project due to lack of resources.

2.6.7 - 4th loop - 3D shape of the main plane and flap assembly

Initially, the development of the rear wing has been bidimensional in a 3D environment. The wing has been generated making a simple straight extrusion of the main plane and flap profile until the endplates. However, any rear wing thoroughly developed is far from being a simple straight extrusion of a simple profile, although this initial step is often seen in the pre-season testing in many cars. Moreover, when there are important changes in the regulations, the complete aero package must be done from scratch, and this “simplified” straight profile is often used.

Fig. 2.88 – Toyota F1 with extremely developed shapes (right) from 2008 season, and the adaptation of the aero packaging for 2009 season (left), with completely straight profiles **[10].**

Fig 2.89 – Renault F1 2010 car launch (left) and the evolution after a few weeks of testing (right) during the winter tests in Jerez, 2010. Notice the "seagull" shape of the main plane **[10]**.

Furthermore, the rear wing of a Formula 1 is very different from a conventional airplane wing. Apart from being regulated by very strict rules, the whole rear wing is at the back of the car. That means that is highly influenced by the elements in front of it. Some of them are developed to clean the airflow, or to redirect some air to improve its performance (front wing, sidepods…). However, other elements exist which make the clean air worse (they create a huge amount of turbulence and drag), and cannot be covered due to regulations, like the wheels or the helmet of the driver, (unlike LeMans Series, where the rules are not so strict). Therefore, the flow in the central section is not the same as the flow close to the endplates. **Visualization is the KEY** to develop the final shape of the rear wing, and CFD is the king in this aspect. There are many different ways to show the flow in any CFD software, like speed/pressure colored streamlines commonly seen, but in fact to "understand" the rear wing the most used are the **Cp videos (pressure coefficient) and the "Oil flow".** The Cp is a sequence of cross-sectional images of the total pressure coefficient values around the car. Animating this sequence of pictures, a video is created, which is a 2D sweep of the whole car, **which is used to understand where the turbulence is, where the vortex are generated and to understand flow energy**, and it is frequently compared with new baselines to understand how a specific change in the car is affecting the whole aero package. **It has extensively been used to check correlation between full 60 million mesh car and progressive mesh downsizing.** The alternative, more intuitive, is the "Oil flow", or constrained streamlines, which are flow streamlines on the surface of the bodywork, just like the paint used in wind tunnel models or track testing. It is very easy and quick to generate (unlike Cp videos), and **is mainly used to detetct if there is boundary layer separation on the suction side of the wings, and to improve the leading edge position of the main plane of the rear wing or the beam wing (lower element**).

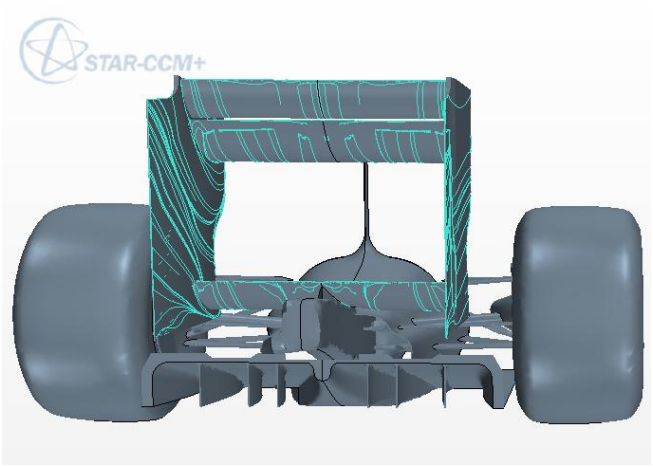

Fig 2.90 & 2.91 – Real Oil flow during testing (green paint) **[10]**, Red Bull F1 2010 season (left) and virtual Oil flow generated on the Epsilon Euskadi F1 prototype with CFD software.

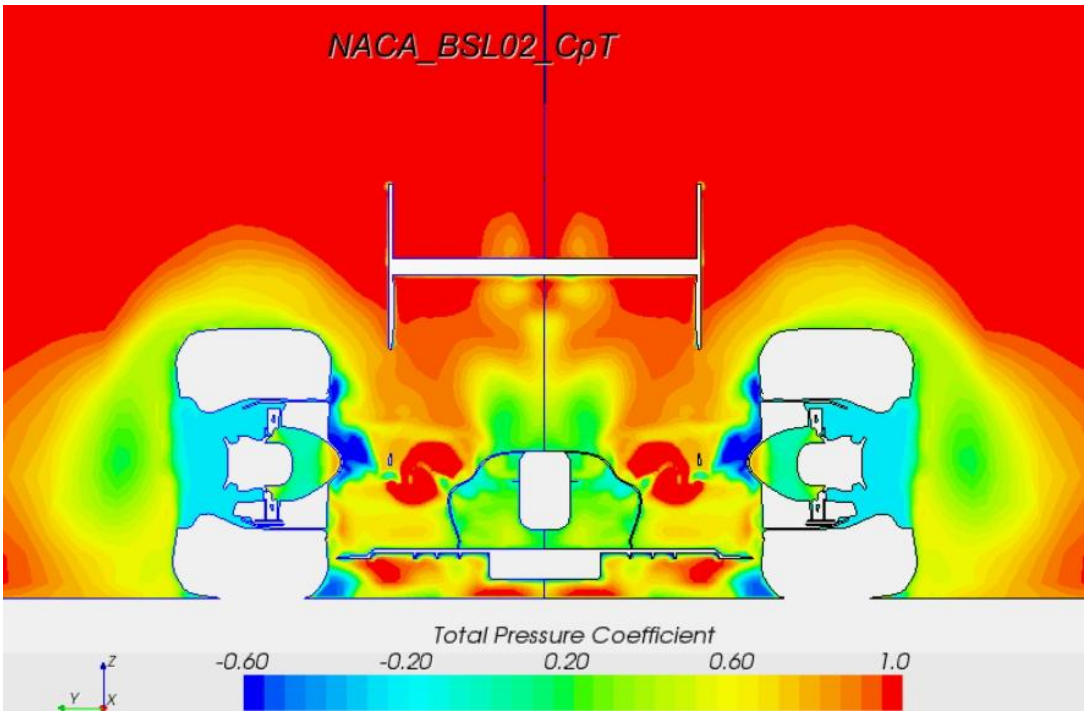

Fig 2.92 – Total Pressure coefficient picture, from YZ plane cross-sectional view, just after main plane leading edge.

Finally, the 4th loop to develop the 3D wing is a mixture between ModeFrontier optimization and the conclusions extracted from it, and the chief aerodynamicist experience to understand the flow behavior. As explained in section 2.4 of this chapter, the parametric design of the main plane and flap assembly is divided into 3 different parts (4 cross-sectional profiles to control the shape). As explained before, graphic

methods will be used to evaluate which parameters should be improved in each group of simulations. In fact, the parameters are always the same (wing chord, angle of attack, Y position of the profile to control the shape), but the range of values is the key parameter. For example, near the endplate, induced drag can be reduced with a more conservative approach (that is, lower angle of attack or lower chord). Therefore, the range in a "group" of simulation can be from original chord length to 20% chord reduction. Depending on results, this reduction could reduce the drag significantly or could be unsatisfactory. Even a chord increase could increase significantly downforce while having a negligible increase in drag. In this situation, the next "group" of simulations would have a different range of values opposite to the former one. **To sum up, the objective is not to find the best rear wing, but the best rear wing working behind the wake of the whole car.** This can lead to take "unusual" solutions, but this is due to the conditions of the flow in front of the rear wing, affected by the wheels, etc.

Considering the methodology of the optimization, the resources and time available, the 4th loop will be an exercise of "fine tunning" rather than a radical evolution. Therefore, corrections will be done in two specific areas: the central section (where the flow is different due to the intake manifold, driver helmet and shark fin interaction) and the area in contact with the endplates, due to the influence of the endplates, wheel turbulence and the possibility to decrease induced drag. Moreover, the central section of the main plane and flap (+/- 75mm from the car centerline) is nearly free of restrictions, so the chord can be increased, and other elements could be added. However, as an exercise of fine tunning, no extra elements will be added (they are only used for high-downforce tracks, and they are not as efficient as the main plane and flap assembly).

Finally, the 4th loop has 4 different optimization groups, each one with slightly different ranges and/or step, and the optimization algorithm parameters where also modified to understand better its behavior. As the improvement with this final loop is very small, the number of simulations is increased significantly. The number of simulations for each group was adjusted to fit into the schedule of the F1 development program and to take advantage of the computing resources available.

The parameters modified are:

Alpha1: central section angle of attack (degrees from baseline, positive for higher leading edge).

C1: central section chord of the main plane (mm). Notice that the flap grows proportionally to keep the same gap and overlap (this central section is not under the regulation box, so the leading edge of the main plane moves forward).

C4: endplate section chord (mm). Notice that this chord cannot grow further than the regulation box (the leading edge of the endplate).

Y3: Position of the third control profile (mm from car centerline).

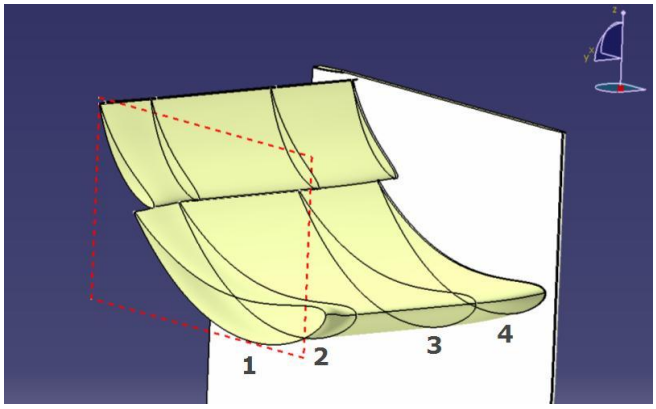

Fig 2.93 – Control profiles of the rear wing numbered (Model split by the symmetry plane).

Group 1

Fx	Fz	L/D	Configuration									
452.68	**1538.4**	**3.3984**	NACA_BSL02	alpha1	0	c1	137.5	c4	122	y3	302.5
456.93	**1554**	**3.4010**	NACA_BSL02	alpha1	0.375	c1	146.88	c4	131	y3	345.62
421.88	**1375.2**	**3.2597**	NACA_BSL02	alpha1	2.625	c1	128.12	c4	113	y3	289.38
452.59	**1532.6**	**3.3863**	NACA_BSL02	alpha1	-1.5	c1	131.25	c4	116	y3	276.25
425.73	**1402.4**	**3.2941**	NACA_BSL02	alpha1	2.25	c1	128.12	c4	113	y3	263.12
450.6	**1538.1**	**3.4134**	NACA_BSL02	alpha1	1.3125	c1	135.94	c4	111.5	y3	303.44
450.32	**1548.1**	**3.4378**	NACA_BSL02	alpha1	0.9375	c1	139.06	c4	132.5	y3	331.56
426	**1410.9**	**3.3120**	NACA_BSL02	alpha1	1.4062	c1	128.91	c4	130.25	y3	296.41
448.74	**1543.1**	**3.4387**	NACA_BSL02	alpha1	2.9062	c1	141.41	c4	118.25	y3	333.91
450.59	**1544.7**	**3.4282**	NACA_BSL02	alpha1	0.65625	c1	135.16	c4	124.25	y3	316.16

Table 2.22 - Results of Group 1, 4th loop

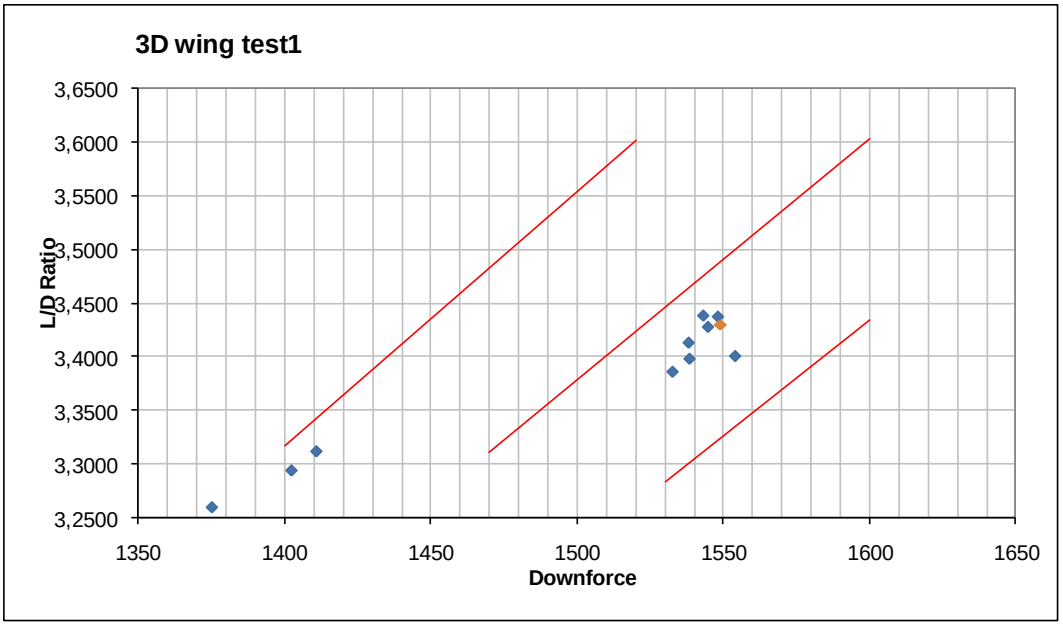

Fig 2.94 – XY graph of Downforce Vs L/D Ratio for the 1st group of the 4th loop. There are several points around the Baseline_02 (orange), but none of them are really better in downforce and efficiency.

Group 2:

Fx	Fz	L/D	Configuration								
452.39	**1553.4**	**3.4338**	NACA_BSL02	alpha1	1.125	c1	140.625	c4	125	y3	326.8750
446.02	**1537.2**	**3.4466**	NACA_BSL02	alpha1	0.09375	c1	133.5938	c4	128.75	y3	310.4687
448.59	**1548.3**	**3.4513**	NACA_BSL02	alpha1	0.375	c1	146.875	c4	131.3572	y3	333.9063
426.82	**1432.9**	**3.3570**	NACA_BSL02	alpha1	1.40625	c1	130.217	c4	130.25	y3	287.0439
444.75	**1529.7**	**3.4393**	NACA_BSL02	alpha1	0.4933	c1	135.9372	c4	111.5032	y3	312.8125
447.42	**1541.3**	**3.4449**	NACA_BSL02	alpha1	0.9375	c1	139.0625	c4	132.4488	y3	331.5625
443.19	**1530.7**	**3.4539**	NACA_BSL02	alpha1	0.4933	c1	135.9372	c4	110.318	y3	310.4687
447.16	**1535.8**	**3.4345**	NACA_BSL02	alpha1	0.9375	c1	139.3902	c4	110.7244	y3	329.2188
452.37	**1544.3**	**3.4138**	NACA_BSL02	alpha1	0.4934	c1	146.875	c4	131.3604	y3	333.9063
448.59	**1548.3**	**3.4513**	NACA_BSL02	alpha1	0.375	c1	146.875	c4	131.3572	y3	333.9086
442.78	**1540.0**	**3.4779**	NACA_BSL02	alpha1	0.09375	c1	133.5938	c4	128.75	y3	291.7441
427.81	**1429.0**	**3.3403**	NACA_BSL02	alpha1	1.40625	c1	130.217	c4	131.0692	y3	287.0439
446.98	**1539.0**	**3.4431**	NACA_BSL02	alpha1	0.9375	c1	139.0625	c4	132.2512	y3	289.3750
426.13	**1429.0**	**3.3534**	NACA_BSL02	alpha1	1.40625	c1	130.217	c4	130.3884	y3	310.4687
446.67	**1532.5**	**3.4310**	NACA_BSL02	alpha1	0.09375	c1	133.5937	c4	131.3572	y3	333.9063
452.37	**1544.3**	**3.4138**	NACA_BSL02	alpha1	0.4934	c1	146.875	c4	131.3604	y3	333.9104
450.82	**1541.4**	**3.4190**	NACA_BSL02	alpha1	1.1814	c1	146.875	c4	131.3572	y3	333.9063

Table 2.23 - Results of Group 2, 4th loop – Notice green candidate, highlighted as best candidate.

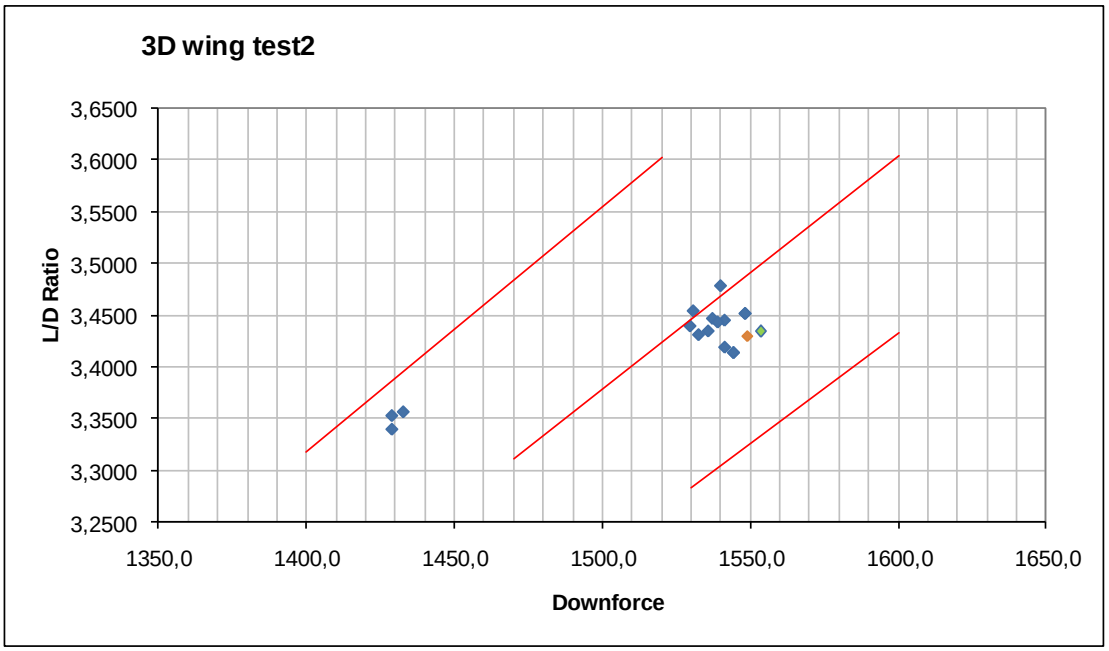

Fig 2.95 – XY graph of Downforce Vs L/D Ratio for the 2nd group of the 4th loop. There are many points close to the Baseline 02 (orange), but perhaps 3 of them can be considered as candidates to become the new baseline. However, only one point is giving both more efficiency and downforce (green point), so having demonstrated that higher efficiency is easily achieved with more conservative wing design, the final candidate to become the Baseline03 is the one with more downforce (green point).

Group 3:

Fx	Fz	L/D	Configuration									
447.20	**1541.9**	**3.4480**	NACA_BSL02	alpha1	1.125	c1	140.625	c4	123.7028	y3	296.4062
417.49	**1371.0**	**3.2839**	NACA_BSL02	alpha1	2.625	c1	128.125	c4	130.25	y3	296.4062
447.32	**1544.4**	**3.4526**	NACA_BSL02	alpha1	0.9375	c1	139.0625	c4	132.6416	y3	345.625
420.59	**1402.6**	**3.3347**	NACA_BSL02	alpha1	1.40625	c1	128.9063	c4	131	y3	345.625
418.48	**1376.8**	**3.2900**	NACA_BSL02	alpha1	2.625	c1	128.5767	c4	132.6416	y3	345.625
446.73	**1542.0**	**3.4518**	NACA_BSL02	alpha1	0.9375	c1	138.6108	c4	130.25	y3	296.4062
420.59	**1402.6**	**3.3347**	NACA_BSL02	alpha1	1.40625	c1	128.9063	c4	131	y3	345.625
447.32	**1544.4**	**3.4526**	NACA_BSL02	alpha1	0.9375	c1	139.0625	c4	132.6416	y3	345.625
445.81	**1543.7**	**3.4626**	NACA_BSL02	alpha1	1.125	c1	140.625	c4	125	y3	345.625
422.68	**1400.1**	**3.3124**	NACA_BSL02	alpha1	1.40625	c1	128.9063	c4	131	y3	345.9176
447.32	**1544.4**	**3.4526**	NACA_BSL02	alpha1	0.9375	c1	139.0625	c4	132.642	y3	345.625
417.49	**1371.0**	**3.2839**	NACA_BSL02	alpha1	2.625	c1	128.125	c4	130.25	y3	296.4062
447.93	**1540.6**	**3.4393**	NACA_BSL02	alpha1	0.9375	c1	139.0625	c4	132.298	y3	296.4062
424.91	**1416.2**	**3.3329**	NACA_BSL02	alpha1	0.37585	c1	128.8653	c4	131	y3	345.625
417.49	**1371.0**	**3.2839**	NACA_BSL02	alpha1	2.625	c1	128.125	c4	130.25	y3	296.4062
447.32	**1544.4**	**3.4526**	NACA_BSL02	alpha1	0.9375	c1	139.0625	c4	132.6416	y3	345.625
423.88	**1402.8**	**3.3094**	NACA_BSL02	alpha1	1.40625	c1	128.9063	c4	129.8224	y3	326.875

Table 2.24 - Results of Group 3, 4th loop

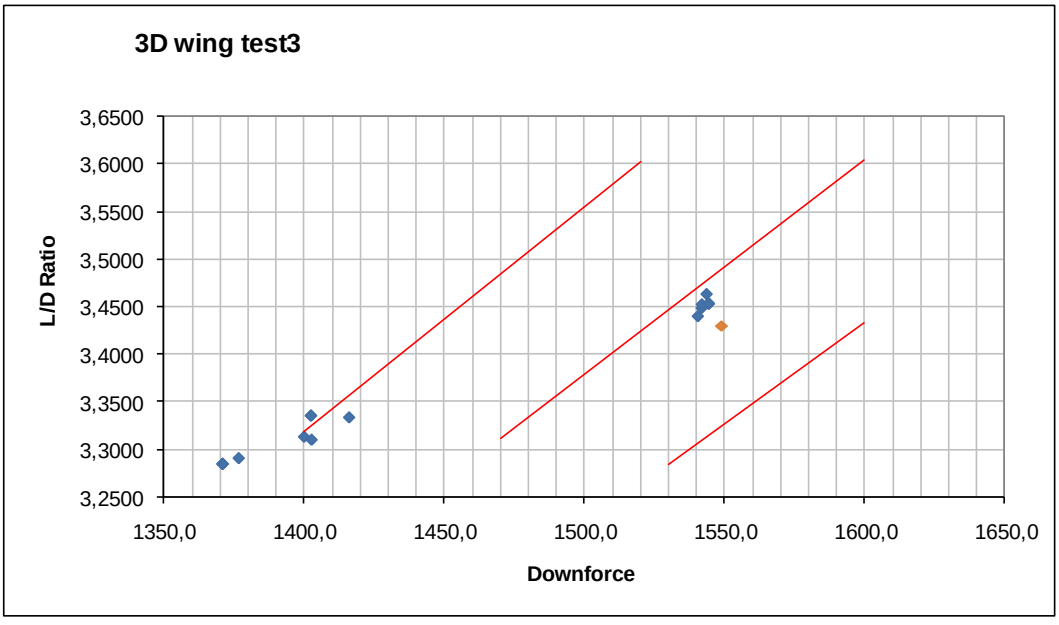

Fig 2.96 – XY graph of Downforce Vs L/D Ratio for the 3rd group of the 4th loop. There are some points close to the Baseline 02 (orange), with higher efficiency but less downforce. As the objective of this loop is to increase downforce and efficiency, no candidates are selected to become Baseline 03, as the increase of efficiency is not enough to justify the loss of downforce.

Group 4:

Fx	Fz	L/D	Configuration									
449.48	**1543.1**	**3.4331**	NACA_BSL02	alpha1	1.125	c1	139.39	c4	130.25	y3	296.41
448.28	**1541.5**	**3.4387**	NACA_BSL02	alpha1	2.9062	c1	140.37	c4	132.5	y3	331.56
445.97	**1525.1**	**3.4197**	NACA_BSL02	alpha1	0.4933	c1	135.94	c4	110.32	y3	315.15
448.64	**1550.1**	**3.4551**	NACA_BSL02	alpha1	0.3826	c1	140.62	c4	125	y3	326.88
420.18	**1380.3**	**3.2850**	NACA_BSL02	alpha1	1.4062	c1	128.83	c4	125	y3	326.88
445.81	**1543.7**	**3.4627**	NACA_BSL02	alpha1	1.125	c1	140.62	c4	125	y3	345.62
446.73	**1542.1**	**3.4520**	NACA_BSL02	alpha1	0.9375	c1	139.06	c4	132.67	y3	345.57
445.92	**1546.9**	**3.4690**	NACA_BSL02	alpha1	2.5759	c1	139.06	c4	132.5	y3	326.88

Table 2.25 - Results of Group 4, 4th loop

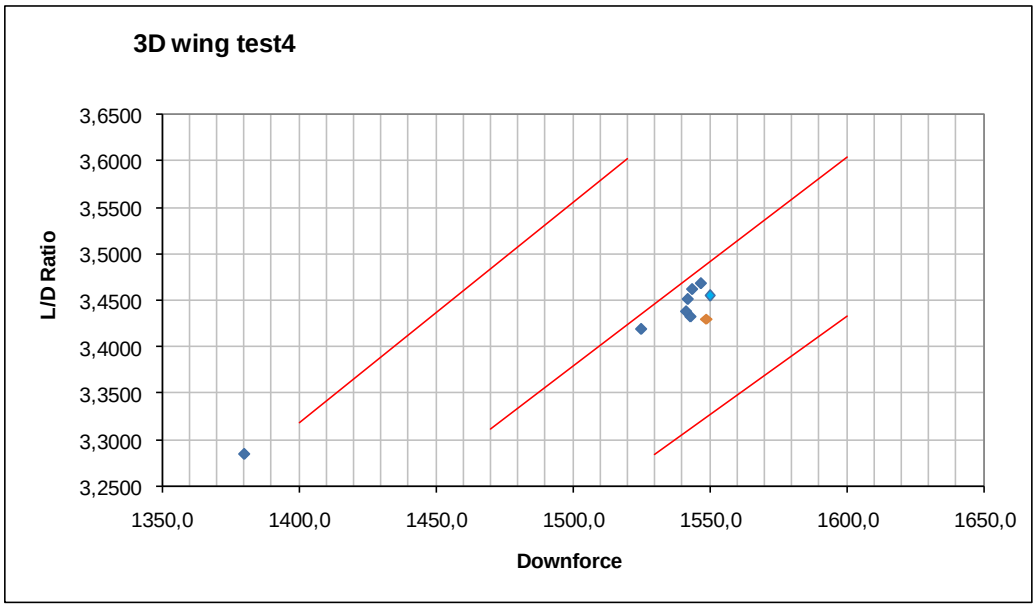

Fig 2.97 – XY graph of Downforce Vs L/D Ratio for the 4th group of the 4th loop. Again, there are some points with higher efficiency but lower downforce than the Baseline 02 (orange). However, there is a single candidate to become Baseline 03 (light blue), which has slightly more downforce and more efficiency.

After analysing the whole group of simulations, there are 2 candidates which are slightly better than the rest to become the new Baseline 03. However, due to limited resources, validation with full model can only be done with one of them. After discussing with the aero department, the most interesting candidate is the green one (from group 2), so it is the one which is going to be tested. Looking closely to both candidates, they are very similar (they share values for c1, c4 and y3), but the green candidate has a more agressive change in the central angle of attack (alpha1), so finally the aero team decided to try this candidate to become **Baseline 03**. Obviously, for further development, dismissed candidate could be re-tested in a second stage of development of the race car when more resources are available as **Alternative**.

2.6.8- Main plane and flap optimization summary

After all the simulation loops, a candidate to become Baseline 02 has been selected, and its evolution to become Baseline 03. Both geometries will be introduced in the full 60 million model and will be re-tested in yaw as all the experiments with the full model to validate the improvements. To sum up, four different loops have been tested, with a computing time around 400 hours using a single, powerful computer (but not a cluster), which means roughly 16 days of processing data non-stop for the computer. However, the set up of the case with Modefrontier, Catia and StarCCM+ has been quite challenging, but a experienced engineer used to work with this kind of software would need approximately 1 month to achieve success in making this optimization.

The final results are quite a big success (although they should be confirmed with the full car model), as the **theoretical** improvements in Baseline 02 and 03 from the original wing are:

BASELINE 02

-Drag reduction: 7.07 N (1.54%)

-Downforce increase: 41.8 N (2.77%)

-Efficiency increase: 0.144 (14 points, 4.38%)

BASELINE 03

-Drag reduction: 6.31 N (1.38%)

-Downforce increase: 46.3 N (3.07%)

-Efficiency increase: 0.148 (15 points, 4.51%)

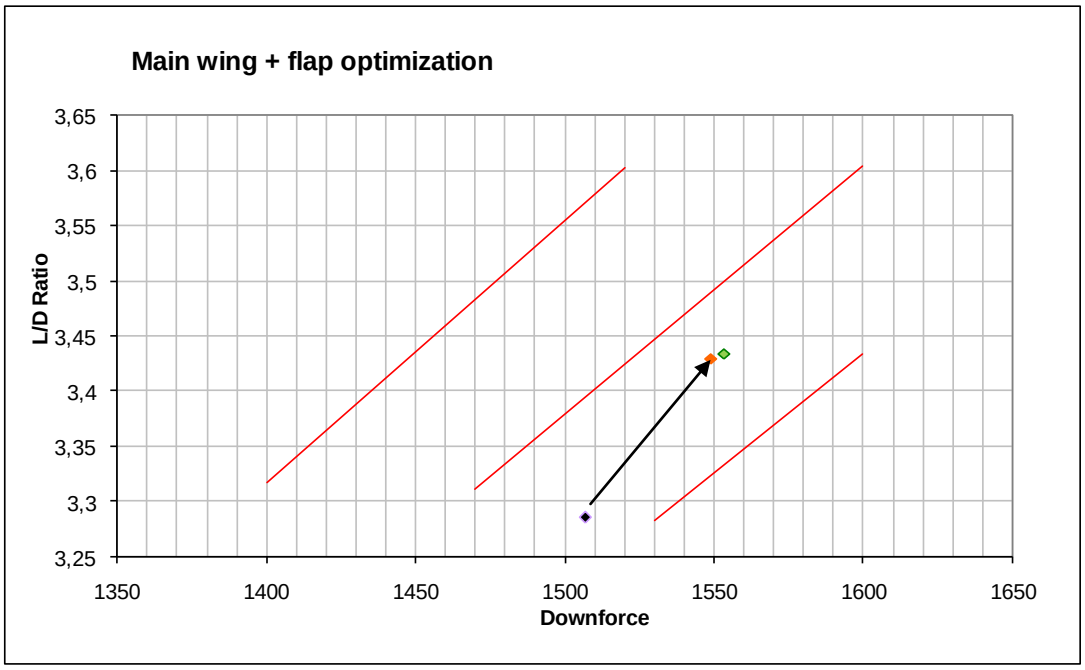

Fig 2.98 – XY graph of Downforce Vs L/D Ratio (efficiency) of the rear wing. Former rear wing is the black point, Baseline 02 is the orange one, and Baseline 03 is the green one. Notice the direction of optimization similar to isodrag lines, so the original target of increasing downforce has been achieved keeping the same drag and even reducing it slightly.

2.7- Beam wing optimization

2.7.1 – Introduction to Beam wing optimization

The optimization of the beam wing (lower element of the rear wing) is more difficult with the aggressive approach of this project, as it works between the diffuser and the upper part of the rear wing. The name of this part is due to its structural function, as it holds the whole rear wing and all the amount of downforce that it generates. However, it is even more important the interaction with the diffuser, as it helps the diffuser to extract more air, creating a low pressure area in its lower surface.

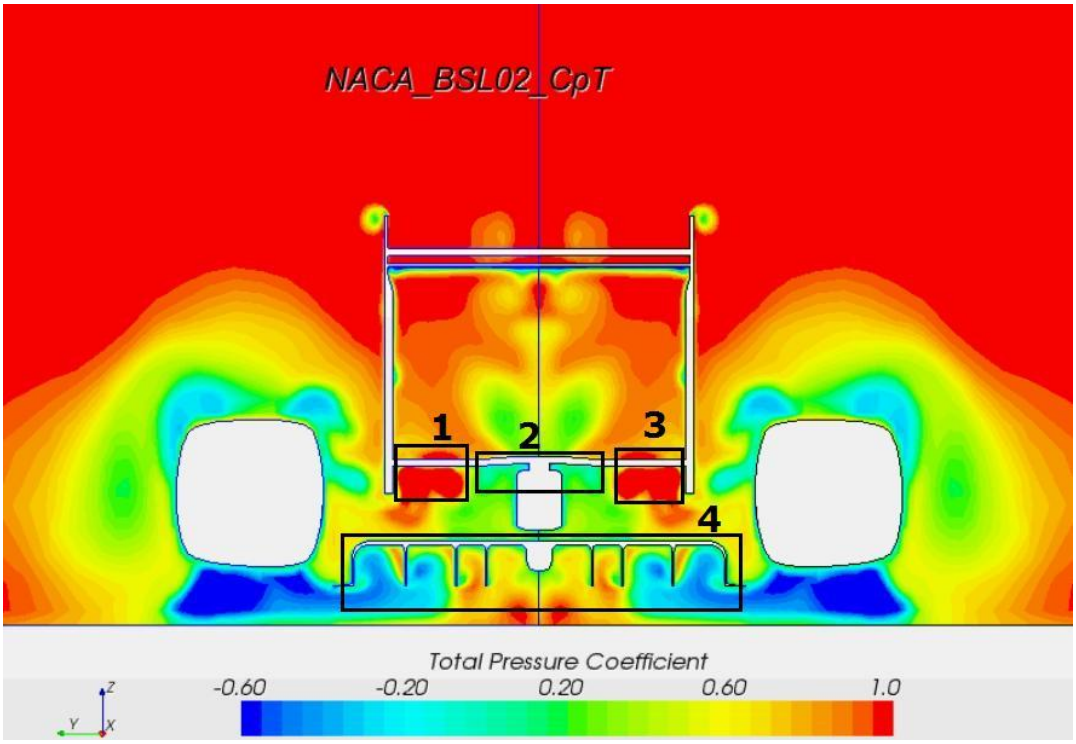

Fig 2.99 – Total pressure coefficient plot of the Baseline 02. Diffuser low-pressure area can be seen in (2), while the diffuser can be seen in (4). Notice the red area in (1) and (3) created by the high energy exhaust gases. In further developments, this should be redirected to the high pressure side of the beam wing.

Unfortunately, the validation of the Baseline 02 and 03 takes some days (3 days to be meshed and processed for each baseline, plus some more days as there are some other aero packages queuing for the cluster). Therefore, the development of the beam wing will be done with Baseline 02 (as the results of correlation seem positive, although not 100% finished).

Moreover, the development of the beam wing is more sensitive that the upper part of the rear wing, as the diffuser is much more complicated, and even more difficult to simulate in CFD. The low-pressure

area created by the diffuser helps to extract more air from the diffuser, so the suction of the diffuser in front of the flat bottom of the car and sidepods will be higher (which is not modeled in our design, which is only the rear part of the car). Therefore, is it clear that the **diffuser is affecting the whole bottom of the car, and the optimization of the beam wing (thus the diffuser as well) would imply a much more detailed approach (full car geometry, bigger mesh size).** However, to continue with the philosophy of this project, the study of the optimization of the beam wing will be done with the Baseline 02 keeping the same mesh, and correlated with the full car as well, to understand how the "local" optimization of the beam wing / diffuser combination with a coarse mesh can affect the whole car.

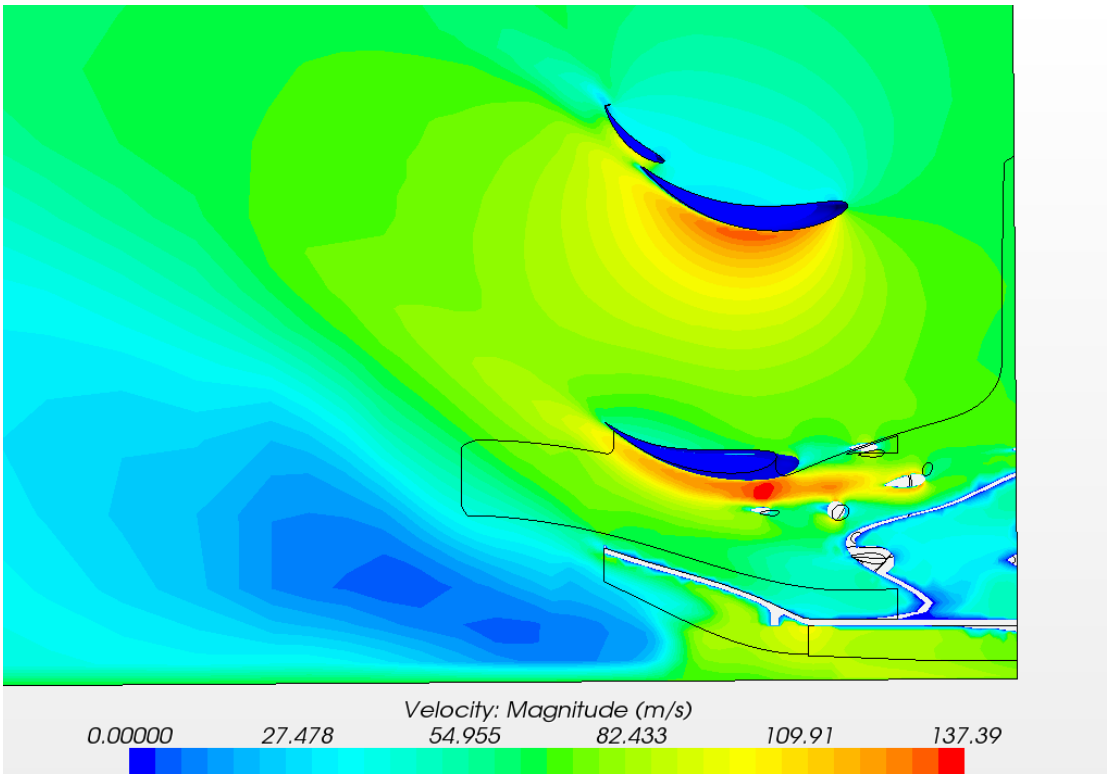

Fig 2.100 – Velocity plot of a longitudinal section of the rear wing with the diffuser, 250mm from the car centerline. The influence between beam wing and diffuser is clearly seen, as its interaction with the rear wing as well.

2.7.2- Beam Wing optimization with 3D parametric design

The optimization using 3D parametric design (explained in section 2.4) follows the same procedure as the main plane + flap profiles, but it is much easier. First of all, it has to optimize one single section instead of two, and it does not deal with relative position between profiles. Moreover, the design is not so strict, as the regulation box only restricts the top, bottom and back of the wing, but not the front section.

Therefore, the size of the beam wing in nearly “free”, but the growth of the profile must be studied carefully, combined with the angle of attack, in order to avoid intersecting with the lower part of the regulation box.

Some loops have been prepared for this optimization. As there is an important restriction in the central section of the beam wing due to its structural properties and the attachment with the bodywork, the optimization is mainly focused where the flow is more effective (between the engine cover and the endplates), although some changes will be done to the endplates as well. The total number of loops for this optimization is 4, with the number of simulations determined by the computing resources availability. The targets are the following ones:

-Loop 1 & 2 variables: AoA 2= AoA3, AoA4, c2=c3, y2, y3. Optimization focused in the cleaner flow between endplates and engine cover. Chord is increased to obtain a bigger low-pressure area to help the diffuser, and to obtain more downforce.

-Loop 3 variables: AoA 1, AoA 2=AoA 3, c2=c3, c4, y3. Keeping the spirit of the first and second loops, the angle of attack of the section 1 (attachment with the bodywork) is modified to try to improve it.

-Loop 4 variables: AoA4, c4, y3: Optimization focused in reducing the induced drag by playing with the profile of the beam wing when it contacts with the endplates.

2.7.3- Beam Wing 1st & 2nd loop with 3D parametric design

Although being 2 separate loops, they share the same variables. The 1st loop was designed to give a good amount of data to analyze, and the 2nd loop is a refinement in the range of the variables.

Fx	Fz	L/D	Configuration											
432.94	**1521.2**	**3.5137**	BSL02	AOA2	0.65	AOA4	2.1	C2	1.065	Y2	119	Y3	252
429.09	**1519**	**3.5400**	BSL02	AOA2	0.1	AOA4	0.8	C2	1.04	Y2	112	Y3	235
451.34	**1547.6**	**3.4289**	BSL02	AOA2	2.3	AOA4	2.6	C2	1.13	Y2	138	Y3	305
428.25	**1505.3**	**3.5150**	BSL02	AOA2	-0.45	AOA4	3	C2	1.02	Y2	106	Y3	217
445.97	**1533.3**	**3.4381**	BSL02	AOA2	1.75	AOA4	1.3	C2	1.105	Y2	131	Y3	288
437.02	**1526.6**	**3.4932**	BSL02	AOA2	0.35	AOA4	3.2	C2	1.095	Y2	141	Y3	314
445.25	**1526.5**	**3.4284**	BSL02	AOA2	2.6	AOA4	1.5	C2	1.01	Y2	115	Y3	244
433.04	**1532.9**	**3.5399**	BSL02	AOA2	-0.75	AOA4	2.4	C2	1.14	Y2	128	Y3	279
440.31	**1521.2**	**3.4548**	BSL02	AOA2	1.5	AOA4	0.6	C2	1.05	Y2	103	Y3	208
437.05	**1537.7**	**3.5184**	BSL02	AOA2	-0.2	AOA4	1	C2	1.16	Y2	135	Y3	296
448.13	**1542.3**	**3.4416**	BSL02	AOA2	2.05	AOA4	2.8	C2	1.075	Y2	109	Y3	226
443.14	**1533.8**	**3.4612**	BSL02	AOA2	0.9	AOA4	0.2	C2	1.12	Y2	147	Y3	332
450.84	**1529.2**	**3.3919**	BSL02	AOA2	3.15	AOA4	1.9	C2	1.03	Y2	122	Y3	261
443.74	**1542.6**	**3.4764**	BSL02	AOA2	1.05	AOA4	1.6	C2	1.145	Y2	111	Y3	274
456.26	**1540.9**	**3.3772**	BSL02	AOA2	3.3	AOA4	3.3	C2	1.06	Y2	136	Y3	204
433.73	**1524.7**	**3.5153**	BSL02	AOA2	-0.05	AOA4	0.7	C2	1.1	Y2	123	Y3	310
443.25	**1522.9**	**3.4358**	BSL02	AOA2	2.15	AOA4	2.5	C2	1.015	Y2	149	Y3	239
429.34	**1527.5**	**3.5578**	BSL02	AOA2	-0.6	AOA4	2.9	C2	1.125	Y2	117	Y3	327

441.15	**1529.3**	**3.4666**	BSL02	AOA2	1.6	AOA4	1.2	C2	1.035	Y2	143	Y3	257
448.18	**1533.1**	**3.4207**	BSL02	AOA2	2.75	AOA4	0.3	C2	1.08	Y2	130	Y3	222
428.77	**1513.7**	**3.5303**	BSL02	AOA2	-0.35	AOA4	1.8	C2	1.045	Y2	146	Y3	248
451.45	**1552.4**	**3.4387**	BSL02	AOA2	2.3	AOA4	1.7	C2	1.15	Y2	147	Y3	260
434.07	**1545.1**	**3.5596**	BSL02	AOA2	0.15	AOA4	3.2	C2	1.13	Y2	148	Y3	287
451.84	**1542.3**	**3.4134**	BSL02	AOA2	2.55	AOA4	3	C2	1.095	Y2	129	Y3	317
448.44	**1529**	**3.4096**	BSL02	AOA2	2.95	AOA4	1.5	C2	1.035	Y2	112	Y3	274
438.38	**1525.4**	**3.4796**	BSL02	AOA2	1.65	AOA4	1.6	C2	1.01	Y2	148	Y3	206
441.49	**1540.9**	**3.4902**	BSL02	AOA2	1.2	AOA4	1.9	C2	1.13	Y2	130	Y3	227
445.32	**1530.3**	**3.4364**	BSL02	AOA2	2.85	AOA4	1.5	C2	1	Y2	113	Y3	286

Table 2.26 - Results of the first and second loops – Notice thicker line to separate loops.

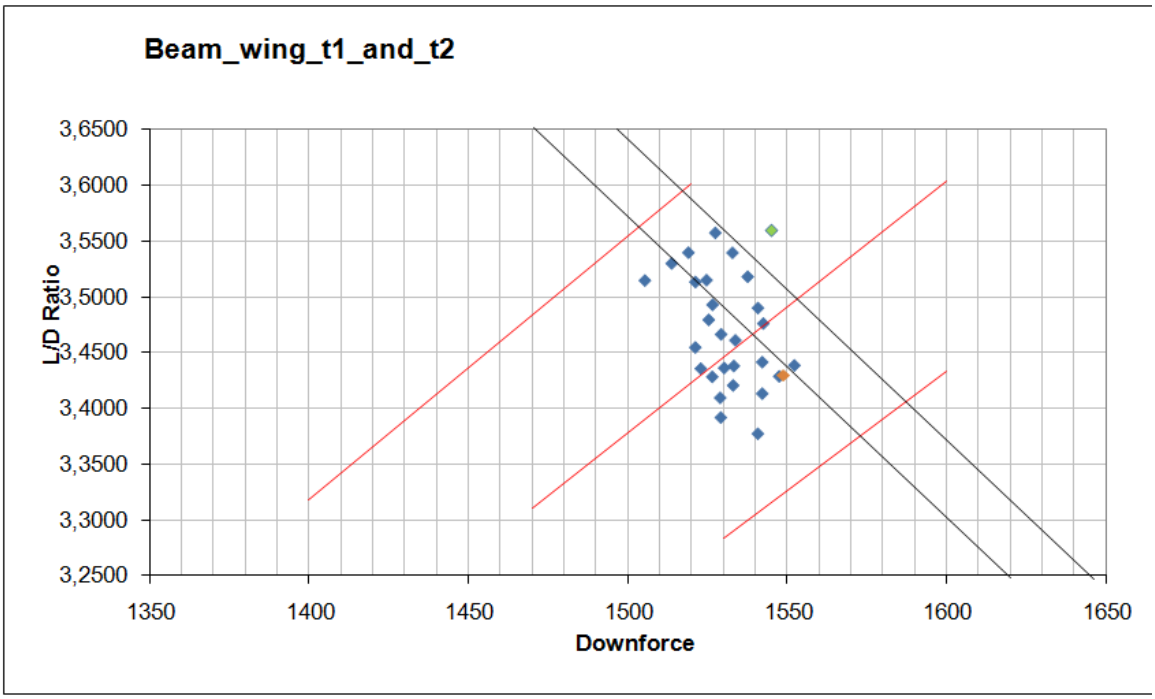

Fig 2.101 – XY graph of Downforce Vs L/D Ratio for 1st and 2nd loop. Baseline 02 is the orange point, and the green point is the best candidate to be testes with as “combined baseline03”.

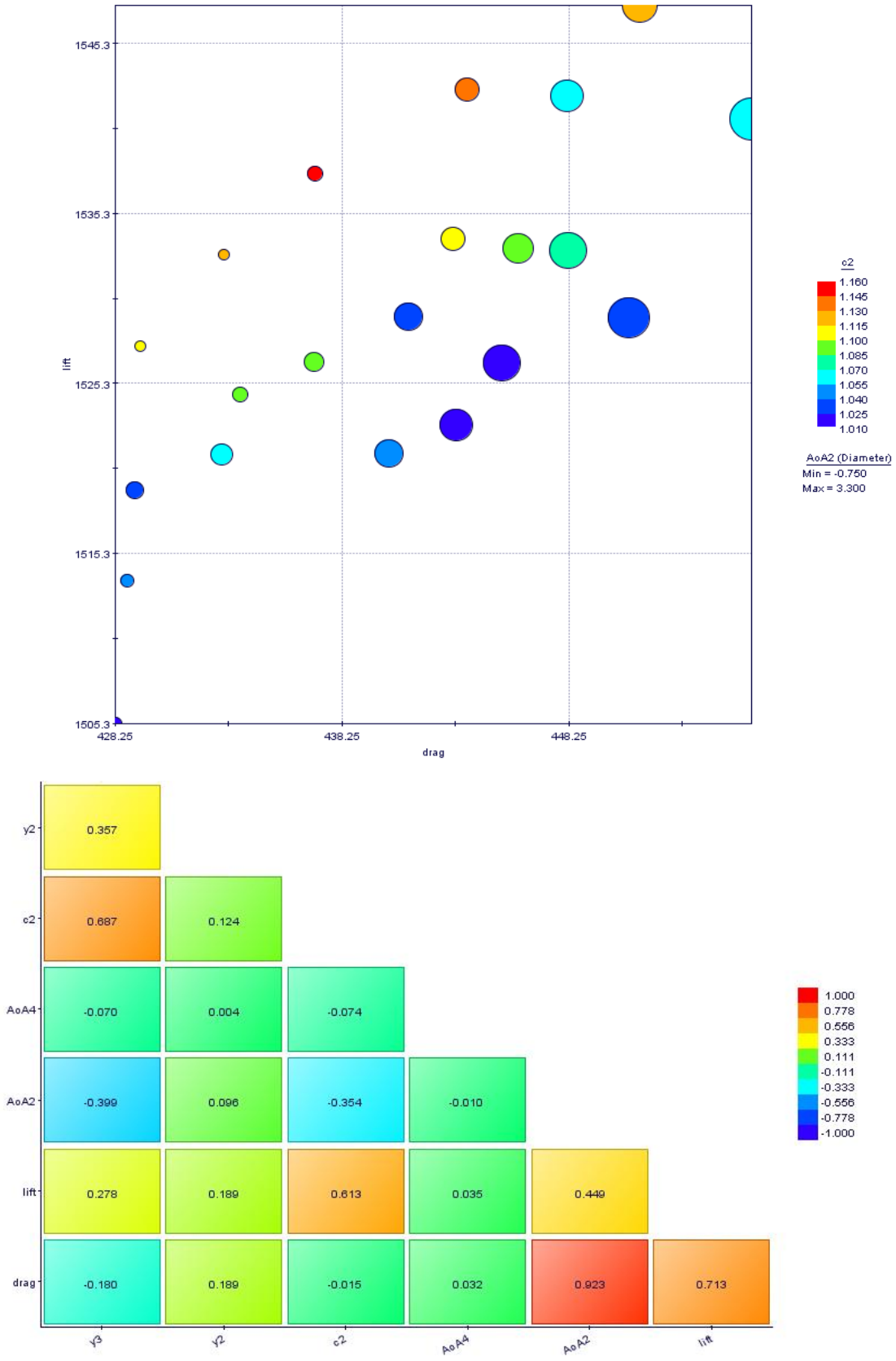

Fig 2.102 & 2.103 -4D Bubble plot of Drag Vs Lift (up) and correlation matrix (down) of 1st loop.

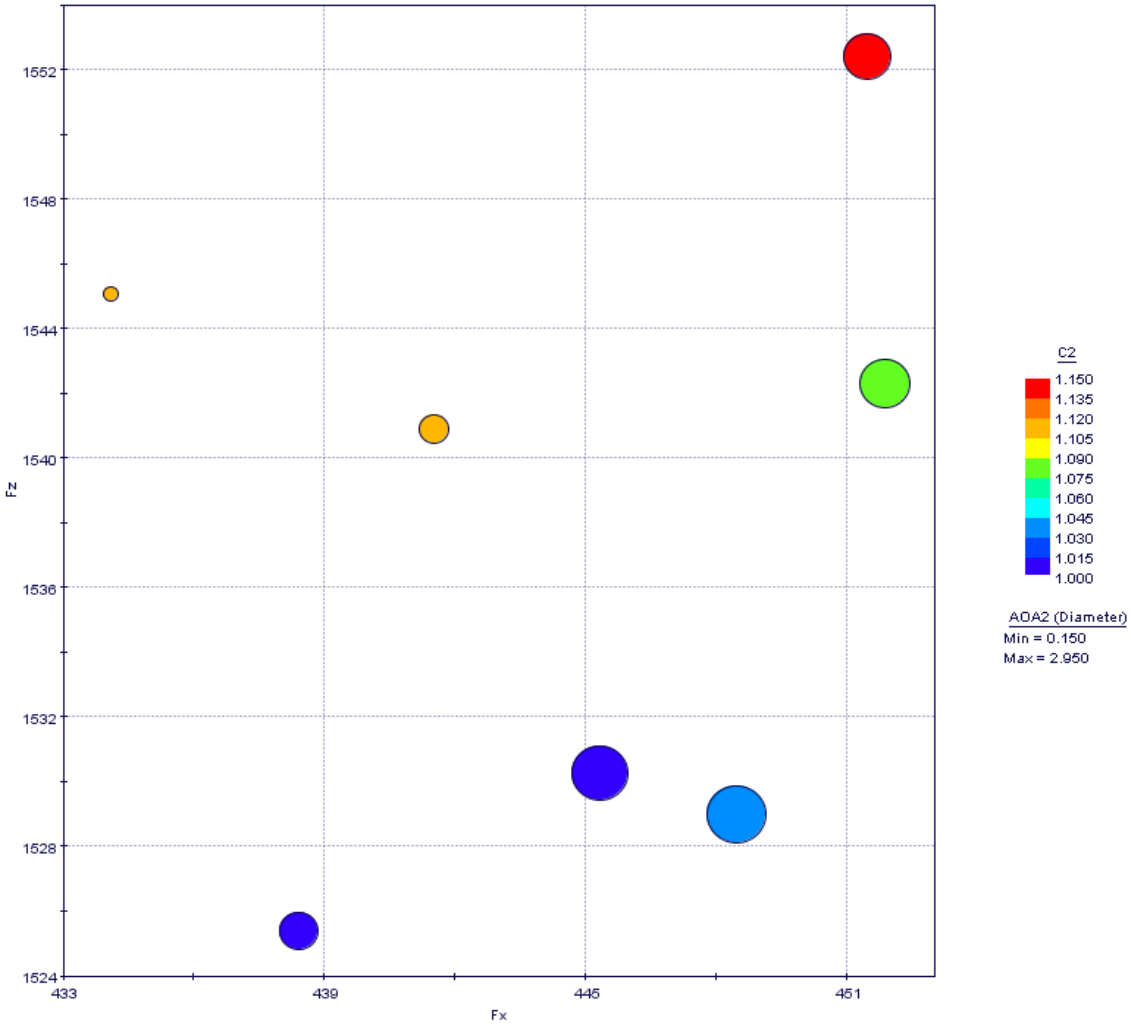

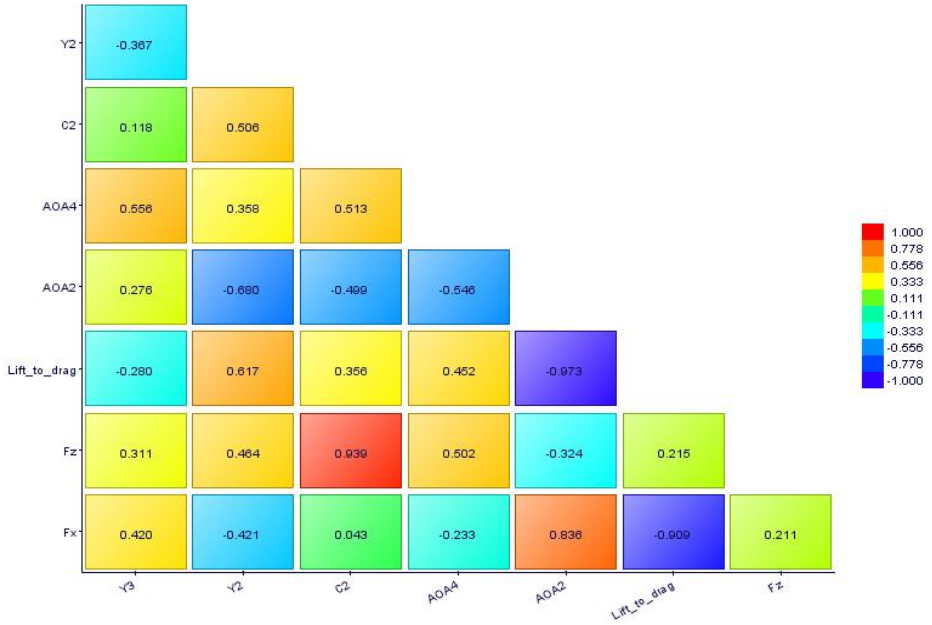

Fig 2.104 & 2.105 – 4D bubble chart of Drag Vs lift (up) and Correlation matrix (down) of 2nd loop.

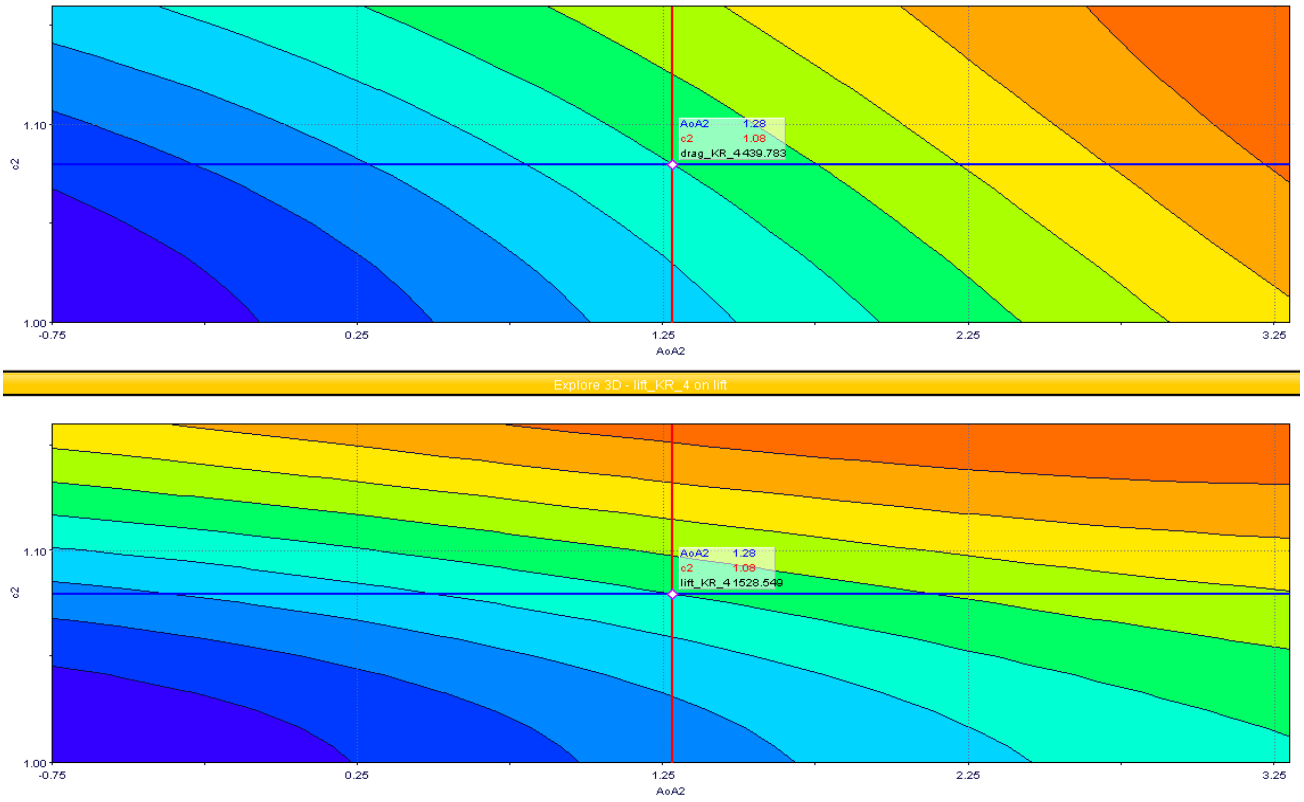

Fig 2.106 & 2.107 – Drag (top) and downforce (bottom) Kriging surfaces. X axis represents angle of attack in the section between the endplates and the engine cover (profiles 2 and 3), and Y axis represents chord of the same section of the beam wing. Notice that high downforce and high drag areas are on top right corner, although reducing the angle of attack slightly will have a significant reduction in drag while keeping a good amount of downforce. Notice also that Kriging surface for 2nd loop would be the similar to this surface.

1st and 2nd loop conclusions:

As a "test" optimization, the results are quite good. The amount of downforce generated is hardly improved, as it was the main focus of the rear wing. However, there is one candidate (highlighted in green), which is 3.79% more efficient, with only 0.25% less downforce. Despite being clearly better in the reduced CFD model, it must be tested in the full car model because of the aforementioned reasons of coarse mesh and lack of representation of the whole bottom of the car.

2.7.4- Beam Wing 3rd & 4th loop with 3D parametric design

Although being two different loops with different variables, the results are very similar. Both are small modifications of the beam wing, the first one focused in the attachment with the bodywork in the central section, and the second in the endplates section.

Fx	Fz	L/D	Configuration											
432.59	1518.2	3.5096	BSL02	AOA1	0.88	AOA2	0.7	C2	1.041	C4	0.65	Y3	250	
427.03	1512.6	3.5421	BSL02	AOA1	0.88	AOA2	-0.7	C2	1.129	C4	0.6	Y3	259	
434.4	1530.5	3.5233	BSL02	AOA1	-0.2	AOA2	0.5	C2	1.165	C4	0.71	Y3	192	
441.8	1519.6	3.4396	BSL02	AOA1	0.88	AOA2	2.4	C2	1.012	C4	0.79	Y3	246	
430.64	1513.2	3.5138	BSL02	AOA1	-1.52	AOA2	0.6	C2	1.012	C4	0.92	Y3	327	
424.9	1515.6	3.5670	BSL02	AOA4	-12.319	C4	0.7	Y3	235					
411.28	1497.9	3.6420	BSL02	AOA4	-18.841	C4	0.5	Y3	187.5					
431.12	1518.6	3.5225	BSL02	AOA4	-6.1594	C4	0.9	Y3	282.5					
427.82	1518.6	3.5496	BSL02	AOA4	-6.1594	C4	0.5	Y3	306.9					
429	1513.6	3.5282	BSL02	AOA4	-3.2609	C4	0.9	Y3	239.1					
426.67	1520.3	3.5632	BSL02	AOA4	-5.0725	C4	0.7	Y3	235					
420.09	1506.7	3.5866	BSL02	AOA4	-9.4203	C4	0.5	Y3	235					
428.28	1523.7	3.5577	BSL02	AOA4	-6.5217	C4	0.9	Y3	286.6					
423.23	1516.3	3.5827	BSL02	AOA4	-10.145	C4	0.8	Y3	233.6					
414.96	1493.1	3.5982	BSL02	AOA4	-16.667	C4	0.9	Y3	1522					
417.07	1499.7	3.5958	BSL02	AOA4	-21.014	C4	0.7	Y3	2065					
411.84	1500.3	3.6429	BSL02	AOA4	-18.841	C4	0.5	Y3	2011					
412.96	1494.8	3.6197	BSL02	AOA4	-18.841	C4	0.5	Y3	187.5					
430.27	1519.3	3.5310	BSL02	AOA4	-6.1594	C4	0.9	Y3	282.5					
427.84	1523.4	3.5607	BSL02	AOA4	-2.8986	C4	0.5	Y3	306.9					
422.26	1512.4	3.5817	BSL02	AOA4	-9.4203	C4	0.6	Y3	259.4					
433.01	1524.8	3.5214	BSL02	AOA4	-17.391	C4	1	Y3	319.1					
428.03	1515.4	3.5404	BSL02	AOA4	-21.377	C4	0.7	Y3	300.1					
421.37	1510.8	3.5854	BSL02	AOA4	-18.116	C4	0.5	Y3	270.1					
425.15	1509.4	3.5503	BSL02	AOA4	-5.4348	C4	0.8	Y3	180.7					

Table 2.27 - Results of the third and fourth loops – Notice thicker line to separate loops.

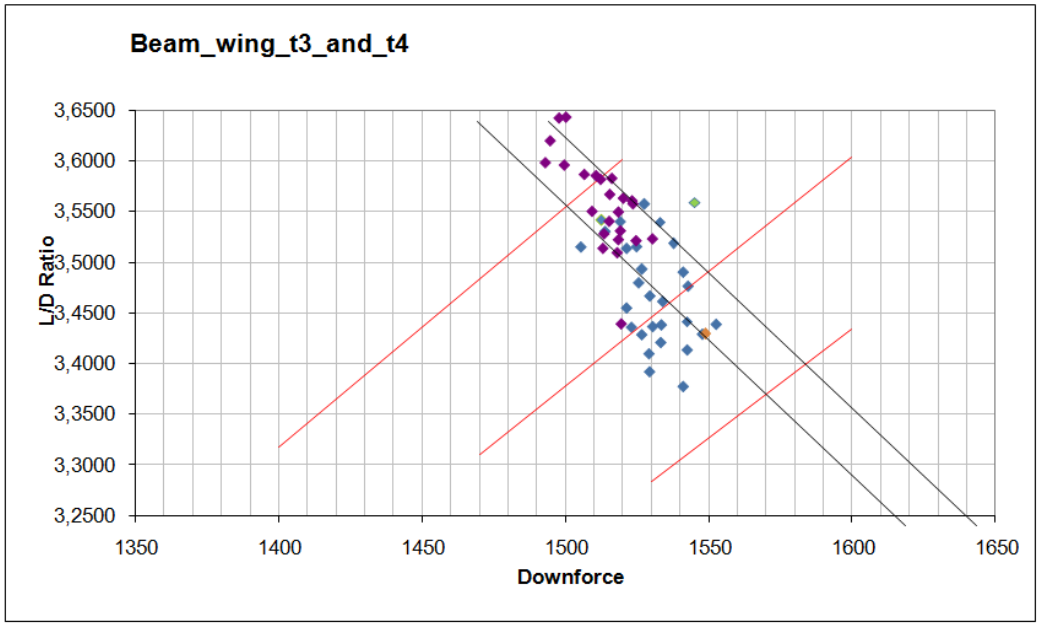

Fig 2.108 – XY graph of Downforce Vs L/D Ratio. Notice that results of 3rd and 4th loop are in purple, while results for 1st and 2nd loop are in blue. Baseline02 is the orange dot, and candidate to become “Combined Baseline 03” is the green dot.

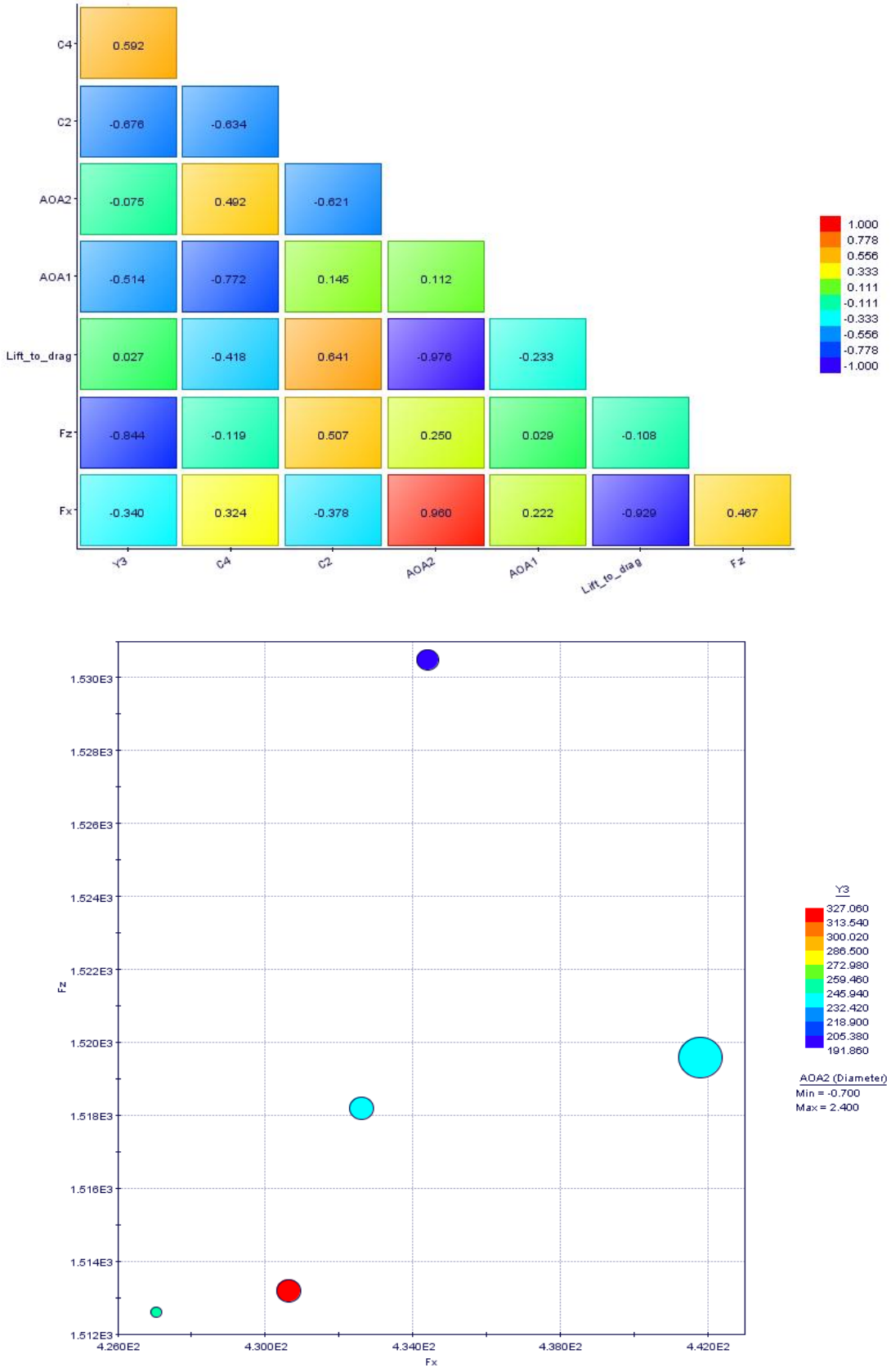

Fig 2.109 &2.110- Correlation matrix (top) and 4D Bubble chart (bottom) of Drag Vs Downforce of 3rd loop.

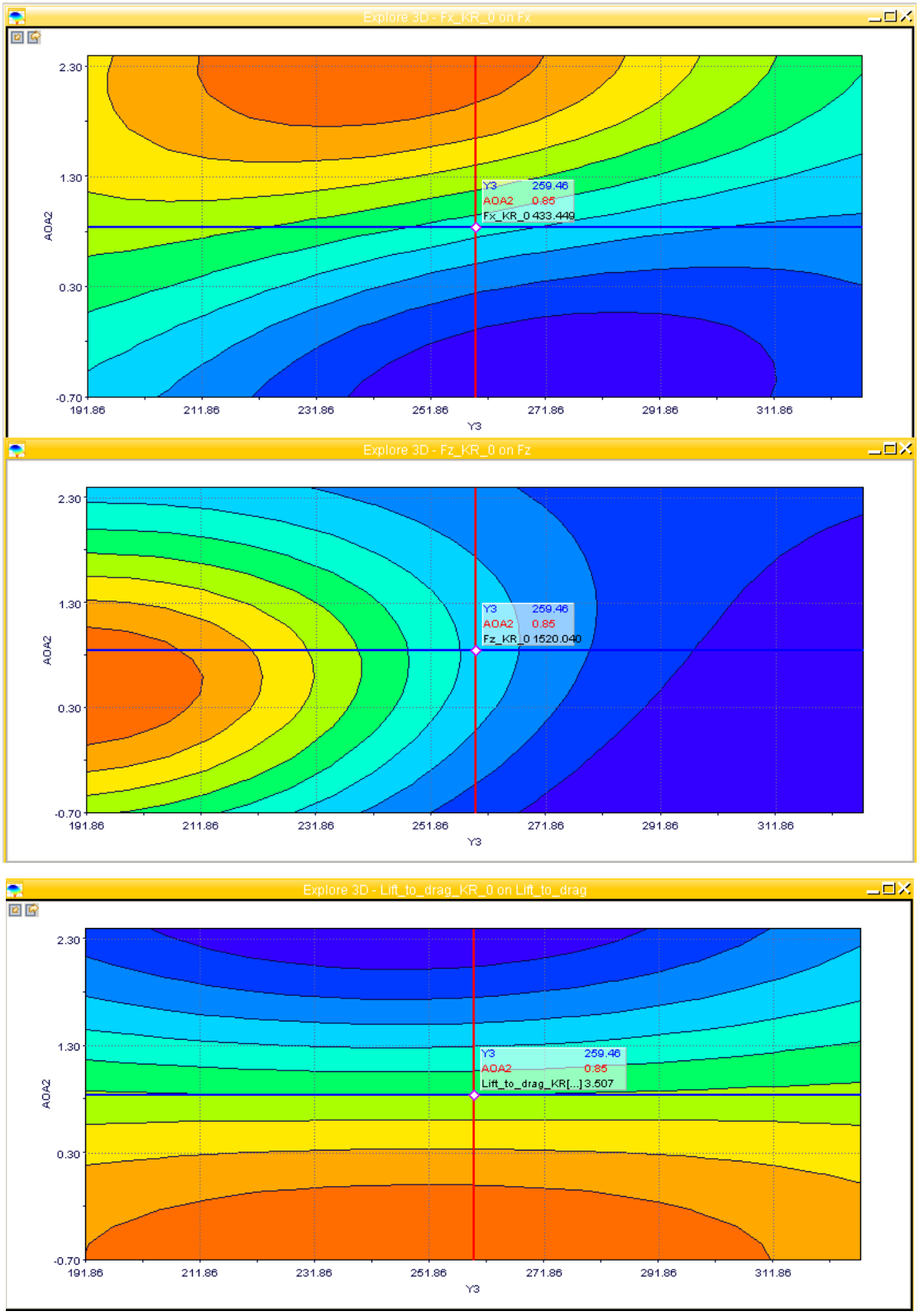

Fig 2.111, 2.112 & 2.113 - Drag (top) and downforce (middle) and L/D ratio (bottom) Kriging surfaces. X axis represents profile 3 position along transversal direction (from car centerline to the wheels), and Y axis represents angle of attack of profile 2&3 (section between engine cover and endplates).

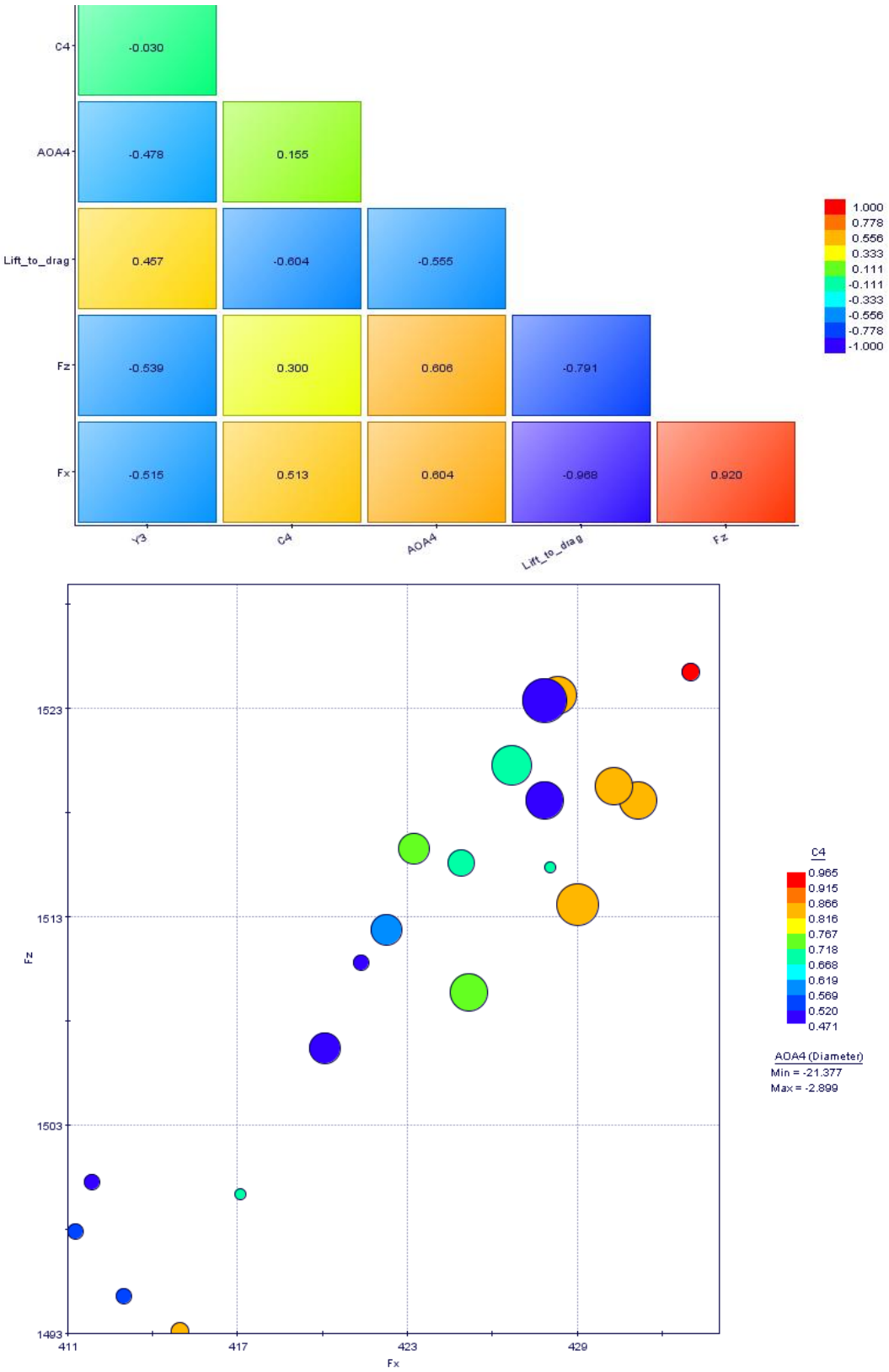

Fig 2.114 &2.115 – Correlation matrix (top) and 4D Bubble chart of drag Vs downforce (bottom) of 4th loop.

3rd and 4th loop conclusions:

Once again, the optimization of the beam wing is able to gain efficiency, but it cannot find extra downforce. Simulations consistently obtain a good efficiency increase, but the decrease in downforce is significant enough to dismiss all candidates. As seen in the development of the main plane and flap, it is easy to increase efficiency by reducing downforce, simply by decreasing the angle of attack, or chord length. In conclusion, despite obtaining interesting results of efficiency, none of them are close to the green candidate of 2nd loop to become the new "Combined Baseline 03".

2.7.5- Beam Wing optimization with NACA profiles

Optimization with NACA profiles is highly compromised by the fact that the structural function of the beam wing implies an attachment with the bodywork, so the profile in the central section of the wing cannot be changed. Therefore, despite having the outer part of the wing as a NACA profile, a small section should link the NACA profile to the former profile of the attachment, so there is an important part of the wing which cannot effectively be optimized with NACA profiles. However, if the NACA optimization were better than the former profile, major changes could be done to the engine cover and the attachment to change completely the beam wing, although this is not the aim of this project, but it is important to understand that it would imply a huge amount of work for other departments which are not involved in this project.

There is only 1 loop, with the three typical parameters for a 4-Digit NACA profile (camber, position of the maximum camber along the chord and thickness). If improvements were shown in the 1st loop, a new series of loops would have been done, but the potential of this optimization was not worthwhile.

Fx	Fz	L/D	Configuration							
434.13	**1495.3**	**3.4444**	NACA_BSL02	Camber	12	X_camber	12	Thickness	4.9
417.52	**1489.5**	**3.5675**	NACA_BSL02	Camber	10.5	X_camber	9.7	Thickness	4.35
451.15	**1506.2**	**3.3386**	NACA_BSL02	Camber	13.5	X_camber	13	Thickness	5.45
427.1	**1489.4**	**3.4872**	NACA_BSL02	Camber	11.2	X_camber	12	Thickness	4.6
456.12	**1515.7**	**3.3230**	NACA_BSL02	Camber	14.3	X_camber	8.8	Thickness	5.75
413.31	**1478.49**	**3.5772**	NACA_BSL02	Camber	9.7	X_camber	14	Thickness	4.05
440.85	**1504.71**	**3.4132**	NACA_BSL02	Camber	12.8	X_camber	11	Thickness	5.2
434.54	**1490.66**	**3.4304**	NACA_BSL02	Camber	10.9	X_camber	15	Thickness	5.9
446.55	**1498.29**	**3.3553**	NACA_BSL02	Camber	13.9	X_camber	11	Thickness	4.75
460.92	**1500.22**	**3.2548**	NACA_BSL02	Camber	14.9	X_camber	15	Thickness	5.25
418.18	**1495.85**	**3.5770**	NACA_BSL02	Camber	10.3	X_camber	9.5	Thickness	4.7
451.28	**1509.34**	**3.3446**	NACA_BSL02	Camber	13.3	X_camber	13	Thickness	5.8
413.56	**1477.57**	**3.5728**	NACA_BSL02	Camber	9.5	X_camber	14	Thickness	4.4
442.43	**1504.19**	**3.3998**	NACA_BSL02	Camber	12.6	X_camber	10	Thickness	5.55
448.23	**1502.5**	**3.3521**	NACA_BSL02	Camber	13.4	X_camber	13	Thickness	5.5

Table 2.28 - Results of the 1st NACA loop.

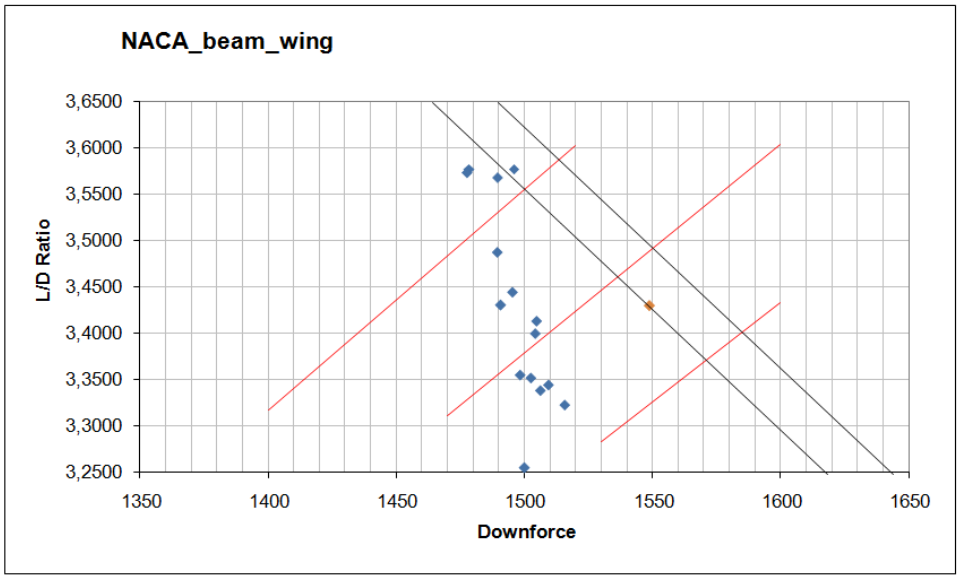

Fig 2.116 –XY graph of Downforce Vs L/D Ratio of 1st NACA loop. The orange dot is the Baseline 02. Notice also the verticality of the results, with a nearly constant downforce, but very variable efficiency.

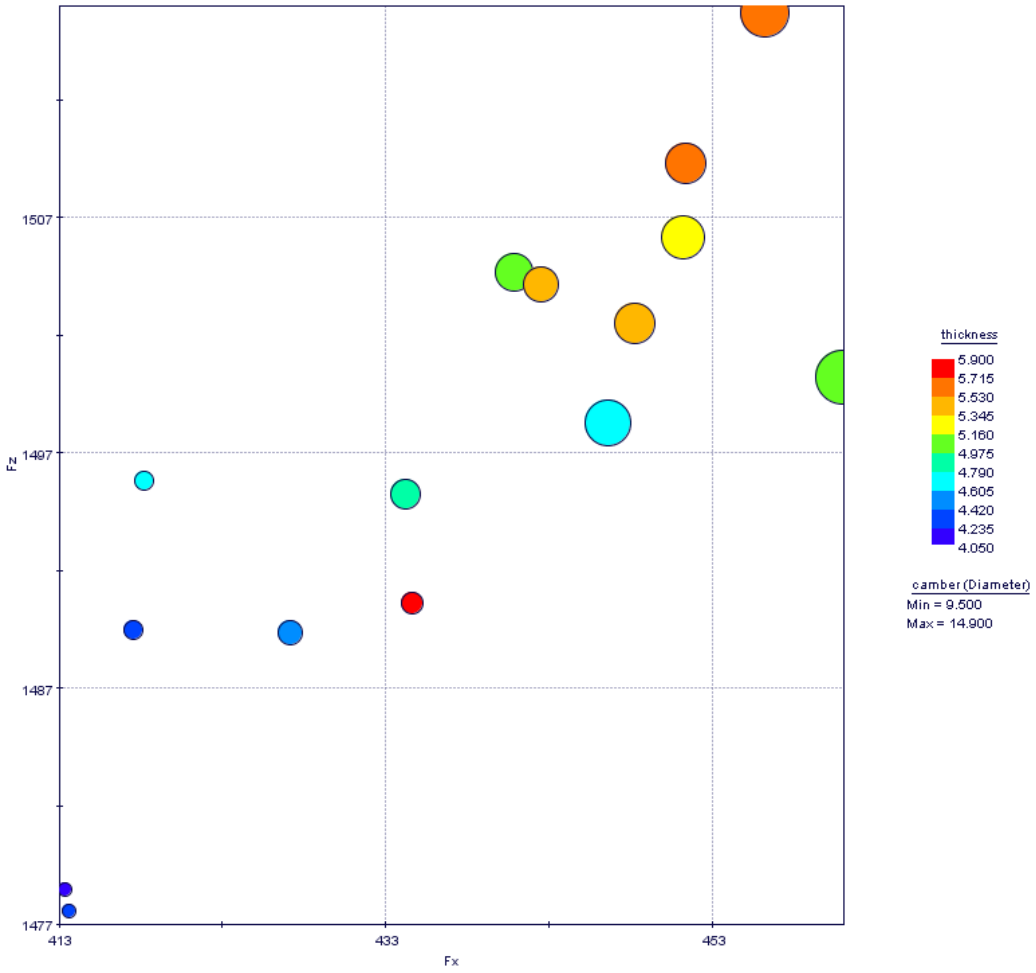

Fig 2.117 – 4D Bubble chart of Drag Vs Downforce for the 1st NACA loop.

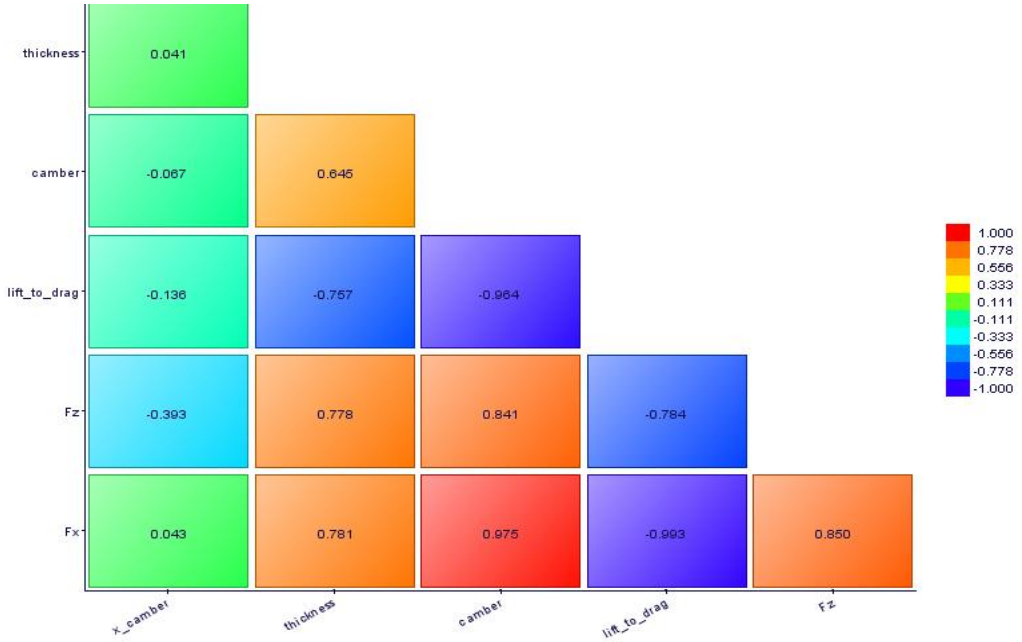

Fig 2.118 – Correlation matrix for 1st NACA loop.

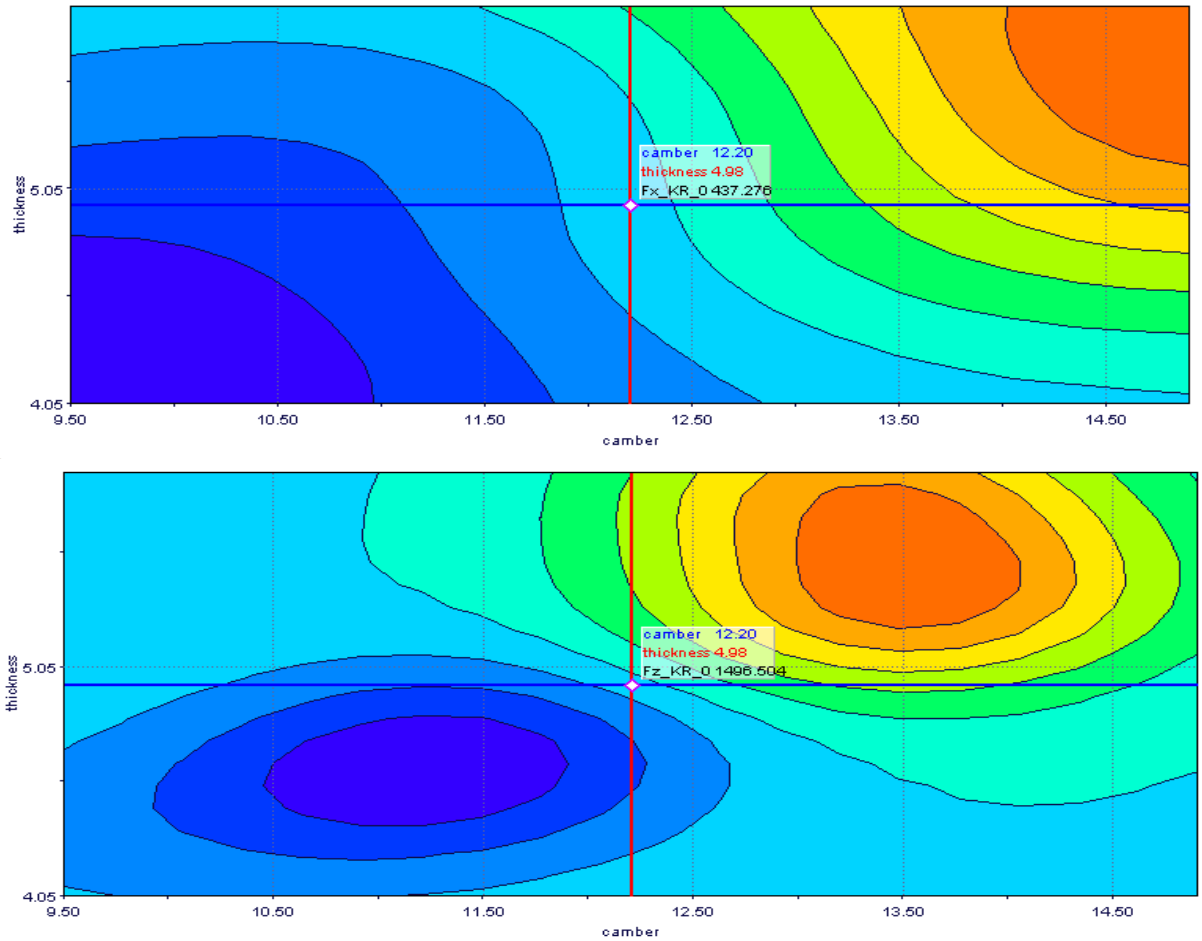

Fig 2.119 & 2.120 - Drag (top) and downforce (bottom) Kriging surfaces. X axis represents camber, and Y axis represents thickness.

1st NACA loop conclusions:

The potential of this optimization is reduced by the attachment with the engine cover which cannot be modified. However, it can reach important peaks of efficiency without changing angle or attack or chord, although not being able to increase downforce. However, the development of this method needs much more time than the 3D parametric design, and it is not worthwhile due to the attachment restrictions. Nevertheless, the potential changing angle of attack, chord, and finally using different angles of attack and chords along the span could be impressive.

2.7.6- Beam wing optimization summary

A good candidate has been found to become the new "Combined Baseline 03", which is the Baseline 02 with a new beam wing, which could be an alternative to Baseline 03 which is currently being tested in the full F1 60 million mesh. It is 3.79% more efficient, with only 0.25% less downforce. The 3D parametric design is clearly a fast, reliable way to improve the efficiency of the wing keeping the same amount of downforce, but the potential is not big. However, the restricted implementation of the NACA adaptation was not good enough to find appropriate candidates. Despite being constrained, some peaks of efficiency were shown. Therefore, the perfect path to develop the beam wing could be a combination of 3D parametric design and the NACA profile, starting with the optimization of NACA profile, adding the chord and angle of attack control (of course deleting the restriction of the attachment with the bodywork). Once achieved the best option, a profile control like in the 3D parametric design should be implemented, only changing chord and angle of attack along the span, or perhaps changing thickness or camber slightly. The potential is clearly higher, it would have clearly more efficiency and probably the same amount of downforce or even more than the original Baseline 02, although it would involve other departments to calculate the new structural analysis and the attachment with the engine cover to handle the load generated by the rear wing.

2.8- Full car simulation results

2.8.1- The necessity of a simulation for each part developed

Before entering into the details of full car simulation results, it is important to understand (and to demonstrate) why each new part developed in CFD needs a full simulation which requires a huge amount of times and resources. It seems logical to try to validate 2 parts (for example the main plane and flap of the rear wing and the beam wing) with only one full simulation to save time and money. Apart from not having the exact contribution in drag and downforce for each part changed (initial results could be extracted from reduced mesh simulations), interaction between them could be harmful, destroying the effects that one single change produces, thus dismissing 2 parts that could work well separately.

The following example will deal with Baseline 02, Baseline 03 and Combined Baseline 03. Currently, validations with Baseline 02 on the full 60 million mesh model demonstrated that the aerodynamics improved as predicted in the reduced mesh model. However, Baseline 03 and Combined Baseline 03 are still being tested. Baseline 03 is a 3D parametric design improvement of the main plane and flap which delivers a little more downforce, and Combined Baseline 03 is the new beam wing which is more efficient. Therefore, in a new simulation, seems logical that introducing both parts together in a new simulation would increase both downforce and efficiency. But nothing could be further from the truth. This example is to illustrate the sensitivity of aerodynamics in general, and the interaction between the rear wing and beam wing in particular.

Baseline 03 increases downforce in 4.5 N and efficiency in 0.0042 (0.42 points) from Baseline 02, and it is represented by the yellow dot in the following graph. Combined Baseline 03 decreases downforce by 3.8 N and increases efficiency by 0.13 (13 points). Therefore, it is possible to think that putting together both parts, the total increase in downforce would be 0.7 N and 0.1258 (12.58 points) in efficiency. However, after testing it in the reduced mesh, the results are far from this theoretical data. Downforce decreases 14.3 N (nearly 1%) and efficiency only increases 0.0687 (6.87 points), half of the predicted increase.

It is not a surprise for any experienced aerodynamicist. The efficiency is in fact increased, but very far from the amount expected. But the downforce has fallen dramatically. This is the result of the interaction of both elements, and the sensitivity of the development of any aerodynamic package. A beam wing could be useful working under the flow of a rear wing, but it could be much worse with a little optimization of the same rear wing. The optimization of the upper part of the rear wing in the 3D parametric design obtained the maximum from the air, thus having an even bigger low pressure area above the beam wing. Therefore, the optimized beam wing, which asked for more effort to the air than the former beam wing, is not working as predicted, or viceversa, the rear wing optimized is not working due to the influence of the new beam

wing. In any case, the Baseline 03 (upper rear wing optimization) and the Combined Baseline 03 (beam wing optimized) are not working correctly together (see graph below).

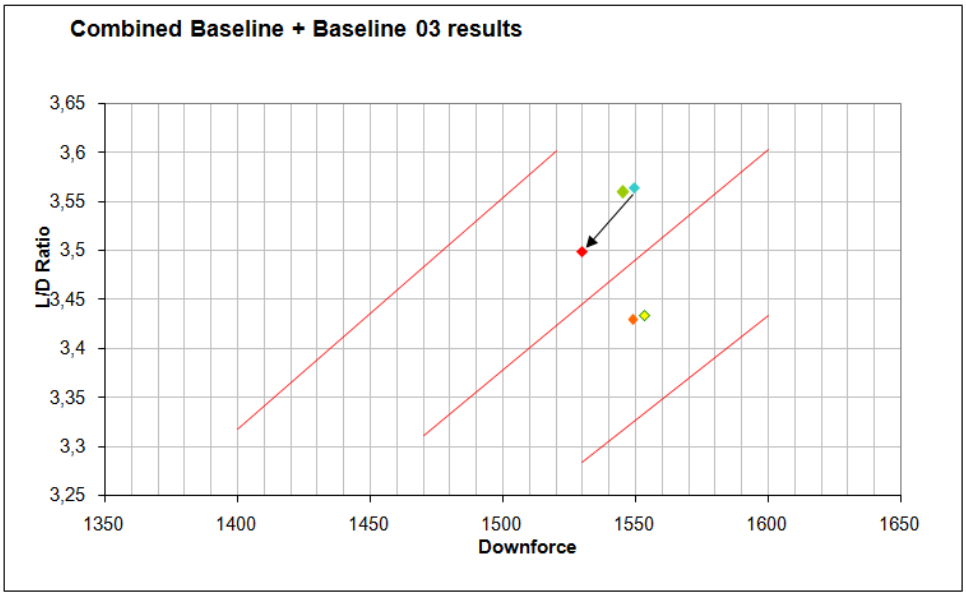

Fig 2.121- XY Graph of Downforce Vs Lift to Drag ratio. Orange dot is Baseline 02, green dot is Combined Baseline 03, yellow dot is Baseline 03, blue dot is the expected result of using together Baseline 03 (rear wing) with Combined Baseline 03 (beam wing), and the red dot is the real (CFD) result.

This result justifies why each part aerodynamically developed must be tested individually, and explains why the car must be developed following a path, all together, and not by parts without taking into account other parts (i.e. a rear wing cannot be developed while the front wing is developed, because the resultant optimization of the rear wing may be useless with a new front wing). This explains the typical division of a F1 aerodynamic department, where different groups (usually 3 or 4) develop the car separately, having always one single baseline, and developing (for example), the front wing one week, the diffuser the next week, and the rear wing the following week. Therefore, after one week of development, two weeks are used to build the wind tunnel parts to validate the CFD development.

2.8.2- Final results with F1 full model – Baseline 02

After selecting Baseline 02, Baseline 03 and Combined Baseline 03 to be tested in the cluster, Baseline 03 was considered not worthwhile to be tested with the cluster due to its small improvement. So finally, **Baseline 02 and Combined Baseline 03 were tested in Epsilon Euskadi cluster**.

BASELINE 02

After testing the new BASELINE 02 with the full 60 million model car, with the complete geometry, in yaw, and steered wheels, it is clear that the new BASELINE 02 is better than the former design. In fact, there is a clear increase in downforce, although a slight increase in drag.

	Former Rear wing	New Baseline 02	Difference
Downforce	3185 N	3285 N	+100 N (+3.14%)
Drag	986 N	996 N	+10 N (+1.01%)
Efficiency	3.2302	3.2982	+0.068 (+2.105%)

Table 2.29 – Baseline 02 results

Notice that this result has a slight offset due to confidential issues, however is perfectly well representing the real study. The following graphs are the “Mean total pressure coefficient” of different sections of the rear wing from the former rear wing and the new Baseline 02. More sections can be seen in the “Appendix”.

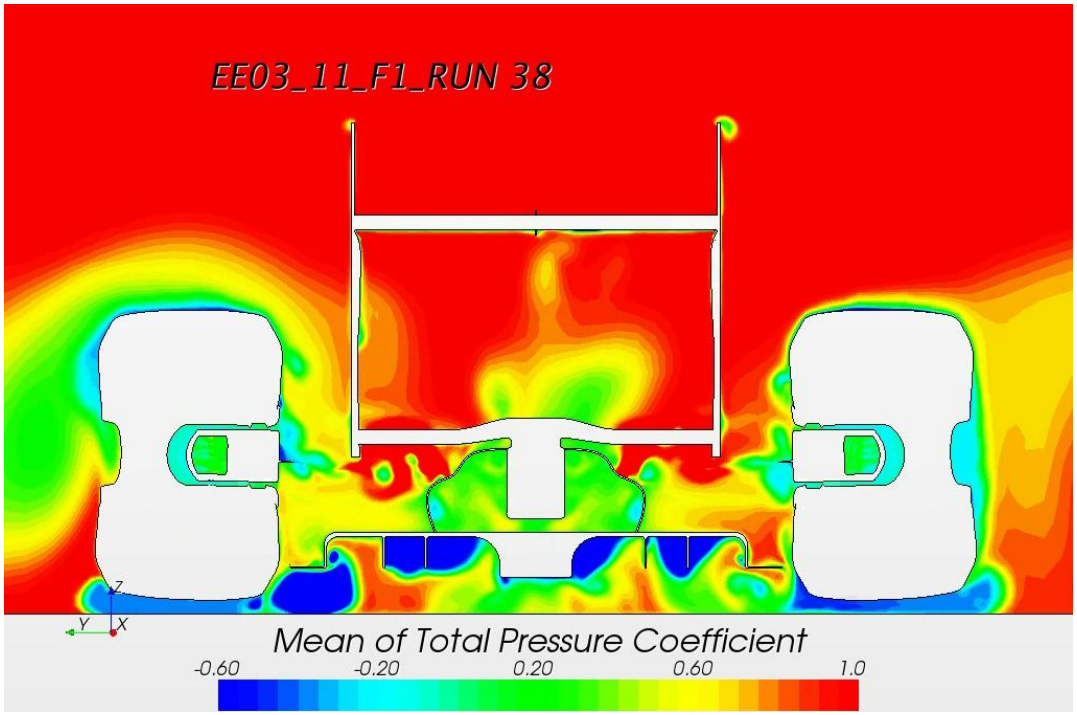

Fig 2.122 – Former rear wing section of the mean total pressure coefficient, at X=3390 from front wheel axis. Notice the asymmetry of the flow, as the car is in yaw.

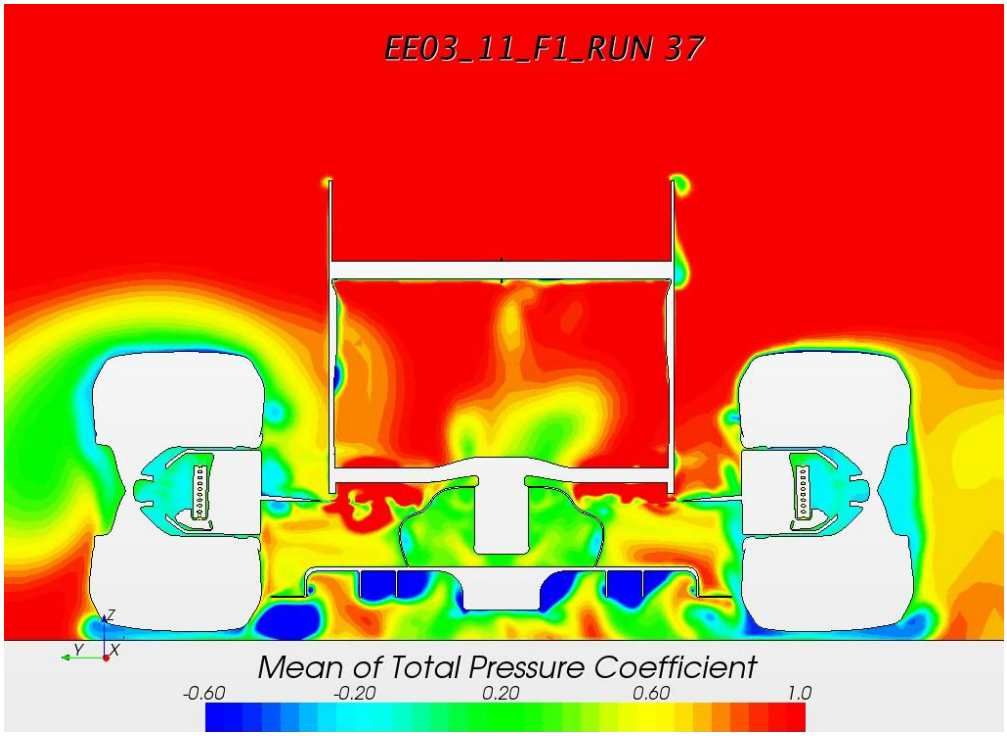

Fig 2.123 – Baseline 02 rear wing section of the mean of total pressure coefficient, at X=3390 from front wheel axis. Notice the asymmetry of the flow, as the car is in yaw. Notice also thicker main plane, as it is thicker and starts earlier than the previous one.

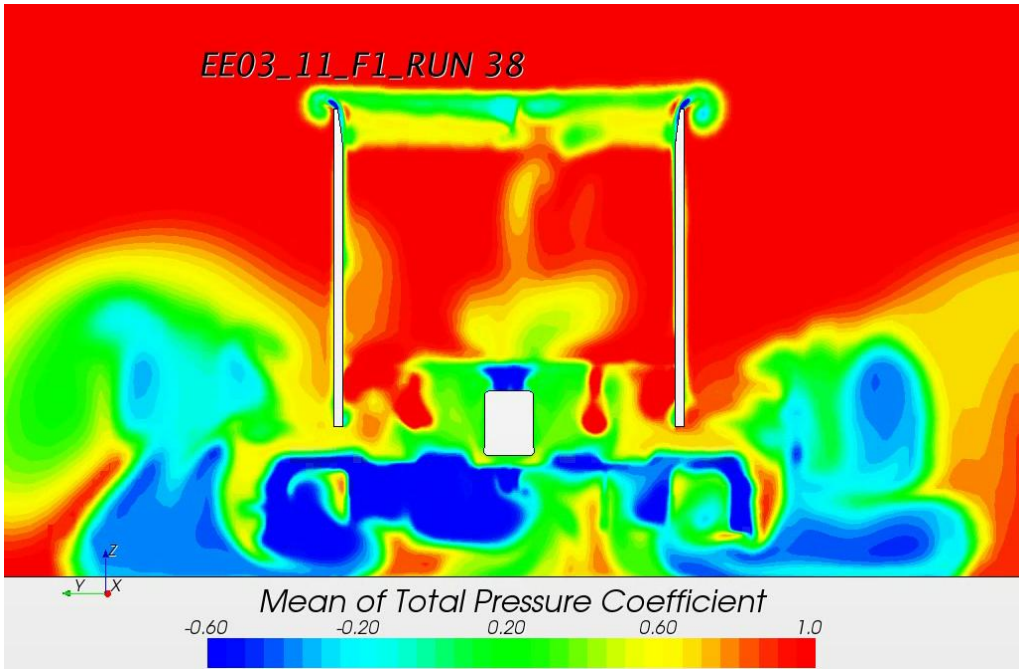

Fig 2.124 – Former rear wing wake generated at X=3610 mm from the front wheel axis. Notice the asymmetry of the flow again, especially in the diffuser area rather than the rear wing.

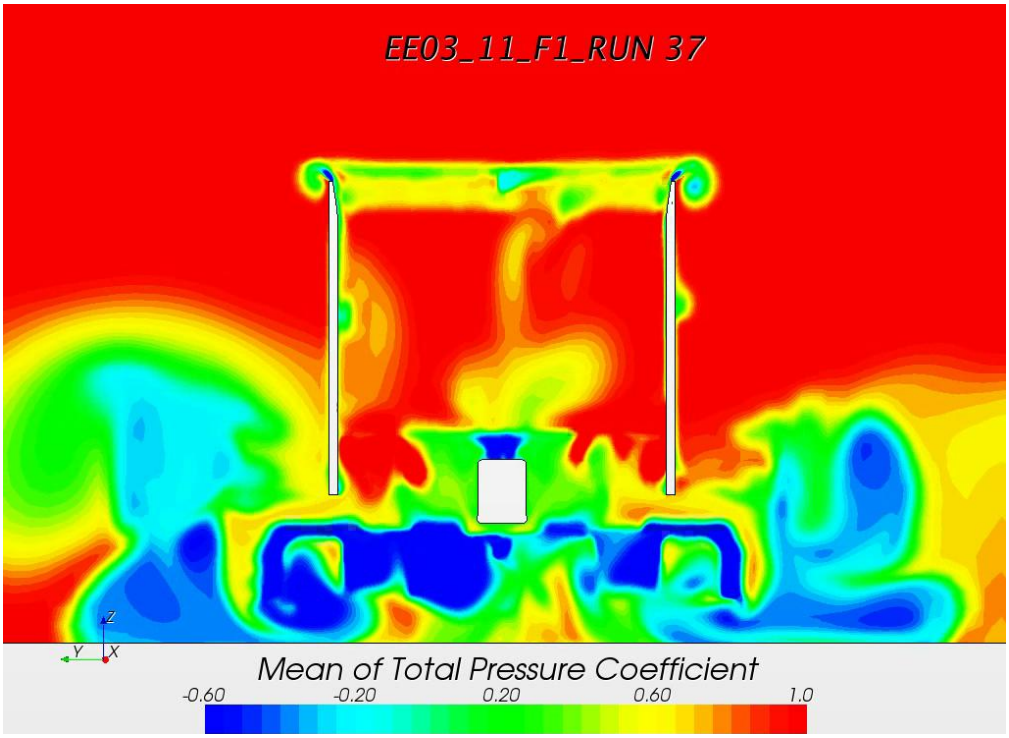

Fig 2.125 – Baseline 02 wake generated by the rear wing, at X=3610 mm. Notice the thinner wake generated by the flap, and the green area generated on the right endplate (which is not in the former wing).

BASELINE 02 CONCLUSION

Data from full car is obviously out of this project and strictly confidential. However, the overall result of the car was positive, so this new Baseline 02 will be definitely converted into a wind tunnel model to be tested, and if the measurements in the wind tunnel show an improvement, it will become the new baseline for further aerodynamic development. Surprisingly, the new CFD simulation affected more than expected the front wing, although it is not an important problem. Nevertheless, to understand the importance of the set up of the front wing, the correlation with the wind tunnel and the **final lap time improvement**, it is necessary to start the wind tunnel analysis protocol.

2.8.3 – Baseline 02 - Example of wind tunnel validation

Although it is not the aim of this validation to explain Wind Tunnel testing protocol, it is important to understand changes in the model to test the car and know the final lap time improvement. First of all, at the beginning of the development, of the real race car, there is a Cx target and a %Front downforce (aerobalance) target, which is set by the Chief Aerodynamicist. Therefore, it is intended to test all models with the same Cx target, and the same %F target. Consequently, a Cz equivalent and an Efficiency

equivalent (which is equal to Cz equivalent divided into Cx target) will be generated, which will indicate if the new aero package improved or not.

When a new aero package is assembled into the scale model of the wind tunnel, front wing and rear wing are used to achieve the %F downforce target and Cx target. Rear wing is used to obtain the amount of drag (Cx) and consequently downforce levels, and front wing is adjusted to obtain the %F balance, but it is not affecting a lot the drag. When both targets are achieved, a full aeromap is done (different ride heights, with different weights according to the importance on aerodynamics performance), and with the new Cz equivalent (and thus Eff. Equivalent) the new aero package is evaluated. If the value is higher, the new aero package is better in terms of performance, and is incorporated into the car. It is said in Formula One that 10 points on the Cz (for medium downforce tracks, the most common in Formula One Championship) is approximately 3 tenths of a second per lap improvement, which is definitely a lot. In big teams, for example Toyota F1, the target is 50 points during the whole season (1 point per week).

The following example is a demonstration of lap time gain with the new Baseline 02, with all data with a small offset due to confidential issues, although the results are quite close to reality.

Targets: %F Downforce: 44%
Cx Target: 1.05

Baseline 01: Front Downforce weight from scales: unknown
Rear Downforce weight from scales: unknown

New aero package introduced: Baseline 02
Drag increase: + 10 N, new Cx higher than Cx target 1.05
Rear downforce increase: +100 N, %F downforce decreased.

Procedure:

1- Decrease rear wing mounting angle of attack, reduce gurney flap height, etc. in order to reduce 10 N drag to achieve Cx target.
2- Check rear downforce balance to calculate new %F downforce.
3- Adjust front wing flap to achieve 44%F downforce (it does not affect total drag).
4- Check new front and rear balance to know new downforce levels.
5- Calculate lap time improvement with new Cz equivalent.

To start with the calculations, the initial Cz must be known, in order to obtain all the unknown data, as well as the frontal area of the car. Looking at some bibliography, it is possible to assume:

Initial Cz: 2.8000

Frontal Area: 1.1 m^2

Air density: 1.22 Kg/m^3

Testing speed (to correlate from CFD): 69.44 m/s = 250 km/h

Remembering basic aerodynamic concepts:

$$Downforce = \frac{1}{2} \cdot density \cdot Frontal\ Area \cdot Cz \cdot speed^2 \quad \text{(Eq. 2.1)}$$

$$Drag = \frac{1}{2} \cdot density \cdot Frontal\ Area \cdot Cx \cdot speed^2 \quad \text{(Eq. 2.2)}$$

Then,

$$Baseline\ 01\ Downforce = \frac{1}{2} \cdot 1.22 \cdot 1.1 \cdot 2.8 \cdot 69{,}44^2 = 9059.41\ N = 923.49\ Kg \quad \text{(Eq. 2.3)}$$

$$Baseline\ 01\ Drag = \frac{1}{2} \cdot 1.22 \cdot 1.1 \cdot 1.05 \cdot 69{,}44^2 = 3397.28\ N = 346.31\ Kg \quad \text{(Eq. 2.4)}$$

With 44%Front downforce:

$$Baseline\ 01\ Front\ Downforce = 44\% \cdot 9059.41\ N = 3986.14\ N = 406.33\ Kg \quad \text{(Eq. 2.5)}$$

$$Baseline\ 01\ Rear\ Downforce = 56\% \cdot 9059.41\ N = 5073.27\ N = 517.15\ Kg \quad \text{(Eq. 2.6)}$$

Baseline 02: Rear wing must be adjusted to obtain Cx target of 1.05.

Baseline 01 Delta Rear Downforce: +70 N (reduction of 30 N)

Baseline 01 Delta Drag: 0 N (reduction of 10 N)

Front wing: Adjusted flap to obtain target 44%F downforce.

Baseline 01 Delta Front downforce: +55 N

Baseline 01 Delta Drag: negligible

Adjusted Baseline 02:

Front downforce = 4041.14 N = 411.98 Kg

Rear downforce = 5143.27 N = 524.29 Kg

Cz Equivalent = 2.8386

Delta Cz = 0.0386 or 3.86 points

If it is assumed that 10 points means an improvement of 3 tenths of a second per lap **[11]** in an average track:

Lap time improvement on average = 1.158 tenths

epsilon EUSKADI

2.8.4- Final results with F1 full model – Combined Baseline 03

The name of combined Baseline 03 is simply because it is the combination of Baseline 02 with a new beam wing. It has been demonstrated that the new Baseline 02 (new main plane and flap of the rear wing) is working correctly, and the increase in performance is significant. Therefore, the development of the beam wing begins with the geometry of Baseline 02.

However, the mesh and the whole simulation was prepared to obtain good correlation results with this upper part of the rear wing, but not the beam wing. Consequently, the results with the full F1 car simulation are different from what was expected. The increase in efficiency is clearly seen, but there downforce has fallen by 1.41%, which was not predicted in the reduced mesh simulation.

	Former Rear wing	Combined Baseline 03	Difference
Downforce	3185 N	3140 N	-45 N (-1.41%)
Drag	986 N	950 N	-36 N (-3.65%)
Efficiency	3.2302	3.3053	+0.0751 (+2.325%)

Table 2.30 – Combined Baseline 03 results.

Efficiency is improved, but this is only on the rear of the car. As said before, the lack of performance of the beam wing will affect the floor and diffuser. The low pressure area under the beam wing is smaller, thus the diffuser is not extracting the same amount of air from the floor, so the performance is also affected in the whole car. Finally, after checking the diffuser, there is a drop of the downforce generated of 6%. The final efficiency of the whole car is decreased by 1 point, so this part will not be tested in the wind tunnel, as the results show that there is not an improvement.

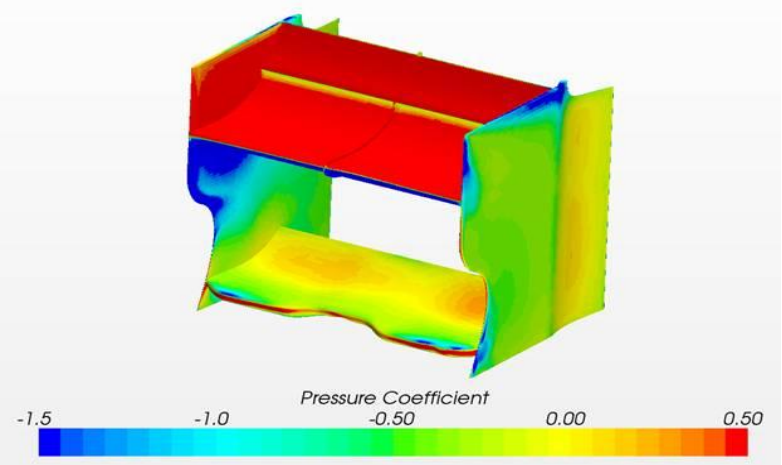

Fig 2.126 – Pressure coefficient graph of the Combined Baseline 03, front view. Notice the high pressure over the main plane and flap, but not so big over the beam wing.

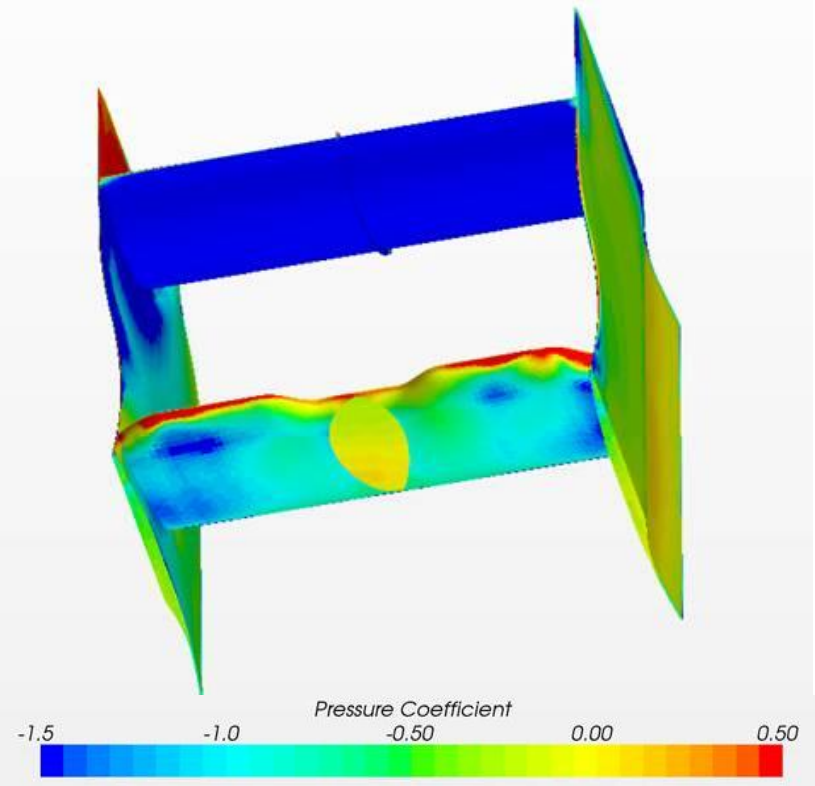

Fig 2.127 – Pressure coefficient graph of the Combined Baseline 03, bottom view. In this picture, the low pressure generated by the main plane is clearly seen, but it is not so strong in the beam wing. The central part (in yellow) of the beam wing is the whole of attachment with the bodywork of the lower surface.
*Graphs are different from Baseline 02 due to confidential issues.

COMBINED BASELINE 03 CONCLUSION

Results are much less accurate as predicted, due to a lack of precision of the mesh, and a model less appropriated (rear half of the car). The beam wing, which looked quite promising in the reduced mesh, was clearly worse than Baseline 02, especially due to the lack of prediction of the downforce generated by the floor + diffuser. A new mesh should be designed, more accurate in the diffuser area, and the model size should be increased (for example, cutting the car after the front wheels, instead of cutting it after the exhaust). Nevertheless, although making this changes (which would imply around 60 or 70% more computing resources per simulation), a correlation analysis should be done to check the reliability of the simulations. It is important to understand that CFD is a very powerful tool, but lack of correlation, mesh accuracy, boundary conditions or model definition can lead to wrong results.

PART 3 – Economical & Environmental analysis

3.1- Economical Analysis

In the budget for the Rear Wing development it is considered only human resources and material resources. However, it is not taken into account some other concepts, like the manufacturing process of a carbon-fiber prototype and wind tunnel testing, as it finally has not been done, although it would be the next logical step.

Therefore, the only costs directly included in the economical study are the ones which has been purchased for the solely purpose of this project. For instance, the computer used, internet access, and licenses of different software are property of Epsilon Euskadi, which has some agreements with Basque Government and software companies as Technological Center and for academic purposes, so they will not be listed as costs. However, all resources needed are listed to show all the resources used to develop the project.

3.1.1 - Resources used not considered in the cost of the project

Item	Units
High performance computer (Workstation)	1
60 CPU low speed cluster (days of use)	9
Internet Access	1
Printer	1
Microsoft Office license	1
Adobe Acrobat Professional license	1
StarCCM+ license (CD-Adapco)	1
ModeFrontier license (Aperio)	1
Catia V5 license (Dassault Systemes)	1
Office material	1

Table 3.1 – Resources used not considered in the cost of the project

Resources like computers, Microsoft Office and Adobe Acrobat Professional licenses come from agreements with the Basque Government. More expensive licenses, like ModeFrontier, StarCCM+ and Catia V5 come from agreements with their companies.

3.1.2 - Human resources cost

Concept	Unit cost (€)	Units (hours)	Total Cost (€)
Working hours, Mech. Engineering student	14	800	11200
Working hours, supervisor (Senior Aerodynamicist)	80	20	1600
TOTAL			12800

Table 3.2 – Human resources cost

The cost for working hour of a Mechanical Engineering student is considered regarding current economical crisis in Spain (2010), and the high demand of jobs in Motorsport. The amount of working hours is the real one, which is considered a workload of 8 hours per day during 5 months. The cost for working hour of the supervisor is approximately the cost of a Senior Aerodynamicist, who should guide the development of the project and frequently assessing the student in short meetings.

3.1.3 - Material resources cost

Item	Unit cost (€)	Units	Total Cost (€)
Office Material			
Printer ink (black)	1	23	23
Printer ink (color)	1	29	29
Paper packs (300)	4	2	8
CDs	0,5	6	3
Rapid-prototyping scale model			
Engineering hours	20	1	20
Polypropylene wire (m)	2	5	10
Support material (wax)	1	5	5
Carbon fiber ply	1	10	10
Modeler hours	20	2	40
Machine power (kWh)	0.15	20	3
TOTAL			151

Table 3.3 – Material resources cost

The cost of the scale model is a 15% scale rear wing, manufactured with a rapid-prototyping machine which heats a polypropylene wire, and uses a kind of wax as a support material. Engineering

epsilon EUSKADI

hours corresponds to the configuration of the rapid-prototyping machine, and modeler hours correspond to the work of the modeler removing the wax and adding the carbon fiber parts in the model.

3.1.4 - Total project cost

Item	Total Cost (€)
Human resources cost	12800
Material resources cost	151
TOTAL PROJECT COST	12951

Table 3.4 – Total project cost

All costs have IVA already included (Spanish VAT).

As it is an in-house project (not for other companies), for academic purpose only, it is considered an internal cost so there is no point in calculating profit margins nor IVA.

3.2- Environmental Analysis

3.2.1 - CFD development

The CFD development of the rear wing has been done using one high performance computer (Workstation), but has been validated with a “cluster”, a 60 CPUs machine to calculate very complex simulations. The impact on the environment of the workstation is minimal, and it has not been purchased for this project only, but it has done a small amount of electrical energy consumption. However, the “cluster” is a “special” computer, which is much bigger, its consumption is more important, and it needs a room with a controlled environment. A small room should be built for several clusters (depending on the size, three cluster in a room of 15 squared meters in Epsilon), with a good system of air conditioning to keep temperature of the room around 22ºC (60 CPUs heats like 60 computers working at maximum power). Moreover, it also needs a UPS (Uninterrupted Power System) to prevent power cuts, and it also filters electricity peaks to improve the electrical quality and to protect CPUs of being damaged. Therefore, the cluster, electricity control and air conditioning devices have a reduced environmental impact, although the energy consumption is quite high, considering also that it is usually working 24 hours per day. After its useful life, it is disassembled by the manufacturing company (Cisco Systems) and they take proper actions to recycle all components in their facilities.

3.2.2 - Wind Tunnel testing

The CFD development objective is to create better rear wing, although wind tunnel testing workload will not be influenced (wind tunnel testing will be done as much as allowed). However, the environmental analysis of a wind tunnel is briefly explained, to understand why it is so restricted in Formula One.

Nowadays, Formula 1 wind tunnel is restricted to 60% model scale testing, and maximum speed of 180 km/h. Moreover, there is an agreement (non-official) of 50 “hours of wind” per day, which means 50 hours of running the fan of the wind tunnel (excluded time of installation of the model inside the wind tunnel). This is due to the aim of making the championship cheaper and more environment-friendly. A wind tunnel fan needs 500 kWh per hour of wind (at maximum speed), plus 50 kWh for the rolling belt (a belt which is moving under the car to avoid development of the boundary layer inside the car), and more energy for instrumentation and control of temperature inside wind tunnel (negligible compared to the wind tunnel fan and rolling belt) and to keep cool the fan and rolling belt. Therefore, there is an important energy consumption which is demanded by the testing procedure. However, to test a new rear wing can only take

a few runs (each run tests around 15 positions of the car at a given speed, which needs around 10 minutes of “wind”). Therefore, testing of the new aero package needs only a couple of hours.

Nevertheless, there is an important visual impact, as a Wind Tunnel facility is huge. However, the wind tunnel and Epsilon Euskadi facilities are built on a land given for free by the Basque Government, to enhance the industry in the area of Vitoria-Gasteiz, as its area it is not as strong as other regions of the Basque Country. Moreover, as Epsilon Euskadi is currently a research & development centre, with an academic MSc to develop young automotive engineers, it is socially accepted as a cutting-edge technological center, and a source of job creation. Moreover, the emission of greenhouse effect gases is reduced, as all wind tunnel facilities are electrical, so it can only be attributed the ones produced by the machinery which built the wind tunnel and other facilities. Other environmental impact can be the destruction of vegetation in the area, construction access roads to the facilities and parking area, thus important building works to adapt the land for the facilities and installation of a proper electrical supply system. Finally, disassemble and recycling of the facility is done by the manufacturing company, although it is a long-term facility.

Fig. 3.1 – Ferrari Wind Tunnel facilities in Maranello, Italy **[12]**

Another environmental analysis must be done in the manufacturing of scale models. A rear wing can be both manufactured in Carbon-Fiber or in aluminium. In this project, it was planned to manufacture a rear wing (main plane and flap, that is, 2 wings) in aluminium, from a CNC machined block. The manufacturing process is quite clean, although it needs a CNC machine to work for 24 hours to manufacture both wings. The electrical energy consumption of modern CNC machines is quite low, and all the residual aluminium shaving is kept in boxes and sent to recycle facilities, where the aluminium is melt

again. During its useful life, there is no residual waste generated, and at the end of its useful life, it is disassembled and it can also be sent to recycle facilities to melt the aluminium part again.

PART 4 - Conclusions

4.1- Conclusions of the project

Formula One is one of the most challenging competitions. Every year, millions of Euros are invested in the development of the car, and aerodynamic development is probably the most important area. Therefore, a project focused on optimization of both performance of the car and resources is really challenging. Having said that, the implementation of the optimizer, a reduced CFD model, and the development of a real Formula One rear wing with a single computer (although supported by a cluster for correlation) is a big success. Moreover, having obtained a new rear wing, which is (theoretically) more than 1 tenth of a second faster on an average track shows the efficiency of the loop created by CATIA V5, StarCCM+ and ModeFrontier – all three reference software in the automotive industry and motorsport world.

Nevertheless, the budget restrictions in the Epsilon Euskadi Formula One project did not allow manufacturing the rear wing to validate it in the wind tunnel, although it would be essential to know the final result of the rear wing in the wind tunnel. As Epsilon Euskadi did not obtain a place in the FIA Formula One 2011 World Championship, the development has been paused, but it can be resumed and all the data is kept for further tests.

The whole process, from the first tests in Catia to the final conclusion of this report has taken up to 5 months, to understand the optimizer, to develop a stable StarCCM+ simulation and to build a parametric model of the rear wing. This includes fixing all the problems related to compatibility issues, licences, etc. which has been a really difficult task to do. However, less than half year to accomplish the project objective is excellent, and a lot of know-how has been generated through the process, especially on the use of StarCCM, and the discovery of ModeFrontier as must-have product in the motorsport industry. Actually, the implementation in a different environment, for example the optimization of a rear wing for a World Series by Renault, or a DTM, would take around 1 month, as all the know-how has been generated and periodically written and shared with the other aerodynamicist, as a very good exercise of what is known as “recurrence prevention”.

To sum up, despite budget problems and lack of computing resources, the optimization method know-how has been implemented into Epsilon Euskadi department successfully, and validated with the development of the rear wing for the Epsilon Euskadi F1 prototype, which has given a better comprehension of CFD software through the process.

4.2- Recommendations for further development

A very aggressive approach has been used to develop the reduced mesh model. However, for a Formula One team (with an adequate budget), a similar reduced mesh method should be used, but more mesh accuracy and more resources should be used. Combined with more simulations of a full car model, a correlation rule could be achieved. For example, for a given CFD model with a reduction of the mesh size by 75% (that is, 75% less number of cells), the prediction of Downforce / Drag is 2% lower than the original simulation. This would release the cluster for optimization and not only for validation issues. Therefore, a better compromise between (optimization resources /full model resources) should be adopted.

ModeFrontier algorithms are also very complicated and difficult to personalize. A deeper research in optimization algorithms should be done, especially to understand how to modify the parameters of the optimizer to fit better the aim of the engineer. Moreover, some kind of controls / intermediate stages could be developed, in order to stop / continue a simulation if an error has occurred. Modefrontier automatically stops the simulation if there is a geometry/CFD failure, but it does not detect if the rear wing is working with an important stall and thus having bad efficiency results. A small modification should automatically detect lower values than expected to run the following simulation immediately. And even better, some kind of signal could be sent to the engineer, for example an e-mail with the efficiency / drag / downforce after 30% of the simulation time.

Finally, with more computing resources and more accurate mesh, another different perspective should be developed, tested and correlated, to maximize the efficiency of the loop and to confirm that the success of this experiment is not only restricted to rear wing developments. For example, exhaust positioning (which is currently very popular in Formula 1 2011 after the prohibition of the blown diffusers). Exhaust diameter, outlet position in the space and direction of the outlet and its interaction with the rear wing could be studied, and combined with a software for engine manifold development, like the ones from Ricardo Software, to test different temperatures and / or speed of exhaust gases, having a loop of ModeFrontier, Catia V5, StarCCM+ and Ricardo Software would be impressive.

Acknowledgements

- First of all, I want to thank my tutor and Chief Aerodynamicist of Epsilon Euskadi Franck Sanchez, and Epsilon Euskadi Technical director Sergio Rinland, for the opportunity to join Epsilon Euskadi Formula One project. The experience after working 4 months in the Aerodynamics department was extraordinary. I really appreciate their support.

- I also want to thank Martin Schudel & Imanol Leizabe, Epsilon Euskadi Aerodynamicists, for their help and knowledge, from the beginning until the end of this project. I hope all the discussions and working hours together can be seen on this project, thank you for your patience and effort. And also thanks to the rest of the Aerodynamics Department / Composites Department for their help when required.

- ModeFrontier Technical Service deserves a special mention. Especially Pascual Guardiola, who spent many hours working on my models and teaching me how to implement the optimizer software on this project.

- From my faculty, I want to thank Dr. Emilio Hernández who helped me with the UPC paperwork and the extended version for the University.

-Finally I want to thank my family and friends, not only for their support on this project, but also to understand my passion and dedication to Motorsport industry.

Bibliographic references

[1] Technical F1 website, [http://www.f1technical.net, September 2010].

[2] Josep KATZ, (1995). *Race Car Aerodynamics. Designing for Speed*. Bentley Publishers.

[3] Pascual Guardiola (2010). *METCA 2010* Optimization *Lectures, from Epsilon Euskadi Master Degree.*

[4] Formula 1 Official website, [http://www.formula1.com, November 2010].

[5] FIA 2010 Formula One Technical Regulations.
FEDERATION INTERNATIONALE DE L'AUTOMOBILE.

[6] Technical F1 website, [http://www.f1technical.net, December 2010].

[7] Sandglass Patrol website, [http://www.sandglasspatrol.com, December 2010].

[8] Epsilon Euskadi website, [http://www.epsiloneuskadi.com, January 2011].

[9] Esteco modeFRONTIER internal documents, [Website not available, January 2011].

[10] Autosport website, [http://www.autosport.com, January 2011].

[11] Franck SANCHEZ, (2010). *METCA 2010* Aerodynamics *Lectures, from Epsilon Euskadi Master Degree.*

[12] Scuderia Ferrari F1 website, [http://www.ferrari.com, January 2011].

epsilon EUSKADI

Complementary bibliography

Although not being used in any particular point of this thesis, this complementary bibliography helped during the whole development of this project, or contributed to the general knowledge to understand some concepts. Books and websites are listed by order of importance:

[12] FIA 2011 Formula One Technical Regulations.
FEDERATION INTERNATIONALE DE L'AUTOMOBILE

[13] William F. MILLIKEN & Douglas L. MILLIKEN, (1995). *Race Car Vehicle Dynamics.* SAE International.

[14] John D. ANDERSON, (2001). *Fundamentals of Aerodynamics.* McGraw-Hill.

[15] J-C. JOUHAUD, P. SAGAUT, B. LABEYRIE. *A Kriging Approach for CFD/Wind Tunnel Data Comparison.* Journal of Fluids Engineering (September 2005).

[16] John D. ANDERSON, (1995). *Computational Fluid Dynamics.* McGraw-Hill.

[17] David TREMAYNE, (2004). *The Science of Formula 1 Design.* Haynes Publishing.